Regulation of T Lymphocyte Growth by Macropinocytosis

by

John C. Charpentier

A dissertation submitted in partial fulfillment
of the requirements for the degree of
Doctor of Philosophy
(Immunology)
in The University of Michigan
2021

Doctoral Committee:

Professor Philip D. King, Chair
Professor Cheong-Hee Chang
Associate Professor Ken Inoki
Assistant Professor Costas Lyssiotis
Professor Joel A. Swanson

John C. Charpentier

jcharpen@umich.edu

ORCID iD: 0000-0001-9488-8239

DEDICATION

To Lauren Flocco

and

Glenn Black

ACKNOWLEDGEMENTS

I thank Phil King for welcoming me into his lab and offering me an exciting project that any graduate student would be lucky to work on. Thanks are also due to my labmate, Di Chen, and my collaborators Phil Lapinski, Jackson Turner, and Irina Grigorova, without whom the quality of this work would have suffered.

I've benefited from conversations and guidance from the rest of my committee members: Joel Swanson, Ken Inoki, Cheong-Hee Chang, and Costas Lyssiotis. In particular, lab rotations with Joel and Ken in my first year helped to clarify the focus of this thesis.

Beth Moore's unconditional support and advice through my graduate career was invaluable. Thanks are also due to the directors of the Graduate Program in Immunology, Malini Raghavan, Gary Huffnagle, and Kanakadurga Singer.

I would never have had the privilege to earn a Ph.D. at the University of Michigan if it weren't for the mentorship I received at Tufts University and my undergraduate alma mater, the University of Massachusetts Boston. The two years I spent in Steve Bunnell's lab at Tufts were transformative. I benefited immensely from the advice and mentorship he and Maria-Cristina Seminario provided me. Thanks are also due to Henry Wortis for introducing me to Steve and for his encouragement and guidance over the past seven years.

The NIH-sponsored Initiative for Maximizing Student Development (IMSD) program at UMass Boston made possible my first experiences in laboratory research and has been responsible for transforming countless first-generation college students into successful Ph.D.

graduates. I am deeply indebted to Claudia Heske, Rachel Skvirsky, and Adan Colón-Carmona, who, through this program, prepared me to succeed in graduate school.

Long before I decided to pursue my education, Mike Stillman encouraged me to expect better things for my life and assured me I was capable when I didn't much believe it. It's been an honor to prove him right.

For twelve years the extended Flocco family has treated me like one of their own, and I am grateful for their kindness and generosity. I will always cherish the time I've spent in Michigan with my friends Melissa and Robert Jasper, who are genuine and generous beyond measure. Thanks also to my best friend for over two decades, Shaun Donnelly, who regularly inspires me and who contributed the excellent illustration shown in the last figure. Lastly, thanks also to my friends Kia Eshghi, Richard Louis, Dave Frank, Steve Spears, Amy Larkin, and Vlad Wormwood, who, as the essayist Charles Lamb once put it, have always allowed me to talk nonsense and have my nonsense be respected.

Ann Arbor, Michigan

March, 2021

PREFACE

In many places in this thesis I refer to “T cells” without further specification. Except where explicitly indicated otherwise, these should be assumed to be murine $CD4^+$ and $CD8^+$ αβ TCR T cells.

TABLE OF CONTENTS

LIST OF FIGURES

LIST OF TABLES

LIST OF ACRONYMS & INITIALISMS

5' TOP – 5' terminal oligopyrimidine tract
ADBE – Activity-dependent bulk endocytosis
ADP – Adenosine diphosphate
AMPK – 5' adenosine monophosphate-activated kinase
APC – Antigen-presenting cell
Arp2/3 – Actin-related protein 2/actin-related protein 3 complex
β1AR – β1 adrenergic receptor
BAR – Bin/Amphiphysin/Rvs
BSA – Bovine serum albumin
CCP/CCV – Clathrin-coated pit/vesicle
CDR – Circular dorsal ruffle
CIE – Clathrin independent endocytosis
CLIC – Clathrin-independent carrier
CME – Clathrin-mediated endocytosis
CSF1 – Colony stimulating factor 1
CtBP1/BARS - C-terminal-binding protein-1/brefeldinA-ADP ribosylated substrate
CTxB – Cholera enterotoxin subunit B
DAG – Diacylglycerol
EIPA – 5-(*N*-Ethyl-*N*-isopropyl) amiloride.
FCS – Fetal calf serum
Fdex – 70 kDa fluorescein-dextran
FEME – Fast endophilin-mediated endocytosis
GAP – GTPase-activating protein
GATOR1/2 - GTPase-activating protein (GAP) activity toward Rags-1/2
GDI – Guanine dissociation inhibitor
GDP – Guanosine 5'-diphosphate
GEEC – GPI-AP Enriched Early Endosomal Compartments
GEF – Guanine nucleotide exchange factor
GPCR – G protein-coupled receptor
GRAF1 – GTPase regulator associated with focal adhesion kinase 1
GRB2 – Growth factor receptor-bound protein-2
GSK3β – glycogen synthase kinase 3β
GTP – Guanosine 5'-triphosphate
HMG-CoA – 3-hydroxy-3-methylglutaryl CoA
J/B – Jasplakinolide/blebbistatin
kDa – Kilodalton
LAT – Linker for activation of T cells
LDL – Low-density lipoprotein

mAb – Monoclonal antibody
M-CSF – Macrophage colony-stimulating factor
MEF – Mouse embryonic fibroblast
MEND – Massive endocytosis
MFI – Median fluorescence intensity
NADPH – Reduced nicotinamide adenine dinucleotide phosphate
NF1 – Neurofibromin 1
NHE – Na^+/H^+ exchanger
OVA – Ovalbumin
Pak1 – p-21 activated kinase 1
PAT – Proton-assisted amino acid transporter
PBMC – Peripheral blood mononuclear cells
PDAC – Pancreatic ductal adenocarcinoma
PDK1 – Phosphoinositide-dependent kinase 1
PFKFB3 – 6-phosphofructo-2-kinase/fructose-2,6-biphosphatase 3
$PI(4,5)P_2$ – Phosphatidylinositol (4,5)-bisphosphate
PIP_3 – Phosphatidylinositol (3,4,5)-trisphosphate
PMA – Phorbol 12-myristate 13-acetate
PRP^{Sc} – Prion protein, Scrapie isoform
PTEN – Phosphatase and tensin homolog
Rasgrp1 – RAS guanyl releasing protein 1
RGBARG – RCC1, RhoGEF, BAR, and RasGAP-containing protein
SEM – Scanning electron microscopy *or* standard error of the mean
SIM – Structured illumination microscopy
SLP-76 - SH2 domain-containing leukocyte protein of 76 kDa
Sos1/2 – Son of sevenless homolog ½
TAP – Transporter associated with antigen processing
TCR – T cell receptor
Tfr – Transferrin receptor
TIL – Tumor-infiltrating lymphocyte
WAVE – WASp family verprolin homologous protein

ABSTRACT

Macropinocytosis is a non-selective form of clathrin-independent endocytosis that has been conserved by evolution from unicellular amoeboids to mammals. The function of macropinocytosis in various cell types, however, is distinct. In amoebae, macropinocytosis facilitates feeding. In mammalian cells it has been shown to aid in, among other things, regulation of receptor density, directed migration, and antigen presentation. Macropinocytosis is implicated in a range of human diseases, including atherosclerosis and transmissable spongiform encephalopathies, as well as being a commonly exploited route of viral infection.

We have discovered that primary mouse and human T lymphocytes (T cells) engage in constitutive macropinocytosis that is enhanced significantly upon TCR ligation and co-stimulation. Unlike macropinocytosis in many other cell types, T cell macropinocytosis is also Ras-independent. We have shown that macropinocytosis is essential for G1 phase growth in activated T cells even under nutrient-replete conditions. Mechanistically, macropinocytosis enables rapid T cell growth, at least in part, by delivering free amino acids obtained from the extracellular space to the lysosomal compartment. There they promote the activation of the mechanistic target of rapamycin complex 1 (mTORC1) by an inside-out signaling mechanism to drive G1 phase blastogenesis and subsequent clonal expansion. Supplementation of minimal cell culture media with the amino acids leucine, glutamine, arginine and serine is sufficient to sustain mTORC1 activation in this period, with leucine and arginine being most important among these.

This work constitutes the first demonstration of a role for macropinocytosis in the regulation of non-cancerous mammalian cell growth. These results suggest that macropinocytosis-mediated activation of mTORC1 may be a feature of other highly proliferative cells. Modulation of T cell macropinocytosis may be therapeutic in the setting of diseases of public health interest.

CHAPTER I:

FORMS OF ENDOCYTOSIS

1.1 ABSTRACT

Endocytosis is a ubiquitous feature of eukaryotic cells that has been implicated in their evolutionary origin. Multiple conserved endocytic modes facilitate a diverse range of cell-specific responses in metazoans. The first-discovered of these, clathrin-mediated endocytosis, is nearly universal with respect to cell type and constitutes the primary "housekeeping" mode of endocytosis in animal cells. Beginning in the 1990s, evidence for a number of endocytic pathways that do not require clathrin has accrued. While flux through these pathways may constitute only a small proportion of endocytic events, they facilitate critical and highly specialized cellular functions. In T lymphocytes, endocytosis regulates, among other things, signal transduction, growth, conjugate formation with antigen-presenting cells, trogocytosis of receptor complexes, and phagocytosis in TCR γδ T cel

1.2 INTRODUCTION

Endocytosis, the generation of internal membranes from the plasma membrane (PM) by extension (or invagination) and vesicle scission, facilitates a range of diverse cellular processes in eukaryotes. In addition to enabling the internalization of extracellular macromolecules, endocytosis permits the compartmentalization of chemistry within cells. Co-evolution of endocytosis and cellular endosymbiosis—the state of one cell living mutualistically within another—may have significantly contributed to the complexity and organization of eukaryotic cells.[1,2] A great number and variety of cellular functions are regulated, at least in part, by endocytosis, including: signal transduction, membrane composition, mitosis, adhesion, lipid homeostasis, motility, and cell morphogenesis. Eukaryotes have evolved many distinct forms of endocytosis, some of which are universal or nearly so with respect to cell type, such as clathrin-mediated endocytosis (CME). Other varieties are limited to specific cell types or lineage states and adapted for specialized functions, such as those that enable the recycling of synaptic vesicles in neurons or the resorption of calcified extracellular matrix by active osteoclasts.[3,4] All endocytic pathways facilitate sensation of, and mediate interaction with, the extracellular environment, making them critical, fundamental components of eukaryotic cells.

Clathrin-Mediated Endocytosis

Endocytic pathways are often broadly classified by their dependence on the hexamer protein clathrin (**Figure 1**). This is in part due to the historical primacy of the characterization of clathrin-mediated endocytosis (CME) in the 1970s but it is also an acknowledgement of its role

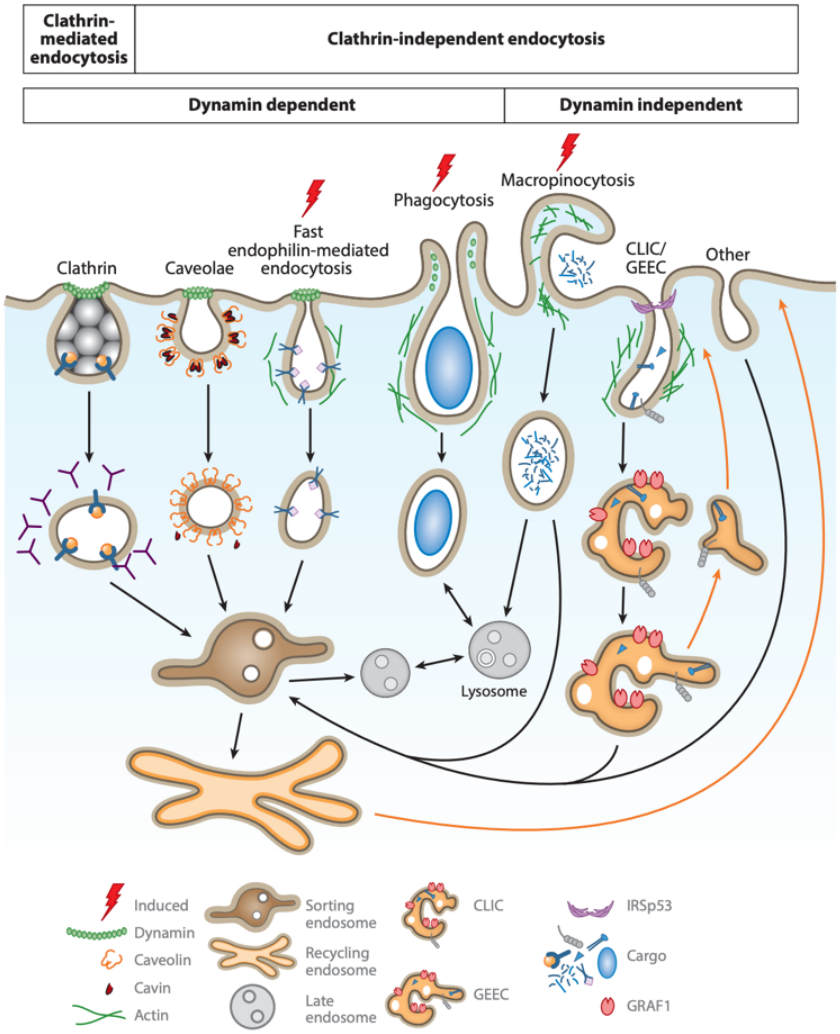

Figure 1: Endocytic pathways in eukaryotic cells. Historically, pathways have been classified by their dependence on the coat protein clathrin and, more recently, the GTPase dynamin. Figure from Mayor et al (2019).[7]

as the primary endocytic route for cellular housekeeping functions.[5,6] In CME, the geodesic assembly of clathrin triskelions on spherical membrane buds promotes the formation of clathrin-coated pits (CCPs) 60-120 nm in diameter.[8] CCPs progress through a series of well-defined morphological intermediates to form clathrin-coated vesicles (CCVs) upon scission from the PM. Post-scission, clathrin assemblies disintegrate, uncoating factors such as synaptojanin 1 remove accessory and adaptor proteins, and uncoated vesicles deliver their contents to endosomes by fusion.[9] CCVs themselves can be further classified by the differential recruitment of over 50 adaptor and accessory proteins, as well as by enrichment of specific lipid and protein cargoes.[8]

For many years, the term "receptor-mediated endocytosis" was used synonymously with CME. However, it is now appreciated that removal of many plasma membrane receptors is accomplished by mechanisms that do not require clathrin. Consequently, this usage has been discouraged and a more descriptive schema, wherein endocytic pathways are classified by the identity of vesicular membrane components and cargoes, has been adopted.

Clathrin-Independent Mechanisms of Endocytosis.

Some cellular functions, such as responding to high intensity stimuli and directed migration, require rapid endocytosis of large patches of membrane or internalization of large boluses of fluid. Since these events require membrane fluxes on the millisecond-to-second scale or are impeded by the size of CCVs, CME is not sufficient to enable them.[10] In recent decades, a number of forms of clathrin-independent endocytosis (CIE) have been discovered and characterized, some of which license rapid, bulk internalization of membrane or otherwise facilitate acute responses. Some evidence suggests that flux through CIE pathways accounts for

only a small fraction of endocytic events compared to CME, though this has only been shown in immortalized mammalian cells.[11] Our present knowledge of CIE is chiefly limited by the lack of validated, path-specific molecular determinants and cargoes, as well as the existence of shared machinery between pathways—both factors which confound interpretation of experimental results. Glycosylation of cell surface proteins and galectin-glycan interactions have also been implicated in cargo-specific regulation of some CIE pathways, but these observations have yet to be confirmed in primary cells or widely replicated.[12] Nevertheless, salient features of each form of CIE have been experimentally elucidated.

Building on the classification of Doherty and McMahon[13], CIE includes: caveolae-dependent endocytosis, clathrin-independent carrier/GPI-AP-enriched early endosomal compartment (CLIC/GEEC) pathway endocytosis, flotillin-dependent endocytosis, interleukin-2 receptor beta (IL-2Rβ) pathway endocytosis, Arf6-dependent endocytosis, phagocytosis, fast endophilin-mediated endocytosis (FEME), activity-dependent bulk endocytosis (ADBE), ultra-fast endocytosis (UFE), massive endocytosis (MEND), and macropinocytosis. Each of these forms of endocytosis, the essential features of which are summarized in **Table 1**, will be discussed.

	Actin-dependent	Scale (vesicle diameter)	Canonical cargoes	Cholesterol-dependent	Dynamin-dependent	Cell type first described in
Clathrin-dependent endocytosis	Depends on cell type[14]	35-200 nm[15]	Tfr[16]	Yes[17]	Yes[18,19]	*A. aegypti* oocytes[20]
Caveolae-dependent endocytosis	Yes[21–23]	50-80 nm[24]	Unclear	Yes[25]	Yes[26]	Murine gall bladder epithelium[27]
CLIC/GEEC pathway endocytosis	Yes[28,29]	Tubulovesicular, 40 nm width[30]	CTxB, CD44[31]	Yes[28]	No[32]	COS, CHO cells[33]
Flotillin-dependent endocytosis	Unclear[34]	Unclear	Unclear	Yes[35]	Unclear	HeLa cells[36]
IL-2Rβ pathway endocytosis	Yes[37]	50-100 nm[37,38]	IL-2Rβ[38]	Yes[39,40]	Yes[41]	IARC 301.5, YT2C2, CIAC cells[42]
Arf6-dependent endocytosis	Yes[43]	60-200 nm	MHC-I, CD59[44]	Yes[44]	Unclear	CHO cells[45]
Phagocytosis	Yes[46,47]	0.5 – 3 μm[48–51]	Microbial pathogens	Yes[52,53]	Yes[54]	Ranine phagocytes[55]
Fast endophilin-mediated endocytosis (FEME)	Yes[56]	Tubulo-vesicular, 100 nm - μm length	β1AR[56,57]	Yes[56]	Yes[56]	BSC1, HEK293 cells[56]
Activity-dependent bulk endocytosis (ADBE)	Yes[58,59]	150 nm	VAMP4[60]	Yes[61]	Yes[62]	Murine cerebellar granule cells[63]
Ultrafast endocytosis (UFE)	Yes[64]	60-80 nm[64,65]	Unclear	Yes[66]	Yes[64]	Nematode neurons[67]
Massive endocytosis (MEND)	No[68,69]	<100 nm[69]	Phospholemman, polypalmitoylated proteins[70]	Yes[71]	No[68,69]	BHK, HEK293 cells[69]
Macropinocytosis	Yes[72,73]	200 nm – 20 μm	Non-selective	Yes[74,75]	Unclear	Murine sarcoma cells[76]

Table 1 – Modes of endocytosis and their salient features. Note that actin-dependency, dynamin-dependency, and canonical cargoes remain to be clarified for multiple pathways.

Caveolae-dependent endocytosis is characterized by a requirement for the integral membrane protein caveolin-1 and a small number of adaptor proteins of the cavin family (four in mammals), as well as by its sensitivity to glycosphingolipid depletion.[25,77] Caveolae, so named for their resemblance to caves, constitute small, flask-shaped membrane bulbs 50-100 nm in diameter and are enriched in vascular endothelial cells, epithelial cells, adipocytes, and fibroblasts.[78,79] Caveolae are relatively stable structures that likely participate in non-endocytic cellular processes. Within them, cavin proteins organize scaffolding microdomains that may be necessary for modulation of intracellular stress and GPCR signaling.[80,81] Despite an initial consensus that caveolae remained attached to the PM, it is now known that the GTPase dynamin positively regulates their budding and scission and that its GTPase activity is required for this function.[26,82] The trafficking of caveolar endosomes and delivery of their lumenal contents to organelles is poorly understood, in part because of overlap between cargoes sorted into the caveolae-dependent pathway and the CLIC-GEEC pathway.[31]

Many proteins that are lipid-anchored to the outer leaflet of the PM, such as GPI-anchored aminopeptidases (GPI-APs), are endocytosed in uncoated, clathrin-independent carriers (CLICs) that are derived from the plasma membrane and enriched in large tubulovesicular structures called GPI-AP Enriched Early Endosomal Compartments (GEECs).[32,33] Endocytosis via the CLIC-GEEC pathway accounts for a significant proportion of internalized membrane and fluid-phase contents and in this respect resembles macropinocytosis. Unlike macropinocytosis, however, CLIC-GEEC endocytosis is insensitive to amiloride inhibition.[83]

The CLIC/GEEC pathway is initiated by plasma membrane recruitment of GBF1, a guanine nucleotide exchange factor (GEF) for the GTP-binding protein ADP-ribosylation factor 1 (Arf1).[84] Consequent to activation of Arf1 by GBF1, the Rho GTPase activating protein (GAP) ARHGAP10/21 is locally recruited and promotes the GTP cycling of the Rho GTPase Cdc42.[84] Cdc42 dynamics at the plasma membrane, in turn, regulate recruitment of downstream effectors that direct actin polymerization and promote vesicle formation. IRSp53, an I-BAR protein that induces negative membrane curvature and interacts with Cdc42, is also required for optimal functioning of CLIC-GEEC endocytosis.[29] GEEC formation is also regulated by recruitment of GTPase regulator associated with focal adhesion kinase1 (GRAF1), a BAR-domain-containing protein capable of sensing and promoting membrane curvature that also negatively regulates activated Cdc42 via its Rho-GAP domain.[30] While the CLIC/GEEC pathway does not require dynamin for endocytosis of its cargoes, dynamin does associate with GEECs post-internalization.[32]

Flotillin-dependent endocytosis is an additional, putative form of CIE requiring flotillin (reggie) proteins, genes for which are highly conserved among metazoans.[85] Flotillins are characterized by N-terminal hydrophobic stomatin/prohibitin/flotillin/HflK/C (SPFH) domains shown to regulate membrane targeting in adipocytes and C-terminal flotillin domains necessary for oligomerization.[86–88] Flotillins associate with lipid rafts and generate membrane invaginations through mechanisms that are largely undefined.[89] The role of dynamin in flotillin-dependent endocytosis is unclear, as is the mechanism governing cargo specificity. For these reasons, some have argued that flotillins may not characterize a distinct endocytic pathway at all but instead function as adaptors in other forms of CIE.[90]

Many cytokine receptors are internalized via a cholesterol-sensitive pathway termed RhoA-dependent IL-2Rβ endocytosis for the receptor that historically first defined it. This form of CIE, which is initiated at the base of membrane protrusions, requires activation of the small GTPases RhoA and Rac1 as well as signaling through p21-activated kinases (Paks).[37,38] Two rounds of actin polymerization drive vesicular budding and maturation. The first, which requires binding of WASP-family verprolin homologous protein (WAVE) to the cytoplasmic tail of the β subunit, is thought to be necessary to drive receptor recruitment and clustering at the base of the invaginated membrane. The second round of actin polymerization required for IL-2Rβ endocytosis is dependent upon the activation of Pak1 and induces the formation of a complex including N-WASP, cortactin, and ARP2/3 that drives receptor scission to form vesicles 50-100 nm in diameter.[37,38] Dynamin has been shown to coordinate progressive recruitment of WAVE and N-WASP in IL-2Rβ endocytosis.[37]

A variety of cell surface proteins are internalized by a mode of endocytosis regulated by the small GTPase ADP-ribosylation factor 6 (Arf6). Arf6-mediated endocytosis also plays an important role in directed migration by down-regulating cell-cell contacts, licenses abscission during cytokinesis, and is essential for cholesterol homeostasis.[91] Arf6 GTP-loading and activation in tubular endosomes promotes membrane recycling to the PM, where Arf6-GTP triggers the generation of actin-rich protrusions.[43] Activation of phosphatidylinositol-4-phosphate 5-kinase downstream of Arf6 recruits additionally needed signaling molecules to sites of active cytoskeletal rearrangement.[92] While Arf6 activation is not strictly required for internalization of cargoes, it is necessary for recycling of endosomes to the PM and hydrolysis to

Arf6-GDP is required for proper cargo sorting.[83] Soon after internalization, Arf6-GDP associates with tubular early endosomes which then fuse with Rab5 positive sorting endosomes.[93] Subsequent trafficking events are regulated by the CME adaptor protein AP-2.[94] While dynamin-2 has been shown to be required for Arf6-activation in CME, its role in Arf6-mediated CIE is less clear.[95]

Phagocytosis is a form of CIE that involves the specific recognition and uptake of particles >500 nm into membrane-derived vesicles known as phagosomes.[96] The posited role of phagocytosis in eukaryogenesis implies an evolutionary origin possibly preceding eukaryotes—far earlier than the likely emergence of most other forms of endocytosis.[97] The contribution of phagocytosis to host defense against microbial pathogens is well-appreciated. Many innate immune cells perform phagocytosis, including macrophages, dendritic cells, monocytes, neutrophils and eosinophils.[98] Phagocytosis in these cells enables presentation of antigen to lymphocytes and parallel activation of adaptive immune responses.[98] Heritable defects in phagocytosis (e.g., in macrophages) are associated with a predisposition to chronic intracellular bacterial infections, usually by mycobacteria.[99]

Less well-appreciated but equally critical are the roles phagocytosis plays in tissue homeostasis and development. In the brain, phagocytosis-competent microglia (as well as possibly astrocytes and oligodendrocytes) are required to prune synapses in the course of neural development as well as to remove inflammatory cellular debris.[100] Many other cell types, including epithelial cells, endothelial cells, and fibroblasts, also perform phagocytosis to promote tissue homeostasis under inflammatory conditions.[96]

Phagocytic target ligands are recognized by surface receptors that can be broadly classified as opsonic and non-opsonic. Opsonic receptors recognize foreign particles indirectly by binding host-derived opsonins. They include receptors for antibody Fc regions (FcγR, FcαR, FcεR), complement (CR3/4), mannan-binding lectin (CR1), and fibronectin ($\alpha 5\beta 1$).[96] Non-opsonic receptors include those that recognize pathogen-associated molecular patterns (CD14, Dectin-1), as well as those that recognize apoptotic and necrotic cells by, for example, detecting oxidized phospholipids (CD36) or phosphatidylserine on the outer leaflet of the plasma membrane (TIM-1/-4).[96] Ligand binding and aggregation of receptors initiates intracellular signaling cascades by recruitment and activation of the non-receptor protein tyrosine kinase Syk, the modulation of membrane phosphoinositides, and the generation of second messengers.[96,101,102] These signals recruit activated Rho GTPases to phagocytic cups where they coordinate actin polymerization in pseudopodial protrusions that engulf the target particle and promote the assembly of a highly complex organelle around it, the phagosome.[96]

In dendritic cells, early phagosomes can fuse with endoplasmic reticulum or Golgi to acquire molecular machinery enabling cross-presentation of acquired antigens on MHC class I, thereby promoting their sentinel function.[103–105] Similarly, neutrophils and macrophages can cross-present peptides derived from phagosomes via mechanisms that do not require the proteasome or the transporter associated with antigen processsing (TAP).[106,107] Alternately, early phagosomes can fuse with early and recycling endosomes in a manner regulated by the small GTPase Rab5.[108] Maturation into intermediate phagosomes is associated with loss of Rab5 and acquisition of Rab7, as well as the accumulation of V-ATPase, which promotes acidification of

the phagosomal lumen by extrusion of protons from the cytoplasm.[96,109] Accumulation of Rab7 also drives fusion with late endosomes and recruits the effector Rab-interacting lysosomal protein (RILP).[110,111] RILP brings late phagosomes into contact with microtubules and promotes their centripetal movement to lysosomes.[110,111] SNARE proteins mediate lysosomal fusion to generate highly microbicidal phagolysosomes.[112]

Fast Endophilin Mediated Endocytosis (FEME) is a form of CIE regulated by the BAR-domain-containing protein endophilin, which has five paralogs in humans (A1, A2, A3, B1, and B2).[57] FEME is a non-constitutive mode of endocytosis that occurs in response to activation of G-protein-coupled receptors (GPCRs) and cytokine receptors by their ligands. Activated receptors are sorted into pre-existing membrane clusters of endophilin that are rapidly (~5-10 seconds) internalized in tubulo-vesicular carriers 100 nm to several microns in length that closely resemble CLICs.[56] This form of CIE is dynamin-dependent and, like many other forms of endocytosis, is regulated by phosphoinositide and kinase signaling.[57] Specifically, phosphorylation of endophilin by ROCK, Src, LRRK2, and DYRK1A, and of dynamin and dynein by Cdk5 and GSK3β, have been shown to negatively regulate FEME.[113–116] In addition, endophilin has been implicated in both IL-2Rβ endocytosis and CME: triple-knockdown of the endophilin proteins known to participate in endocytosis (endophilin A1, A2, and A3) by RNA interference has been shown to decrease the rate of IL-2Rβ internalization and prevent the uncoating of CCVs.[56,117]

Two high-capacity modes of CIE of special importance in neurons are Activity-Dependent Bulk Endocytosis (ADBE) and Ultrafast Endocytosis (UFE). Both are dynamin-dependent forms of

CIE that, like FEME, are characterized by their rapidity. ADBE has been shown to internalize large patches of membrane and aid in the retrieval of synaptic vesicles (SVs) at central nerve terminals in response to high neuronal activity.[58] Mechanistically, ADBE requires interaction between dynamin and syndapin 1, which associates with N-WASP, an effector of actin nucleation and polymerization.[118] ADBE of SVs also requires cyclin-dependent kinase 5 (Cdk5)-mediated activation of Dynamin-1.[119] UFE occurs in response to more mild stimulation, 50-100 milliseconds after propagation of an action potential, and enables the recycling of synaptic vesicle components, such as SNAREs and synucleins.[64,120] Like FEME, endophilin has been implicated in regulation of UFE.[121]

Lastly, Massive ENDocytosis (MEND) is a dynamin-independent form of CIE that does not require actin remodeling.[69] As the name suggests, MEND enables the internalization of very large membrane patches in response to metabolic stress, Ca^{2+} signaling, and other stimuli, in a process driven by membrane phase separation.[68,122] In this process, membranes of heterogeneous lipid composition can partition into different nanodomains with intrinsic curvature, which facilitates endocytosis without actin remodeling.

1.3 ENDOCYTOSIS IN T CELLS

CME and CIE facilitate a range of T cell specific functions, as summarized in Table 2. Chief among these are the regulation of plasmalemmal immune receptors, including internalization and recycling of T cell antigen receptors (TCRs). Endocytic mechanisms are also critical for stable conjugate formation between T cells and APCs. They also enable trogocytic exchange of receptor complexes between individual T cells, as well as between T cells and APC.

	Described in T cells	Function in T cells
Clathrin-dependent endocytosis	Yes	PM receptor regulation[123,124], TCR αβ endocytosis[125–127]
CLIC/GEEC pathway endocytosis	Yes	TCRζ endocytosis[128]
Flotillin-dependent endocytosis	Yes	TCR αβ recycling[129], conjugate formation with APCs[129]
IL-2Rβ pathway endocytosis	Yes	IL-2R complex endocytosis[37,130]
Arf6-dependent endocytosis	Yes	Conjugate formation with APCs[131]
Phagocytosis	Yes	Host defense/immune surveillance (γδ T cells)[132,133], trogocytosis (TCR αβ T cells)[134]
Macropinocytosis	Yes	Regulation of G1 phase growth by bulk acquisition of amino acids.[135]
Caveolae-dependent endocytosis	No	No
Fast endophilin-mediated endocytosis	No	N/A
Activity-dependent bulk endocytosis (ADBE)	No	N/A
Ultrafast endocytosis (UFE)	No	N/A
Massive endocytosis (MEND)	No	N/A

Table 2 – Evidence of endocytic adaptations in T lymphocytes prior to this investigation.

Plasma membrane immune receptor and ligand regulation

Endocytosis of PM receptors and the trafficking, recycling, and targeted degradation of their components are integral to many cellular responses, including those of T cells. Both CME and CIE pathways have been shown to regulate localization of immune receptors in both TCR αβ and γδ T cells.

The immune checkpoint protein CTLA-4, which negatively regulates TCR αβ T cell activation by capturing from APCs and endocytosing in trans the CD28 ligands CD80 and CD86, is constitutively internalized by CME.[123,124] This occurs in a ligand- and dynamin-independent manner and results in both recycling to the cell surface and trafficking to lysosomes for degradation. Constitutive CTLA-4 internalization continues even as its surface expression is upregulated during T cell activation.[124]

In thymus-dependent humoral immune responses, transient expression of the transmembrane glycoprotein CD40-L on $CD4^+$ TCR αβ T cells provides an essential, contact-dependent, co-stimulatory signal to cognate B cells. $CD4^+$ T cell CD40-L binding to CD40 on B cells initiates an intracellular signaling cascade that promotes the generation of class-switched, high-affinity antibodies, as well as the establishment of B cell memory and differentiation into long-lived plasma cells. In addition to the transfer of CD40-L from T follicular helper (Tfh) cells to cognate B cells via an uncharacterized exocytic mechanism, down-modulation and lysosomal degradation of PM CD40-L has also been shown to occur in T cell tumor lines.[136] Endocytosis of

CD40-L in these cells requires actin polymerization, though its dependence on clathrin and dynamin have not been established.

By contrast, the rapid internalization of IL-2R complexes from the surface of activated TCR in αβ T cells has been shown to occur by CIE.[130] IL-2Rβ endocytosis was first demonstrated to be clathrin-independent in studies employing dominant-negative mutants of the essential clathrin coated pit and vesicle component Eps15.[130] Endocytosis of IL-2Rβ complexes in these experiments occurred normally in the absence of CME, which was confirmed by the loss of transferrin uptake. In addition to dynamin, IL-2Rβ internalization requires the cytoplasmic tail of the component γ_c chain, as well as both the catalytic activity and p85 regulatory subunit of PI3K.[137,138] The constituent subunits of the receptor partition into different compartments soon after internalization, with the comparatively stable α chain confined to transferrin-positive recycling endosomes (suggesting partial utilization of the CME pathway) whereas the β and γ_c chains are sorted into late endosomes and thereafter targeted to lysosomes for degradation.[139] The proteasome has also been shown to be important, not for the initial phase of IL-2Rβ endocytosis but for its continuance and lysosomal targeting of the β and γ_c subunits.[140] The co-localization of endophilin with IL-2Rβ vesicular cargoes in the human T cell line Kit255, as well as the specific diminution of IL-2Rβ internalization in cells depleted of endophilin, implicate FEME as a mechanism of IL-2Rβ endocytosis.[56]

WC1 proteins are transmembrane glycoproteins of the scavenger receptor cysteine-rich family that in γδ T cells are thought to function as activation coreceptors through co-ligation with the γδ TCR.[141] In Jurkat T cells, sustained co-ligation of the TCR and a transmembrane fusion protein,

consisting of the CD4 extracellular domain fused to the WC1 transmembrane and cytoplasmic domains, enhanced T cell activation, as measured by elevated IL-2 production.[141] Like the CD3γ, CD3δ, and CD4 intracellular domains, the proximal cytoplasmic tail of WC1 contains an [DE]XXXL[LIM] dileucine motif known to promote endocytosis by binding to the adaptor protein (AP-2) components of CCPs andCCVs.[141] Moreover, mutation of the same motif in the aforementioned fusion protein enhances IL-2 production upon co-ligation with the γδ TCR and significantly impairs endocytosis of the co-receptor. These findings suggest an important role for CME in regulating the co-receptor function of WC1 in γδ T cells.[142]

Endocytosis of the TCR

While endocytosis of the TCR in TCR αβ T cells is constitutive, its downmodulation in response to ligation by peptide:MHC complexes is an essential event in T cell activation. Non-engaged TCRs are constitutively internalized by CME into CCPs in a manner dependent upon dynamin.[125] In the absence of stimulation these non-engaged receptors are recycled back to the cell surface. Selective triggering of the TCR complex, however, has been shown to cause the concomitant downregulation of non-engaged TCRs in a manner regulated by protein kinase C θ (PKCθ). Phosphorylation of the CD3γ subunit at S126 by PKCθ[143] renders a downstream dileucine endocytosis motif more accessible to the adapter AP-2, thereby recruiting CME machinery.[125,143] Interestingly, bystander TCR downmodulation that occurs concomitantly with TCR ligation, however, uniquely require protein tyrosine kinase (PTK) activity.[125]

Endocytosis of engaged TCRs occurs by both CME and CIE.[129] Mechanosensory cues appear to play a role in dictating which endocytic mode predominates: TCR triggering with soluble anti-

CD3 antibodies promotes internalization by CME, whereas triggering by anti-CD3 immobilized on plastic promotes CIE of engaged TCRs.[125] The clathrin-dependent pathway requires dynamin and is similarly regulated by a CD3γ dileucine endocytosis motif. Endocytosis and signaling from engaged TCRs is tightly coupled, as it is for other signaling components of TCR microclusters, such as LAT, ZAP-70, and SLP-76. It has been shown in $CD4^+$ and $CD8^+$ human T cell lines that the Src family kinase Lck, a key component of the T cell signalosome, promotes CME of the TCR upon receptor engagement and lysosomal degradation.[126,144] It does so by inducible phosphorylation of tyrosine residues on the clathrin heavy chain (CHC) that interacts with the clathrin light chain to regulate triskelion assembly.[126] Basal Lck phosphorylation of the CHC also plays a role in constitutive endocytosis of the TCR, as unstimulated cells deficient in Lck exhibit no TCR internalization.[126] Fyn, another Src family kinase that regulates proximal TCR signaling, also promotes CME of the TCR, since human T cell lines deficient in CD45, and therefore unable to activate Lck or Fyn, exhibit less internalization than those deficient in Lck alone.[144,145]

An adaptor protein critical for the early-stage assembly of CCPs, the FCH domain only 1 (FCHO1) protein, plays a critical role in CME of engaged TCRs. First identified by whole exome sequencing in human patients with combined immunodeficiency, loss-of-function mutations in FCHO1 profoundly impair ligand-induced TCR clustering and endocytosis.[127,146] FCHO1 deletion in Jurkat T cells recapitulates this phenotype and can be rescued by expression of wild-type FCHO1.[127]

Also in Jurkat T cells, the cytoplasmic protein intersectin 2 has been shown to promote the translocation of Cdc42 and its effector Wiskott-Aldrich Syndrome protein (WASP) to CCVs.[147] Intersectin 2 also activates Cdc42 by the action of its Dbl homology (DH)/RhoGEF domain. Overexpression of intersectin 2 in these cells substantially increases TCR internalization whereas expression of an intersectin 2ΔDH construct markedly reduced it.[147] In this way, intersectin 2 may link the machinery of actin polymerization with that of CME.

The clathrin-independent pathway of TCR endocytosis also requires dynamin but uniquely utilizes the R-Ras subfamily GTPase TC21 (R-Ras2). TC21 promotes internalization by a mechanism reliant on the small GTPase RhoG, previously implicated in both phagocytosis and caveolar endocytosis.[134,148,149] However, global TCR down-modulation occurring in response to T cell activation is apparently achieved not by increasing the rate of internalization but by inhibition of TCR recycling and degradation of ligated complexes in the lysosome and proteasome.[150] Some evidence suggests that the basal TCR internalization rate is negatively regulated by intracellular TCRζ chain length.[151]

In activated Jurkat T cells, the actin-binding protein HIP-55, is recruited to the immunological synapse and has been shown to associate with early endosomes as well as dynamin.[152] Its expression in this system promotes TCR down-modulation, most likely by interfering with receptor recycling.[152]

Members of the EPS15 Homology Domain-containing (EHD) family of endocytic traffic regulators are known to be expressed in murine $CD4^+$ T cells and have been implicated in the

regulation of cell surface receptors. $CD4^+$ T cells from T cell-specific knockout EHD1/3/4 mice exhibit reduced proliferation and IL-2 secretion in response to antigen stimulation *in vitro*, as well as impaired TCR recycling, and enhanced lysosomal degradation of TCR components.[153] Support for a role for EHD proteins in these processes is indicated by their association with Rab effector proteins that regulate endocytic trafficking.[153]

Membrane-organizing flotillin proteins incorporate into pre-assembled signaling platforms that asymmetrically localize to one pole in hematopoietic cells, including T cells.[154] Immediately upon internalization, engaged TCRs are incorporated into a stable, mobile endocytic network defined by flotillins.[129] Consistent with the idea that flotillins may function as adaptors for other endocytic pathways, as opposed to demarcating a distinct, bona fide form of endocytosis, they are not required for internalization of engaged TCRs. Like EHD proteins, flotillins may regulate TCR surface expression by promoting endocytic recycling. Flotillins are required for the trafficking of downmodulated TCRs to Rab5-positive sorting endosomes, from Rab5- to Rab11a-positive recycling endosomes, and their recycling to the immunological synapse.[129,155] Additionally, flotillins are required for the formation of stable conjugates with antigen-presenting cells and interact with signaling phosphoproteins to facilitate TCR signaling.[129]

The CLIC-GEEC pathway of CIE has also been implicated in TCR endocytosis in activated Jurkat T cells. In this system, CD3 triggering resulted in TCRζ accumulation in tubular invaginations of the PM that are shaped by actin polymerization downstream of the Rho GTPase Cdc42.[128] The BAR domain-containing protein GRAF1 is recruited to these structures, where it promotes Cdc42 GTP hydrolysis via its GAP domain. These tubular invaginations mature into

endocytic vesicles that show co-localization of the internalized TCR with cholera toxin B (CTxB) and CD44, established cargoes of the CLIC-GEEC pathway.[128]

Arf6-mediated endocytosis in APC conjugate formation

The formation of stable conjugates between T cells and APCs requires Arf6-mediated endocytosis, in addition to flotillins. A number of cargo proteins important for T cell activation, such as MHC class I, CD4, and LFA-1, co-localize to Arf6-positive vesicles in Jurkat cells.[131] Expression of a constitutively-active form of Arf6 in these cells inhibits endocytosis of MHC class I, and causes other cargoes important for immunological synapse formation, such as CD4 and LFA-1, to accumulate in enlarged Arf6-positive vacuoles.[131] Consequently, conjugate formation with APCs is impaired. Both Arf6 and the small GTPase Rab22 have been implicated in stable conjugate formation and cell-spreading in Jurkat T cells.[131] In these cells, expression of a dominant-negative form of Rab22, Rab22S19N, is alone sufficient to impair MHC class I endocytosis and conjugate formation.[131]

Trogocytosis

Trogocytosis refers to the exchange of intact membrane patches between cells. While not, strictly-speaking, a form of endocytosis, *in vitro* studies have has suggested a mechanism with qualitative similarity to that of phagocytosis. An increasing body of evidence suggests not only that T cell trogocytosis is a ubiquitous phenomenon *in vivo*, but that it constitutes an important mechanism of intercellular communication and immune modulation.[156–159] Trogocytosis has even been shown to convey novel functional capabilities from one cell type to another through the acquisition of membrane-associated molecules.[156,160]

In Jurkat T cells, TCR-mediated trogocytic uptake of peptide:MHC complexes from antigen-presenting cells requires the previously described phagocytosis-associated GTPases R-Ras2 (TC21) and RhoG.[134,161] In $CD4^+$ TCR αβ T cells, trogocytic exchange of peptide:MHC complexes has been shown to influence T effector cell polarization.[158] When stimulated by murine fibroblasts and peptide-pulsed bone marrow-derived dendritic cells expressing peptide:MHC complexes, trogocytosis-positive $CD4^+$ T cells activated the transcription factor GATA-3 and produced IL-4 both *in vitro* and *in vivo*, consistent with Th2 polarization.[158] The mechanism responsible for this polarization remains to be elucidated, though it may relate to the strength and duration of TCR stimulation.

Even more remarkably, virus-specific $CD8^+$ cytotoxic T lymphocytes (CTLs) are capable of transferring their TCRs via trogocytosis to recipient CTLs of different clonotypic specificity.[162] Acquisition of donor TCRs confers the ability to recognize additional antigen and enables expansion of virus-specific clones independent of proliferation.[162]

Phagocytosis in TCR γδ T cells

Previously thought to be limited to cells of the myeloid lineage, it is now known that human peripheral γδ T cells not only have phagocytic capabilities but can act as "professional" phagocytes in that they are capable of presenting processed antigen on MHC class II to TCR αβ T cells.[132,133] Indeed, TCR γδ T cells can ingest entire bacteria, such as *L. monocytogenes* and *E. coli*.[132,133] Presumably the maturation of phagosomes in these cells resembles and depends on the

same machinery as other professional phagocytes (e.g., Rab5/7, RILP, etc.) though very little is currently known about this.

1.4 MACROPINOCYTOSIS

Pinocytosis ("cell drinking") refers to non-specific endocytosis of solute contents dissolved in the fluid phase into vesicles of any size.[163] Micropinocytosis, the ingestion of fluid-phase contents into vesicles <100 nm in diameter, is today an archaic term as it is now known to encompass a number of distinct endocytic pathways described previously in this document. All forms of fluid-phase endocytosis contribute to the regulation of cellular absorption of water, nutrients, and ions from the extracellular environment. For example, dynamin-dependent "pinocytosis" in microvilli of epithelial cells aids in the absorption of nutrients in the digestive tract.[164]

Macropinocytosis, however, refers to a distinct, evolutionarily-ancient, and non-selective form of endocytosis that generates double membrane-bound vesicles (macropinosomes) ranging in size from 200 nm to >5 μm in diameter.[165] In perhaps the earliest description of macropinocytosis, by Warren Lewis in the early 1930s, plasma membrane ruffling and the centripetal movement of ingested fluid contents was observed by light microscopy.[76,166] What was likely macropinocytosis was also observed early in the 20th century in social amoebae.[167] One in particular, the soil amoeba *Dictyostelium discoideum*, has become a primary organism for macropinocytosis research since the isolation of anexic laboratory strains in the late 1960s.[168–170]

Macropinosomes are dynamic vesicular organelles that form from stochastically-generated plasma membrane ruffles that project from the apical cell surface. Some of these protrusions meet and fuse with other, contraposed ones at their distal margins to generate a macropinosome. Other ruffles, created by rapid polymerization of branching actin filaments, collapse singularly back into the plasma membrane with the same effect: enclosure of a double membrane-bound vesicle. Membrane ruffles originating dorsally or peripherally produce concave, somewhat heterogenous, cup-like structures that close to form a macropinosome. Alternatively, larger circular dorsal ruffles (CDRs) form nested actin ring structures that are thought to generate macropinosomes upon centrifugal contraction, much like the "purse-string" mechanism of phagosome closure.[171]

Morphologically, the extension and folding of the plasma membrane form cup-like structures in macropinocytosis bears a closer resemblance to phagocytosis than any other form of endocytosis. CME, cavaeolae-mediated endocytosis, IL-2Rβ endocytosis, and other small-scale forms of endocytosis, by contrast, generate vesicles by invagination of and budding from the membrane following local concentration of pathway-specific cargoes.

As organelles, macropinosomes are still relatively uncharacterized. They share many features in common with the phagolysosomal and endolysosomal systems. In macrophages, macropinosomes acquire markers of early endosomes, then late endosomes, before fusing with the lysosome.[172]

Cell-specific adaptations of macropinocytosis

Macropinocytosis has never been observed in plants or fungi, presumably because their rigid cell walls preclude the ruffling and extension of membrane necessary to generate macropinosomes. It does occur, however, in a wide variety of vertebrate cells and has been adapted for cell-specific functions including, but not limited to, directed cell migration, morphogenesis, feeding, and immune surveillance in antigen-presenting cells.[165,173,174] The latter activity, where soluble antigens and sometimes whole pathogens are constantly ingested by macropinocytosis and processed for presentation by dendritic cells, macrophages, and others, is critical for both innate and adaptive immunity. The rate and scale of macropinocytic fluid uptake in macrophages is impressive: M-CSF-stimulated macrophages can ingest 25% of their cell volume in 5 minutes.[175]

Like other endocytic pathways, macropinocytosis regulates composition of the plasma membrane, and therefore signaling, through internalization of membrane-embedded molecules and the regulated trafficking of endocytic vesicles. The rate and scale of membrane internalization during macropinocytosis necessitates a retrieval system that salvages and selectively recycles surface proteins before they are lysosomally-degraded, which in *Dictyostelium* is accomplished by the concerted action of the Retromer sorting complex and WASP and SCAR homologue (WASH).[176] It's likely this system or a comparable one has been conserved in mammals as WASH has a homolog in mammalian cells.

In *Dictyostelium* and related amoebae, macropinocytosis facilitates feeding and nutrient acquisition alongside phagocytosis.[177] As will be detailed below, it has been discovered recently that mammalian cells can also utilize macropinocytosis for nutrient uptake and its occurrence

under both normophysiologic and pathological conditions is of central interest to this investigation.

1.5 MACROPINOCYTOSIS AND PATHOPHYSIOLOGY

Macropinocytosis has been implicated in a number of disease states, including atherosclerosis, neurodegenerative diseases, viral infection, and cancers. Macropinocytosis of native, oxidized or aggregated LDL cholesterol mediates the conversion of monocyte-derived macrophages into foam cells, which can accumulate to form plaques and atheromas in the tunica intima of blood vessels.[178] Macropinocytosis of exogenous PRP^{Sc}, the pathological prion protein conformation implicated in transmissable spongiform encephalopathies, enables cell-to-cell spreading of misfolded prion protein.[179] There is also considerable evidence that inclusion bodies (protein aggregates) in the brain themselves can stimulate plasma membrane ruffling of neurons, triggering their macropinocytic uptake and spread.[180–182] Also in the brain, hyperstimulation of neuronal macropinocytosis by methamphetamine is associated with impaired lysosomal function and neurotoxicity.[183]

Exploitation by viruses

Many viruses have evolved to exploit endocytic machinery to facilitate infection and macropinocytosis is no exception. In fact, its relative non-selectivity makes it an especially vulnerable route of entry for a range of pathogens, including a wide variety of both enveloped and non-enveloped, DNA and RNA viruses. Vaccinia virus, respiratory syncytial virus, coxsackievirus B, African swine fever virus, herpes simplex virus 1 (HSV-1), echovirus 1, human immunodeficiency virus 1 (HIV-1), murine amphotropic retrovirus (A-MLV), influenza

A, and adenovirus 3 are among those known to productively infect cells by macropinocytosis.[184–188] Others, such as rubella and adenovirus 2/5, enter cells by other endocytic mechanisms but appear to require macropinocytosis to enable cytoplasmic penetration.[186]

Some viruses that induce or opportunistically exploit macropinocytosis to promote infection, such as β-coronaviruses, require trafficking to lysosomes to promote viral egress.[189] In HeLa-mcc1a and Vero E6 cells, these viruses deacidify lysosomes (and thereby inactivate resident lysosomal proteases) by an unknown mechanism before inducing lysosomal exocytosis in a manner dependent upon the small GTPase Arl8b, a known regulator of lysosomal trafficking.[189,190]

Cancer

Macropinocytosis and cancer have been linked since the former's discovery: Lewis's initial description of what we now know as macropinocytosis was in, among other cell types, rat and mouse sarcomas. The recent discovery that certain tumor cells can use macropinocytosis to scavenge nutrients has stimulated interest in the process in the cancer biology community, with the hope that a better understanding of it may inform therapeutic development.

The rapid growth and proliferation of cancer cells requires, among other things, the continuous supply of nutrients which are quickly depleted from inhospitable tumor microenvironments. Oncogenic mutations in some signaling proteins, such as isoforms of the GTPase Ras, stimulates macropinocytosis and enables tumor cells to grow under conditions of nutrient scarcity.

Similarly, expression of the oncogenic v-Src protein, a gene found in Rous sarcoma virus, is sufficient to stimulate constitutive macropinocytosis in fibroblasts.[191]

In a landmark paper, Commisso et al. described macropinocytosis of extracellular protein in tumor cells driven by oncogenic K-Ras under conditions of amino acid starvation.[192] In these cells, macropinocytosed extracellular protein is trafficked to lysosomes where it is degraded to amino acids that subsequently enter central carbon metabolism. In K-Ras-driven pancreatic ductal adenocarcinoma (PDAC) cells that exhibit this behavior when deprived of glutamine, macropinocytosis of extracellular protein depends on EGFR-Pak signaling.[193] More recently, PTEN-deficient prostate cancer cells under conditions of nutrient deficiency (and AMPK activation) have been similarly shown to macropinocytose protein and necrotic cell debris, which are then degraded to yield amino acids for growth.[194]

Indeed, the adaptation of macropinocytosis for scavenging and feeding may be a pervasive phenomenon in many cancers; in addition to those previously mentioned it has been observed in colorectal, lung, ovarian, hepatocellular and bladder urothelial carcinomas, osteosarcoma, glio- and medulloblastomas, and other tumor types.[195] A study of senescent U2OS (human osteosarcoma) and Hs68 (human foreskin fibroblast) cells found that the lymphocyte antigen 6 complex, locus D (LY6D), an extracellular protein attached to the plasma membrane by a GPI-anchor, was required for macropinocytic uptake of extracellular protein and growth.[196]

As the breadth of macropinocytosis research expands to include the study of additional cell types and tissues there will doubtless be additional roles identified for macropinocytosis in the shaping of health and disease.

1.6 MOLECULAR MECHANISM OF MACROPINOCYTOSIS

The formation of macropinocytic cups and their closure to form macropinosomes depends on the complex and incompletely understood interaction of phosphoinositides, kinases, GTPases, and cytoskeletal proteins, which cooperate over time and space to produce a global increase in actin excitability and polymerization at the cell surface. Signaling in macropinocytosis is through pathways associated with growth factor receptors, Fc receptors, and chemoattractant receptors that converge on activation of class I phosphatidylinositol 3-kinases (PI3K), which link the plasma membrane and the cytoskeleton.

The Ras family of small GTPases play a central role in canonical descriptions of macropinocytosis. In general, Ras GTPases transduce signals from activated growth factor receptors to class I PI3Ks. Anexic strains of *Dictyostelium* that have evolved the ability to grow in liquid media show dramatically elevated rates of macropinocytosis due to a deletion of neurofibromin 1 (NF1), a Ras GTPase-activating protein (GAP) that spatially regulates Ras inactivation in forming macropinosomes, underlining the importance of Ras signaling in the process.[197] In fibroblasts, expression or injection of constitutively active (oncogenic) Ras is sufficient to cause membrane ruffling and macropinocytosis to occur.[198] In macrophages and *Dictyostelium*, active Ras is enriched and spatially coordinated during the formation of macropinocytic cups alongside PIP_3 and active Rac1.[199–201] Also in *Dictyostelium*, the

multidomain protein RCC1, RhoGEF, BAR, and RasGAP-containing protein (RGBARG) coordinates macropinocytic cup formation by promoting activation of Rac1 at the protruding edge and suppressing Ras activation in the cup interior.[202] Also in *Dictyostelium*, the IQGAP-related protein IqgC associates with macropinosomes and negatively regulates their size by exerting GAP activity toward the Ras isoform RasG.[203]

Humans have at least three Ras genes (H-, K-, and N-Ras), though transcripts from these genes undergo extensive alternative splicing to yield splice variants with distinct structural properties. Translated Ras proteins are also extensively post-translationally modified.[204] Like other GTPases, Ras proteins exhibit switch-like behavior, cycling between two conformations: an inactive, GDP-bound state and an active, GTP-bound state in which numerous effector proteins (e.g., TIAM1, RAF1, RASSF, etc.) can be bound to regulate signaling through multiple pathways.[205] Most of the post-translational modifications of Ras proteins, including prenylation, carboxyl methylation, and palmitoylation, are confined to the C-terminus.[205] The most important of these is farnesylation of a C-terminal CAAX sequence, where C is cysteine, A is usually an aliphatic amino acid, and X is any amino acid.[205] Farnesylation of this motif enables tethering of Ras GTPases to the inner leaflet of the plasma membrane where Ras GEFs and GAPs can activate or deactivate them by promoting, respectively, GDP dissociation or GTP hydrolysis. Restriction to the 2D plane of the inner membrane represents an effective increase in the binding constant between these proteins of five orders of magnitude compared to that of the proteins in free solution.[206]

Ras can be downregulated from the membrane by K63 ubiquitination, which promotes its internalization on endosomes.[207] Components of the ESCRT-III complex regulate the fate of Ras-laden endosomes, which can be stored, destroyed, or recycled back to the plasma membrane.[208]

Ras plasma membrane localization is critical for its signaling functions. Given that fact and the prevalence of Ras mutations in a wide variety of tumors (estimated to be 33%), there has been extensive development and investigation of the therapeutic potential of inhibitors of Ras farnesylation and membrane recruitment.[209] Farnesyl thiosalicylic acid (FTS, salirasib) and similar farnesylcysteine mimetics inhibit H-, N-, and K-Ras by competing with Ras for binding Ras-escort proteins that mediate membrane association.[210,211]

Ras may promote PI3K activation in macropinocytosis by multiple mechanisms. Different Ras isoforms may activate specific PI3K isoforms with distinct functional capabilities. Class IA PI3Ks consist of a p85 regulatory subunit and a p110 catalytic subunit (p110α, p110δ or p110γ).[212] They also possess an N-terminal Ras-binding domain (RBD) and each of the class IA catalytic subunits are also Ras effectors.[213] PI3Ks are also activated by ligand-induced dimerization and autophosphorylation of receptor tyrosine kinases (RTKs). Phosphotyrosine motifs on dimerized receptors recruit the adaptor protein GRB2, which activates the Ras GEF son of sevenless 1 (SOS1).[214] SOS1 promotes GTP-loading and activation of Ras, which in turn activates class IA PI3K catalytic subunits.[215]

Class I PI3Ks converts membranous phosphatidylinositol (4,5)-bisphosphate ($PI(4,5)P_2$) to phosphatidylinositol (3,4,5)-trisphosphate (PIP_3), which accumulates at the base of macropinocytic cups and localizes signaling cascades there. The generation of PIP_3 in macropinocytic cups is a universal hallmark of macropinocytosis that has been noted in a wide variety of cell types. Plasma membrane enrichment of PIP_3 in turn recruits proteins with PIP_3 binding domains, including PLCγ1, PDK1, Akt (protein kinase B), and GEFs that locally activate Rho-family GTPases such as Rac1, RhoG and Cdc42.[216]

GTP-loading of Rho-family GTPases by their respective GEFs results in the recruitment of effector proteins that promote membrane ruffling and coordinate cup formation and closure. RhoG and its GEF Trio modulate the size of CDRs via unknown downstream effectors.[217] The Rac1 effector p21-activated kinase 1 (Pak1) has been shown by itself to promote dramatic actin remodeling and generation of lamellipodia in some cell types.[218] Additionally, Pak1 and the C-terminal-binding protein-1/brefeldinA-ADP ribosylated substrate (CtBP1/BARS) have both been implicated cup closure. CtBP1/BARS appears to be the direct mediator of cup closure but is regulated by phosphorylation on serine 147 by Pak1, which licenses vesicle scission, at least in epidermoid carcinoma cell lines performing EGF-stimulated macropinocytosis.[219] Recently another molecular player involved in cup closure has been identified: Rab5a, which promotes sealing and scission of macropinosomes by recruitment of inositol 5-phosphatases that eliminate membranous $PI(4,5)P_2$.[220] Other critical downstream effectors of Rho GTPases are WASP family verprolin homologous (WAVE) proteins, which bind phosphatidylinositol phosphates, stabilize lamellipodial extensions, and activate Arp2/3, a nucleator of branched actin filaments.[221]

Hydrolysis of PI(4,5)P2 by PLCγ1 produces the second messengers inositol 1,4,5-trisphosphate (IP_3) and diacylglycerol (DAG). DAG in turn activates protein kinase C (PKC) which indirectly promotes cup closure. In M-CSF-stimulated macrophages, administration of DAG analogs like phorbol 12-myristate 13-acetate (PMA) alleviates PI3K dependence and promotes downstream Ras and PKC activation. Additional evidence from macrophages suggests that PKCδ is the predominant isoform of PKC directing cup closure.[222] Other molecules implicated in macropinocytic signaling include, Arf6, phospholipase D, and DAG kinase.[216,223–225]

A great deal of macropinocytosis research has focused on the actin cytoskeleton while there has been comparatively little focus on the role intermediate filaments and microtubules play in the process. Recently it was shown in HT1080 (fibroscarcoma) cells that Arf6, a GTPase active in multiple CIE pathways, cooperates with dynein and the microtubule motor scaffold protein JIP3 to promote the centripetal movement of macropinosomes on microtubules.[224] Similarly, the kinase PIKfyve and the calcium channel TRPML1 (mucolipin) associate with and mediate shrinkage of macropinosomes as they mature.[226] How exactly they do this is poorly understood but TRPML1 also regulates interactions between lysosomes and dynein, the retrograde (minus-end-directed) microtubule motor protein. SEPT2, a member of the septin family of GTP-binding proteins, mediates macropinosome maturation and lysosomal fusion in canine epithelial cells (MDCKs).[227]

Macropinocytic signaling in cancers

Recently an unbiased screen designed to detect changes in the PDAC cell surface protein repertoire induced by K-Ras identified a syndecan, syndecan-1, as a critical regulator of

macropinocytosis in these cells.[228] Syndecans are co-receptors for GPCRs but have also been shown to regulate the activity of small Rho-family GTPases, such as Rac1, RhoA, and RhoG, which may explain their reported influence on macropinocytosis.[228,229] Also in oncogenic Ras-driven tumor cell lines, Ras activation of protein kinase A (PKA) promotes the translocation of the vacuolar-ATPase (V-ATPase) to the plasma membrane.[230] In these cells, accumulation of V-ATPase is required for macropinocytosis because it promotes the cholesterol-dependent membrane targeting of Rac1. Wnt signaling has also been shown to promote macropinocytosis in cell lines: expression of Wnt3a, the canonical activator of the Wnt signaling pathway, alone induces macropinocytic uptake of extracellular protein and its digestion in lysosomes.[231]

These findings may be restricted tumor cells and only reflect the aberrant behaviors of tumor cells. The potential influence of Wnt signaling on macropinocytosis in non-transformed cells in particular has been little explored. It remains to be seen whether these studies will inform our understanding of normophysiologic macropinocytosis.

Similarities and differences with other CIE pathways

As nearly all forms of CIE require mobilization of the actin cytoskeleton there is, perhaps unsurprisingly, considerable overlap in their signaling and effector requirements. The molecular mechanism of macropinocytosis bears the most obvious similarity to that of phagocytosis. The study of Fc receptor-mediated phagocytosis has yielded the most insight into phagocytic signaling, and it has revealed a similar convergence on PI3K, Rho GTPases and their effectors, and PKC.[232] Similarly, IL-2Rβ endocytosis also depends crucially on PI3K signaling and the recruitment of actin-remodeling effectors like Pak1, WAVE, and Arp2/3.[233] Apart from

macropinocytosis, a significant proportion of fluid-phase uptake in cells occurs by CLIC-GEEC endocytosis which, as previously mentioned, depends critically on the Rho GTPase Cdc42.[33]

Selective inhibition by EIPA and J/B

Despite this shared signaling and actin-remodeling machinery—which underlines the difficulty of selectively targeting CIE pathways—macropinocytosis is uniquely inhibited by amilorides, pyrazine derivatives that inhibit plasma membrane Na^+/H^+ exchangers (NHEs).[72,234] These channels are antiporters that extrude cytoplasmic protons (H^+) in exchange for extracellular Na^+. The mechanism that connects ion exchange to macropinosome formation is poorly understood but involves the regulation of submembranous pH. NHE blockade, and in particular selective inhibition of NHE-1 by the amiloride derivative 5-(*N*-Ethyl-*N*-isopropyl) amiloride (EIPA), promotes submembranous acidification that dramatically impairs the activity of Rac1 and Cdc42.[235] The current consensus is that this inhibitory influence on actin-remodeling Rho GTPases is how amilorides selectively inhibit macropinocytosis.

More recently, a combination of the actin-depolymerization inhibitor jasplakinolide and the myosin II inhibitor blebbistatin (J/B) have also been shown to be selective inhibitors of macropinocytosis in macrophages.[236,237]

1.7 SCOPE OF THESIS

The utilization of macropinocytosis for feeding in transformed metazoan cells may be seen as something of an atavistic trait—a reversion to the behaviors of unicellular eukaryotes like *Dictyostelium*—but conceivably also dismissed as an aberration of cancer cells. The principle

motivation of this research project, which arose in discussions between Joel Swanson, Phil King, and myself in 2016, was to investigate the possibility that non-transformed cells with high proliferative capacity, namely activated T cells, perform macropinocytosis and, if so, under what conditions and for what purpose.

Chapter II describes results from *in vitro* and *in vivo* experiments demonstrating the capacity of primary murine and human T cells to internalize high molecular weight macropinocytosis probes under various conditions, and the enhancement of this uptake upon stimulation. Experiments employing scanning electron microscopy and confocal microscopy highlight similarities between plasma membrane features in T cells and macropinocytosing macrophages. The temperature dependency and sensitivity of probe uptake to abolition by EIPA is also shown by flow cytometry and confocal microscopy.

In Chapter III I explore the signaling requirements of T cell macropinocytosis. In addition to demonstrating the abolition of probe uptake using established selective inhibitors of macropinocytosis (EIPA and the combination of jasplakinolide and blebbistatin), I show that inhibition of PI3K, Rac1, or Pak1 also inhibits T cell macropinocytosis, but to a lesser extent. In contradistinction to canonical macropinocytosis signaling in other cell types such as macrophages, T cell macropinocytosis exhibits Ras-independence, as confirmed by experiments testing probe uptake in Rasgrp1 knockout mice and in the presence of a Ras inhibitor.

Chapter IV examines the relationship between macropinocytosis and growth in nascently-activated T cells under nutrient-replete conditions. After identifying the period following

stimulation and activation corresponding to G1 phase, I show how inhibition of macropinocytosis during this period is accompanied by a proportional reduction in growth and that this relationship is approximately linear.

How macropinocytosis regulates activated T cell growth is the subject of Chapter V. Given that macropinocytic cargoes are frequently targeted to lysosomes in other cell types and the observed relationship between macropinocytosis and growth, it was reasonable to suspect involvement of the mechanistic target of rapamycin complex 1 (mTORC1). I confirmed lysosomal targeting of macropinocytosed contents by flow cytometry and confocal microscopy. Next, I examined mTORC1 signaling kinetics in stimulated T cells through G1 phase and confirmed its continuous, sustained activation. I then show evidence that mTORC1 activation in this period is abolished in a dose-dependent manner by inhibition of macropinocytosis and that inactivation is consistently more pronounced than that achieved with the selective mTORC1 inhibitor Torin 1. I also show that abrogation of mTORC1 signaling by inhibition of macropinocytosis does not impair activation-induced ERK (MAPK) and NFκB signaling. Additional experiments show that inhibition of lysosomal proteolysis in this context does not impair mTORC1 activation, suggesting that macropinocytosis of free amino acids sustains signaling. Lastly, I share results demonstrating that minimal medium containing four particular amino acids is sufficient to sustain G1 phase mTORC1 activation, and emphasize the special importance of two of them (leucine and glutamine). The chapter concludes by discussing a proposed model of mTORC1 activation in stimulated T cells.

Chapter VI summarizes the thesis and discusses additional findings related to the extent of

macropinocytosis in thymocytes and other T cell subsets. I discuss the probability that macropinocytosis facilitates growth in other primary mammalian cell types and suggest some lines of inquiry to be explored further by future researchers.

CHAPTER II:

MACROPINOCYTOSIS IN T CELLS[1]

2.1 ABSTRACT

To test whether T cells engage in macropinocytosis, flow cytometry uptake assays were performed using high molecular weight, flurochrome-congjuated macropinocytosis probes. Primary $CD4^+$ and $CD8^+$ murine T cells incubated *in vitro* at 37°C were found to constitutively ingest two macropinocytosis probes: 70 kDa fluorescein-dextran (Fdex) and 67 kDa Alexa 488-bovine serum albumin (BSA). Stimulation with anti-CD3 and anti-CD28 antibodies for 24 (Fdex) or 20 (BSA) hours prior to probe incubation in the final 8 (Fdex) or 4 (BSA) hours resulted in a 3-4 fold increase in probe uptake compared to unstimulated cells. In stimulated cells, probe internalization was coincident with an increase in cell size. Uptake was due to a temperature-dependent process, occurring at the permissive temperature of 37°C but abrogated by incubation at 4°C. Confocal microscopy confirmed temperature-dependent probe uptake into putative macropinosomes. Adoptive transfer of OT-II TCR Tg T cells into recipient mice followed by immunization with whole ova protein permitted the demonstration of BSA probe uptake *in vivo*. Constitutive and stimulated uptake was also tested and confirmed *in vitro* in primary human cells; $CD4^+$ and $CD8^+$ T cells stimulated with either anti-CD3/CD28 mAbs or the

[1] The contents of this chapter were adapted and reproduced from the following publication: Charpentier, J. C. *et al.* Macropinocytosis drives T cell growth by sustaining the activation of mTORC1. *Nat Commun* **11**, 180 (2020).

T cell mitogen phytohemagglutinin recapitulated enhanced probe uptake relative to constitutive internalization in unstimulated cells. Scanning electron microscopy of murine $CD4^+$ and $CD8^+$ T cells resolved morphological features of the plasma membrane consistent with macropinocytosis in macrophages—namely macropinocytic cups in various stages of evolution. Confocal microscopy of murine $CD4^+$ T cells stimulated for 16 hours with anti-CD3 and anti-CD28 antibodies, then stained with phalloidin revealed polymerized actin loops directed 1-2 um from the cell surface. Most importantly, probe uptake was significantly inhibited by addition of 5-(N-Ethyl-N-isopropyl) amiloride (EIPA), a selective inhibitor of macropinocytosis that blocks plasmalemmal Na^+/H^+ exchangers (NHEs), prior to probe incubation. EIPA inhibition of probe ingestion was confirmed by flow cytometry and confocal microscopy. Similarly, incubation with a combination of the actin-depolymerization inhibitor jasplakinolide and the myosin II inhibitor blebbistatin (J/B), which together selectively inhibit macropinocytosis in macrophages, also blocked probe uptake as assayed by flow cytometry. Both EIPA and J/B inhibited probe uptake in a dose-dependent manner but probe internalization was not inhibited by incubation with a selective inhibitor of clathrin-mediated endocytosis, PitStop 2. Inhibition by EIPA and J/B was also confirmed in primary human cells. Taken together, these findings suggest that both murine and human primary $CD4^+$ and $CD8^+$ T cells constitutively perform macropinocytosis and upregulate it 3-4 fold upon stimulation and cell activation.

2.2 INTRODUCTION

Compared to CME, which uses unique protein machinery to transport pathway-specific cargoes, distinct CIE pathways share machinery and can transport identical cargoes, making their study considerably more challenging. Macropinocytosis, for example, requires the activity of Rab and Rho-family GTPases and their effectors, but so do IL-2Rβ endocytosis, phagocytosis, CLIC/GEEC endocytosis, and a host of other unrelated cellular processes. As a result, ablation or deletion of the genes encoding proteins that cooperate to perform these modes of endocytosis nearly always compromises the activity of multiple pathways and/or impairs other critical cell functions. In other words, most of the genetic targets that have been evaluated are highly pleiotropic.

One way to overcome the difficulty of studying macropinocytosis in isolation is to use high molecular weight (>10 kDa) probes. As macropinocytosis is a non-selective mode of endocytosis the selectivity of probe uptake occurs by virtue of its size in solution (i.e. by size exclusion from alternative routes of entry). While high molecular weight probes cannot be assumed to be internalized exclusively by any one mode of endocytosis, it's reasonable to assume that the larger their size, the stronger will be their bias for macropinocytic uptake.

One widely used high molecular weight macropinocytosis probe is 70 kDa fluorescein-dextran (70 kDa Fdex). Dextrans are highly soluble, elastic, non-immunogenic polysaccharides of α-linked D-glucopyranose monomers widely used in research, food, cosmetics, and medicine (especially as blood plasma volume expanders).[238–241] They are generally recognized as safe (GRAS) by the U.S. Food and Drugs Agency (FDA) and their long use in many industries attests

to their safety and biocompatibility. Studies in mammalian cells have demonstrated that whereas 10 kDa dextran is internalized by both CME and macropinocytosis, 70 kDa dextran enters cells predominantly through macropinocytosis.[242]

Another macropinocytosis probe of comparable size is bovine serum albumin (BSA). Its unconjugated molecular weight is 66.5 kDa, which the addition of a fluorophore (such as Alexa 488) increases by <1 kDa. BSA is an endogenous bovine blood protein made in the liver. It is the most abundant protein found in plasma and has multiple important functions including maintaining plasma colloid oncotic pressure and serving as a carrier for hydrophobic molecules.[243] The advantage of using fluorophore-conjugated BSA over dextrans in macropinocytosis studies is that, as proteins, they are fixable by formaldehyde, which permits fluorescence microscopy.

We endeavored to first test the capacity of unstimulated and nascently-stimulated primary murine and human $CD4^+$ and $CD8^+$ T cells to macropinocytose 70 kDa Fdex and Alexa-488 BSA *in vitro*. We developed a standard uptake assay (detailed in Materials and methods below) with a focus on the period 12-24 hours post-stimulation since this corresponds with rapid G1 phase growth in activated T cells. Macropinocytosis being an energy-dependent process, we included negative controls incubated with macropinocytosis probes at 4°C in all experiments. Uptake of both 70 kDa Fdex and Alexa 488-BSA probes was measured by multi-parameter flow cytometry.

Next we planned to assay BSA probe uptake into intracellular vesicles by confocal microscopy. To compare findings between murine and human cells, we performed identical uptake assays in primary human T cells. To test the capacity of primary murine T cells to macropinocytose the BSA probe *in vivo*, we performed adoptive transfer experiments using OT II ($CD4^+$) Tg TCR T cells stimulated with cognate peptide-MHC ligand (OVA).

Unstimulated and CD3/28-stimulated murine T cells were also examined by scanning electron microscopy to identify features of the plasma membrane, such as CDRs and cups, consistent with macropinocytosis. Additionally, to visualize the distribution of filamentous actin in T cell membranes, we used phalloidin, a cyclic F-actin-binding peptide isolated from the fungus *Amanita phalloides*, in confocal microscopy imaging assays.

Lastly, as previously discussed in **Chapter 1.6**, the best tools currently available for assessing macropinocytosis are the selective inhibitors EIPA and J/B. If probe internalization were due to macropinocytosis, we would expect it to be significantly inhibited if not abolished by treatment with EIPA or J/B. Sensitivity of probe uptake by EIPA and J/B treatment was assessed in both murine and human T cells (stimulated by various means) by flow cytometry and confocal microscopy.

2.3 MATERIALS AND METHODS

Animals. Wild-type mice were bred in house and were on a mixed 129S6/SvEv X C57BL/6 genetic background. One exception was recipient mice in *in vivo* experiments that were on a CD45.1 C57BL/6 background (JAX). OTII TCR Tg mice (JAX) were on a C57BL/6 genetic

background. Mice ranged in age from 6 weeks to 3 months. Mice of both sexes were used in experiments. All experiments performed with mice were in compliance with University of Michigan guidelines and were approved by the University Committee on the Use and Care of Animals.

T cell macropinocytosis assays. Murine splenocytes from wild-type or pan-T cells, purified from splenocytes of wild-type mice by column depletion (Miltenyi Biotec), were resuspended in RPMI 1640 medium (Thermo Fisher) supplemented with 10% heat-inactivated FCS (Gibco). Splenocytes were seeded into U-bottomed 96-well plates at a density of 1×10^6 cells per well and were stimulated or not with anti-CD3 (1μg/ml; eBioscience, clone 145–2C11) and anti-CD28 (1μg/ml; eBioscience, clone 37.51) mAb for the indicated times. Pan-T cells were seeded at a density of 1×10^6 cells per well into the wells of flat-bottomed 96-well plates pre-coated with anti-CD3 mAb (10μg/ml) and soluble CD28 mAb (1μg/ml) was added to wells. 70 kDa Fdex or Alexa 488-BSA macropinocytosis probes were added to wells at final concentrations of 1 mg/ml, 0.4 mg/ml, respectively, at the indicated times. Incubation with probes was for the indicated times at 37°C or 4°C. Pharmacological inhibitors were added to cultures 15 min prior to addition of macropinocytosis probes in a range of concentrations as indicated or at the following final concentrations: EIPA (Sigma), 50μM; jasplakinolide (Tocris), 1μM; (S)-(-)-blebbistatin (Tocris), 75μM; PitStop 2 (Sigma). Cells were harvested, washed, stained with APC-Cy7-CD4 (BD Pharmingen, clone GK1.5,cat. no. 552051, dilution 1:100) and APC-CD8α (BD Pharmingen, clone 53-6.7, cat. no. 553035, dilution 1:100) mAb and analyzed by flow cytometry on BD Fortessa or BD FACSCanto instruments (BD Biosciences). Gating strategies are illustrated in the Appendix. Percentage macropinocytosis in the presence of inhibitors was

calculated as follows: [(MFI in presence of inhibitor at 37°C - MFI in absence of inhibitor at 4°C)/(MFI in absence of inhibitor at 37°C - MFI in absence of inhibitor at4 °C)] × 100.

To assess human T cell macropinocytosis, human peripheral blood mononuclear cells (PBMC) were isolated from buffy coats obtained from the New York Blood Center and resuspended in RPMI 1640 with 10% FCS. PBMC were seeded into 96 well U-bottomed plates at a density of 5 × 10^5 cells per well and were stimulated or not with anti-CD3 (1μg/ml; Invitrogen, clone OKT3) and anti-CD28 (1μg/ml; Invitrogen, clone CD28.2) mAb or PHA (1.5% final; Thermo Fisher) for 20 h. Cells were incubated with BSA-Alexa 488 at 0.4 mg/ml for the last 8 hours of culture. EIPA and J/B were added to cultures 15 min prior to addition of probe at the above concentrations. Cells were harvested, stained with APC-Cy7-CD4 (Biolegend, cloneRPA-T4, cat. no. 300518, dilution 1:100) or PerCP-Cy5-5-A-CD4 (Biolegend, cloneOKT4, cat. no. 317428, dilution 1:100) and Alexa 700-CD8α (Biolegend, clone SK1, cat. no. 344724, dilution 1:100) or BV-605-CD8 (Biolegend, clone RPA-T8,cat. no. 301040, dilution 1:20) mAb and analyzed by flow cytometry. The gating strategy is illustrated in the Appendix.

Confocal microscopy. Murine splenic pan-T cells or $CD4^+$ T cells (isolated by column depletion) were stimulated with CD3 and CD28 mAb for 12 h as above before incubation in the presence or absence of BSA-Alexa 488 (0.4 mg/ml) at 37°C or 4°C in the presence or absence of EIPA (50 μM) for a further 4 or 8 h. Cells were harvested, washed, resuspended in PBS and sedimented for 1 h on ice at 1 g onto coverslips previously coated with 0.1% poly-L-lysine (Sigma). Cells were fixed *in situ* by addition of an equal volume of 4% paraformaldehyde and incubation for 30 min at room temperature. Coverslips were then washed and cells were stained

with rat anti-mouse CD4 (R&D Systems, clone GK1.5) or CD8α (R&D Systems, clone 53-6.7), mAb overnight at 4°C. The following day, coverslips were washed, blocked with 5% donkey serum for 1 h, incubated with Alexa 488- or Alexa 594-labeled donkey anti-rat secondary antibody (Thermo Fisher, cat. nos. A-21208 and A-21209, dilution 1:200), and stained with 10 μg/ml Hoechst 33258 (Thermo Fisher). For imaging of polymerized filamentous actin, cells were permeabilized with Triton X-100 and stained with Actistain-488 fluorescent phalloidin (0.1 μM; Cytoskeleton, Inc.) prior to the antibody staining steps. Coverslips were mounted in ProLong Gold Anti-Fade (Thermo Fisher) and images were captured on a Leica upright SP5 confocal microscope (Leica). Data showing the percentage of T cells with indicated numbers of macropinosomes are based upon counts of >150 cells.

Scanning electron microscopy. Murine BM-derived macrophages were prepared as described.[244] After 6 days culture, macrophages were stimulated for 15 minutes with CSF1. Murine $CD4^+$ T cells were stimulated for 16 hours with CD3/28 mAb and prepared as indicated in confocal microscopy. Macrophages and T cells were fixed for 1 hour at room temperature with 2% glutaraldehyde in 0.1 M cacodylate buffer, pH 7.4, containing 6.8% sucrose. After rinsing the coverslips in buffer they were next post-fixed for 1 hour at 4°C in 0.1 M cacodylate buffer containing 1% osmium tetroxide, incubated for 30 minutes in 1% tannic acid in distilled water, and then treated with 1% osmium tetraoxide for 30 minutes at 4°C. Fixed coverslips were then dehydrated in an acetone series followed by hexamethyldisalizane. The coverslips were then air-dried, coated with gold particles using an ion-coater, and imaged on an Amray 1900 field emission scanning electron microscope.

Macropinocytosis *in vivo*. One million TCR Vβ5$^+$CD4$^+$T cells from CD45.2OTII TCR Tg mice were injected into the tail veins of CD45.1 wild-type recipients. After 24 hours, recipient mice were immunized i.d. in footpads with Ova (0.5 mg/ml) in RIBI adjuvant (Sigma) or with RIBI adjuvant alone (25µl per footpad). Twelve hours later, all mice were injected i.d. in footpads with BSA-Alexa 647 (5 mg/ml in 25µl of PBS per footpad; Thermo Fisher) and mice were euthanized after an additional 8 hours. Draining popliteal lymph nodes were harvested from mice, stained with PerCP-Cy5-5-A-CD45.2 (BioLegend, clone 104, cat. no. 109828, dilution1:200), Alexa Fluor 700A-CD45.1 (BioLegend, clone A20, cat. no. 110724, dilution1:200), V500-CD4 (BD BioSciences, clone RM4-5, cat. no. 560782, dilution 1:400), APC-Cy7- CD8α (Invitrogen, clone 53-6.7, cat. no. A15386, dilution 1:100), and PE-TCR V-β5 (BD Pharmingen, clone MR9-4, cat. no. 553190, dilution 1:200) mAb, and analyzed by flow cytometry to assess BSA-Alexa 647 uptake by OTII TCR Tg T cells. The gating strategy is illustrated in the Appendix.

2.4 RESULTS

Murine T cell internalization of macropinocytosis probes *in vitro*

To determine if murine T cells perform macropinocytosis, we tested the ability of primary, splenic pan-T cells to endocytose a widely-used macropinocytosis probe, high molecular weight, fluorochrome-labeled dextran (70 kDa fluorescein dextran, Fdex). The large size of this probe generally precludes its uptake via other, small-scale forms of endocytosis, such as clathrin-mediated endocytosis, making it a reliable marker of macropinocytosis. Splenic T cells were either stimulated for 24 hours *in vitro* with monoclonal antibodies (mAbs) against the CD3 component of the T cell receptor complex and the CD28 co-receptor, or were left unstimulated.

For hours 20-24 post-stimulation, cells were incubated with 1 mg/mL 70 kDa Fdex at 37°C or at 4°C. After 24 hours, the cells were washed and stained with anti-CD4 and anti-CD8 antibodies prior to live analysis by flow cytometry.

As **Figure 2** shows, both $CD4^+$ and $CD8^+$ murine T cells readily endocytosed the macropinocytosis probe at 37°C, as determined by acquisition of cell fluorescence. Probe uptake was observed in both unstimulated and stimulated $CD4^+$ (**a-b**) and $CD8^+$ (**c-d**) T cells, with the extent of probe internalization significantly increased in stimulated cells coincident with an increase in cell size as measured by forward scatter area (FSC-A, also called forward angle light scatter area). FSC-A is a flow cytometry parameter that approximates cell size (cross-sectional area) by measuring incident light scatter in cells with the same refractive index. Uptake of the Fdex probe was enhanced by 3-4 fold in stimulated vs. unstimulated cells (**e**). By contrast, stimulated cells chilled to 4°C prior to probe incubation for hours 20-24 did not substantially endocytose it (**a-d**). Lack of probe uptake at 4°C and the non-saturability of uptake over a range of Fdex concentrations (unpublished data) demonstrated that fluorescence acquisition was the result of an energy-dependent process and not triggered by binding to a cell surface receptor.

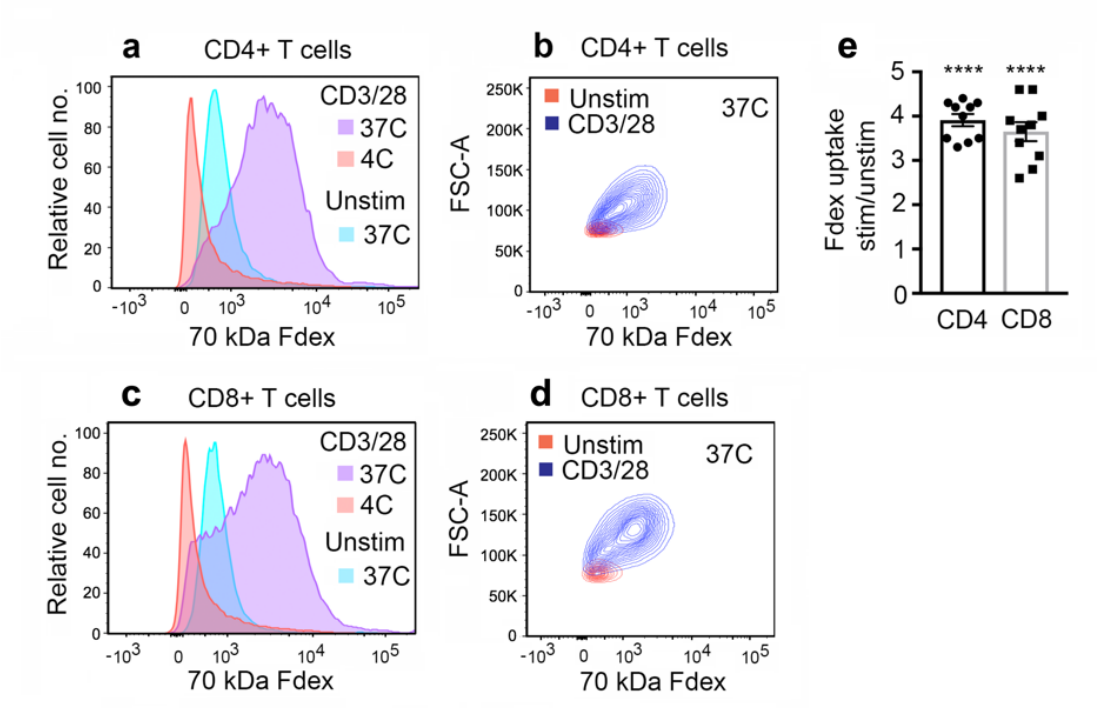

Figure 2 – Murine T cell uptake of Fdex probe. Murine splenocytes were unstimulated or stimulated with CD3/28 mAb for 24 h. 70 kDa Fdex probe was added to cells for the last 4 hours of culture, at the indicated temperatures. **a-d** Representative flow cytometry histogram plots of $CD4^+$ and $CD8^+$ T cell probe uptake and contour plots of probe uptake vs. FSC-A. **e** Mean ± 1 SEM of the ratio of Fdex probe uptake in stimulated vs. unstimulated $CD4^+$ and $CD8^+$ T cells at 37°C **(a–e)**, n = 10 independent experiments. ****$P < 0.0001$ by Student's 1-sample, 2-sided *t*-test.

To visualize putative T cell macropinosomes, we used an alternative macropinocytosis probe of comparable size, fluorochrome-labeled bovine serum albumin (66 kDa), which unlike 70 kDa Fdex can be fixed for imaging applications. Similar to the previous uptake assay, primary, splenic murine pan-T cells were stimulated or not with anti-CD3/28 mAbs for 20 hours in total, and incubated with BSA probe for hours 12-20 at either 37°C or 4°C. As **Figure 3** illustrates, flow cytometry analyses confirmed probe uptake into $CD4^+$ and $CD8^+$ T cells at the permissive temperature of 37°C but not at 4°C. We observed an approximately 3-fold enhancement of uptake of the BSA probe coincident with an increase in cell size in stimulated cells, consistent with results obtained from experiments performed with the Fdex probe (**Figure 2**).

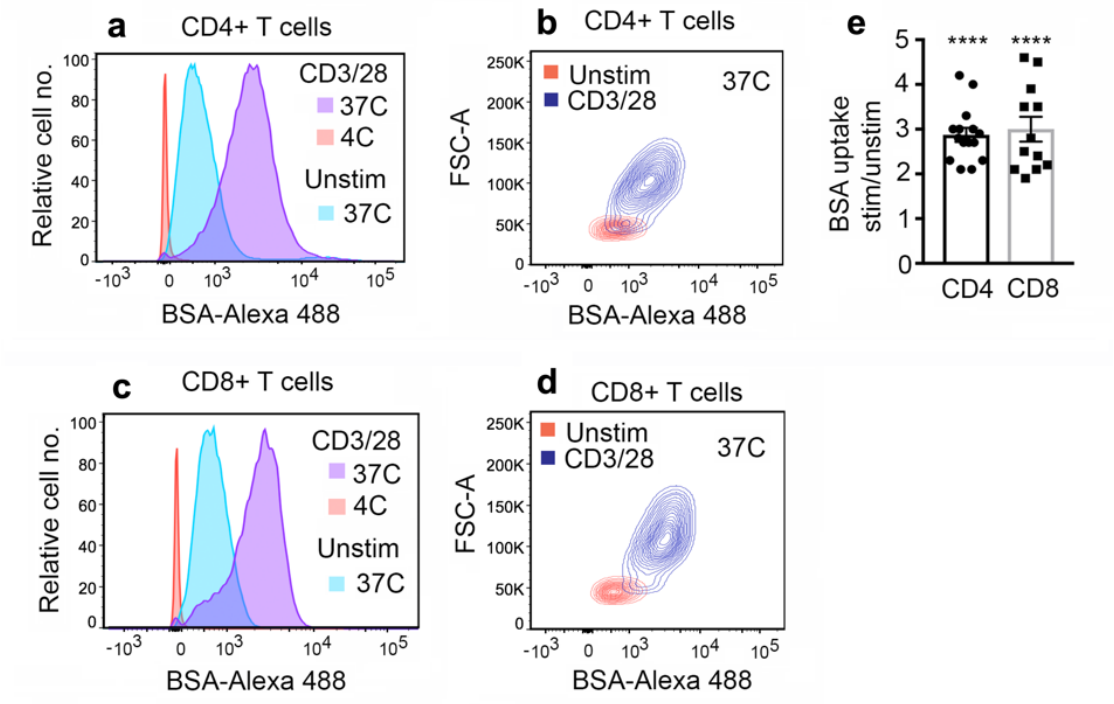

Figure 3 – Murine T cell uptake of BSA probe. Murine splenocytes were unstimulated or stimulated with CD3/28 mAb *in vitro* for 20 h. BSA-Alexa 488 probes were added to cells for the last 8 hours of culture at the indicated temperatures. **a-d** Representative flow cytometry histogram plots of $CD4^+$ and $CD8^+$ T cell probe uptake and contour plots of probe uptake vs. FSC-A. **e** Mean ± 1 SEM of the ratio of BSA probe uptake in stimulated vs. unstimulated $CD4^+$ and $CD8^+$ T cells at 37°C (n = 15 and 12 independent experiments for $CD4^+$ and $CD8^+$ T cells, respectively). ****$P < 0.0001$ by Student's 1-sample, 2-sided *t*-test.

To visualize putative T cell macropinosomes, purified, murine pan-T cells were stimulated for 20 hours, incubated with BSA probe for hours 12-20 post-stimulation then prepared for confocal microscopy as described in Materials and methods. As shown in **Figure 4** for a representative field of CD4-labeled cells (outlined in red), bright green fluorescence with a wavelength of 490-525 nm was observed accumulated within distinct vesicles approximately 200 nm to 1 μm in diameter, consistent with the size of macropinosomes, at 37°C (**a, left**) but not in cells chilled to 4°C (**a, right**) prior to probe incubation for hours 12-20. The nucleus was stained with Hoechst 33342 dye (blue). Vesicles were roughly circular, though slightly heterogenous in morphology, and predominantly localized to the cell periphery. The number of putative macropinosomes per $CD4^+$ or $CD8^+$ T cell at the moment of fixation varied from cell to cell with around 50% of them having 5 macropinosomes or fewer, though some cells contained 10 or more (**b-c**).

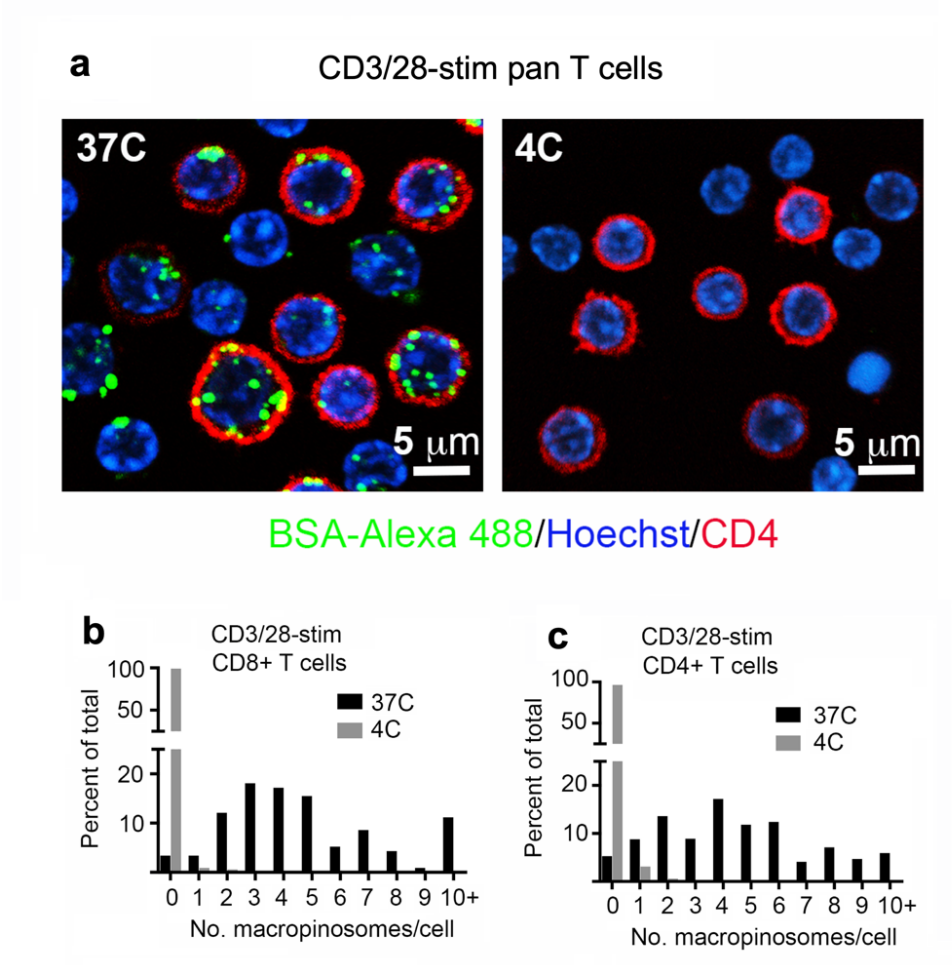

Figure 4 – Confocal microscopy of BSA probe uptake. a Images show temperature-dependent uptake of BSA-Alexa 488 by anti-CD3/28 mAb-stimulated purified murine pan T cells (probe incubation from 12 to 20 hours) into structures that resemble macropinosomes. Representative images of six repeat experiments are shown. **b-c** Quantitation of the number of macropinosomes per $CD8^+$ T cell (**b** n = 116 cells each at 37°C and 4°C) and $CD4^+$ T cell (**c** n = 169 and 196 cells at 37 °C and 4 °C, respectively).

Murine T cell internalization of macropinocytosis probes *in vivo*

To ensure that probe uptake was not artifactual and secondary only to artificial, *in vitro* TCR triggering and co-stimulation with antibodies, we conducted probe uptake assays using T cells from TCR transgenic mice. If enhancement of probe internalization was a consequence of bona fide TCR signaling and physiological activation, we predicted that stimulation with cognate peptide-MHC ligands *in vivo* would reproduce the elevation in uptake we saw in previous experiments using CD3/28 mAbs. T cells from OTII TCR transgenic (Tg) mice are $CD4^+$ and specific for ovalbumin (OVA) peptide 323-29 in complex with the $I\text{-}A^b$ MHC Class II molecule. To determine if endocytosis of fluorochrome-BSA by murine $CD4^+$ T cells increased upon TCR stimulation by cognate peptide-MHC ligands, we adoptively transferred OTII TCR Tg T cells into wild-type mice, waited 24 hours, immunized the wild-type recipients with OVA protein (or not), waited 12 additional hours, injected the Alexa-488-BSA probe into their footpads, and 8 hours later sacrificed the mice. This method is summarized in **Figure** 5a. After isolating T cells from the draining popliteal lymph nodes, we then measured the uptake of BSA probe in OTII TCR Tg T cells by flow cytometry, using antibodies specific for the transgenic TCR to identify and examine probe uptake only in these cells. As predicted, OTII TCR Tg T cells readily took up the probe, whether stimulated with peptide-MHC or not. As **Figure 5b** shows, uptake was enhanced in stimulated cells and was coincident with an increase in cell size as measured by FSC-A. OTII TCR Tg T cells stimulated with cognate peptide-MHC showed an approximately 3-4-fold increased uptake of BSA compared to unstimulated OTII TCR Tg T cells from non-immunized mice (**Figure 5c**).

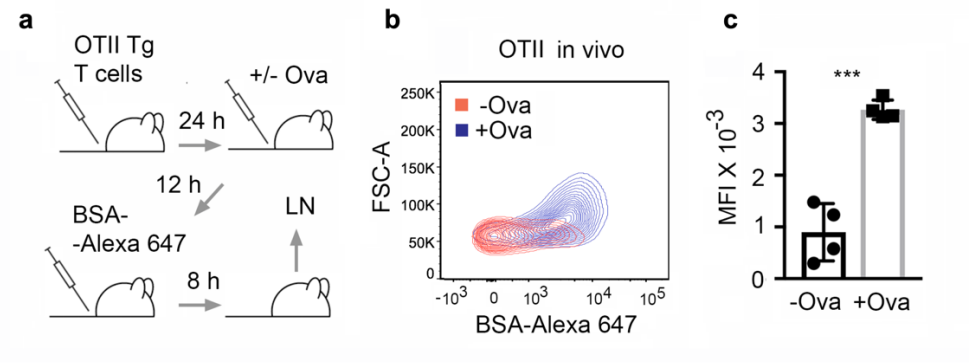

Figure 5 – *In vivo* uptake of BSA probe. a Method used to assess uptake of BSA-Alexa 647 by OTII TCR Tg T cells *in vivo* following immunization with whole OVA protein. **b** Representative flow cytometry contour plot of probe uptake vs. FSC-A. **c** mean ± 1 SEM of median fluorescence intensity (MFI) of Alexa 647 fluorescence of OTII TCR Tg T cells from unimmunized and immunized mice (n = 4 mice for each condition) ***$P < 0.001$ by Student's 2-sample, 2-sided *t*-test.

Human T cell internalization of macropinocytosis probes *in vitro*

To test whether uptake of macropinocytosis probes was unique to primary murine T cells, peripheral blood mononuclear cells (PBMCs) were prepared for uptake assays as described in Methods and materials. Primary human $CD4^+$ and $CD8^+$ T cells within the PBMC culture were stimulated (or not) with anti-human CD3/28 mAbs for 20 hours, then incubated with Alexa 488-BSA for hours 12-20 prior to washing, staining with CD4 and CD8 antibodies, and analysis by flow cytometry. Representative results from $CD4^+$ T cells are shown in **Figure 6a-b** and the fold-change in stimulated vs. unstimulated uptake for both $CD4^+$ and $CD8^+$ T cells are shown in **Figure 6c**.

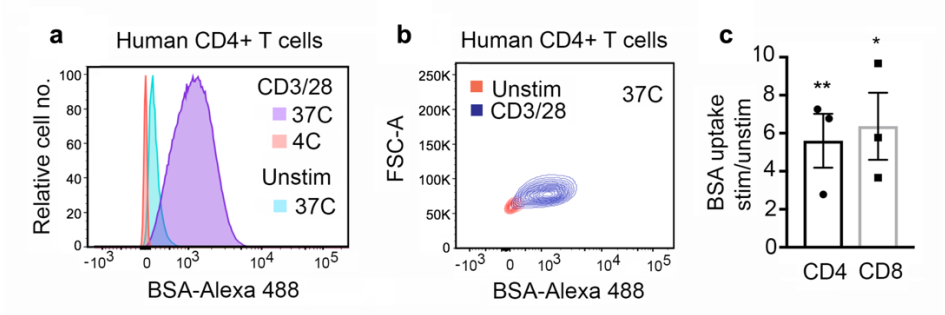

Figure 6 – Human T cell uptake of BSA probe. Human PBMCs were unstimulated or stimulated *in vitro* with CD3/28 mAb for 20 hours. BSA-Alexa 488 was added to cells for the last 8 hours of culture at the indicated temperatures. **a-b** Representative flow cytometry histogram plots of $CD4^+$ T cell probe uptake and contour plots of probe uptake vs. FSC-A. **c** Mean ± 1 SEM of the ratio of BSA uptake in stimulated vs. unstimulated $CD4^+$ and $CD8^+$ T cells at 37°C (n = 3 independent experiments). **P*< 0.05, ***P*< 0.01, by Student's 1-sample, 2-sided *t*-test.

As in experiments employing primary murine T cells, primary human $CD4^+$ and $CD8^+$ T cells internalized the BSA macropinocytosis probe in a temperature-dependent manner that was significantly enhanced upon stimulation with anti-CD3/28 mAbs. The mean fold-change in stimulated vs. unstimulated cell uptake was higher in human T cells compared to murine T cells, however these data exhibited considerably higher variance.

These experiments were then repeated with phytohemagglutinin (PHA) substituted for anti-CD3/28 mAbs to assess the effect of using an alternate mode of *in vitro* stimulation. Phytohemagglutinin is a mitogenic lectin isolated from the red kidney bean which promotes polyclonal T cell activation by cross-linking CD2 receptors and inducing cytoplasmic calcium influx.[245] Results from these experiments are summarized in **Figure 7**.

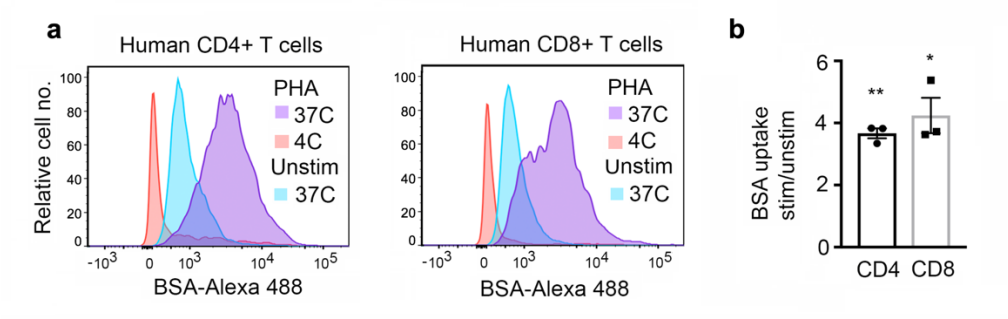

Figure 7 – BSA probe uptake in human T cells stimulated with PHA. Human PBMC were unstimulated or stimulated *in vitro* with CD3/28 mAb for 20 hours. BSA-Alexa 488 was added to cells for the last 8 hours of culture at the indicated temperatures. **a** Representative flow cytometry histogram plots of $CD4^+$ and $CD8^+$ human T cell probe uptake. **b** Mean ± 1 SEM of the ratio of BSA probe uptake in stimulated vs. unstimulated $CD4^+$ and $CD8^+$ T cells at 37°C (n = 3 independent experiments). $*P < 0.05$, $**P < 0.01$ by Student's 1-sample, 2-sided *t*-test.

Similar to results obtained using anti-CD3/28 mAbs, stimulation of primary human $CD4^+$ and $CD8^+$ T cells with PHA internalized the BSA macropinocytosis probe in a temperature-dependent manner that was significantly enhanced upon stimulation with PHA (**Figure 7a-b**). The mean fold-change in stimulated vs. unstimulated cell uptake was 3-4, consistent with previous results (**Figure 6c**).

To discern features of the plasma membrane during probe internalization, we prepared murine $CD4^+$ T cells stimulated in vitro with anti-CD3/28 mAbs for 16 hours, as well as unstimulated, naïve T cells, for imaging by scanning electron microscopy (SEM). **Figure 8a-b** shows representative images from this experiment.

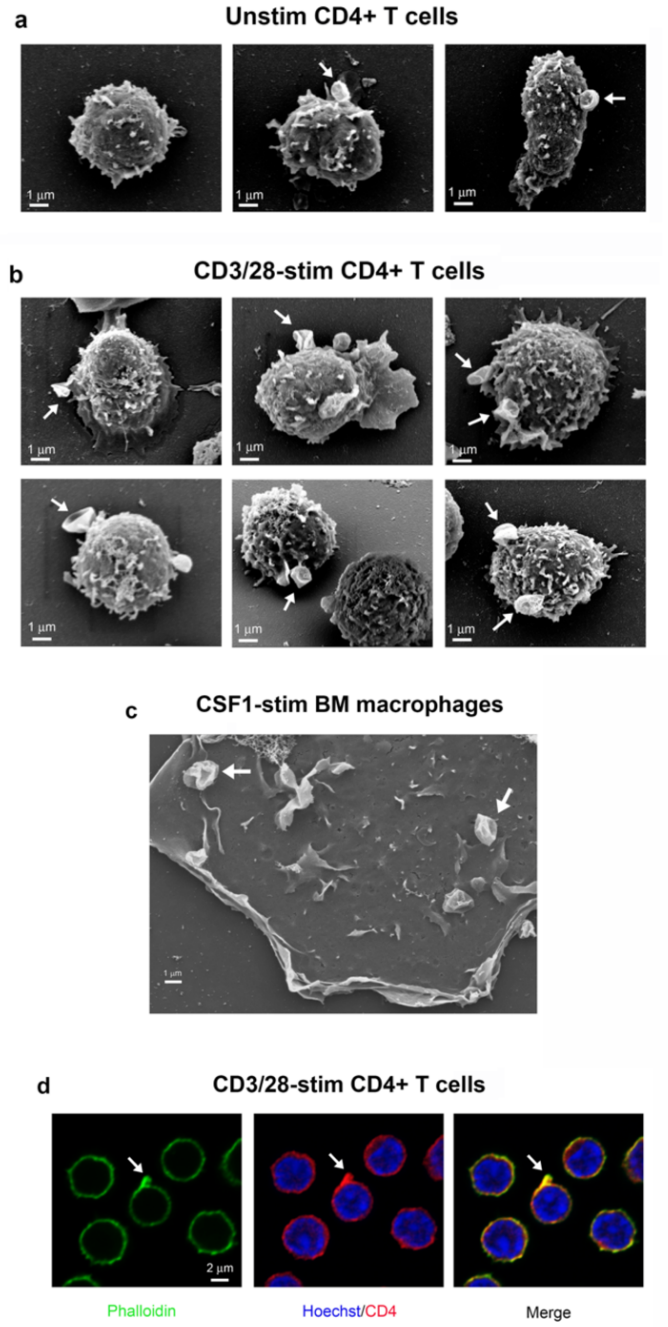

Figure 8 – Scanning electron and confocal microscopy reveal plasma membrane features consistent with macropinocytosis. a, b SEM images of murine $CD4^+$ T cells, unstimulated or stimulated with anti-CD3/28 mAbs for 16 hours. Macropinocytic cups at different stages of development are indicated (arrows). **c** SEM image of a murine BM macrophage stimulated with CSF1 for 15 minutes. Note similarity of macropinocytic cups to those identified in T cells (arrows). **d** Murine $CD4^+$ T cells, stimulated with CD3/28 mAb for 16 hours, were fixed and permeabilized, stained with Alexa 488-labeled phalloidin and anti-CD4 mAb, and analyzed by confocal microscopy. Shown images are 3 µm above the plane of T cell contact with the substratum. Note cell surface projected loop of polymerized actin (arrows).

SEM images of unstimulated and stimulated murine $CD4^+$ T cells show approximately spherical cells, 5-7 um in diameter, with many small, spiky surface projections. Also apparent are large plasma membrane protrusions and what appear to be macropinocytic cups in various stages of evolution, some with quite apparent concavity (**Figure 8a-b**, arrows). These protrusions and cups are more numerous on stimulated $CD4^+$ T cells compared to unstimulated cells. SEM of bone marrow-derived macrophages stimulated with CSF1 for 15 minutes prior to fixation reveals highly similar plasma membrane structures, including cups (**Figure 8c**, arrows). Additionally, murine $CD4^+$ T cells stimulated for 16 hours with anti-CD3/28 mAbs were fixed, permeabilized, and stained with Hoechst nuclear stain, fluorochrome-conjugated anti-CD4 mAb, and phalloidin, a bicyclic heptapeptide that selectively stains filamentous actin (F-actin), prior to visualization by confocal microscopy. A representative cross-sectional image slice from these experiments, taken 3 um above the plane of T cell contact with the substratum, is shown in **Figure 8d**. On the central cell in the image, a large loop of filamentous actin that is coincident with CD4 staining projects from the plasma membrane (denoted by an arrow).

Effect of macropinocytosis inhibitors on probe uptake in murine T cells

To definitively determine if the uptake of high molecular weight probes we observed in murine and human T cells was due to macropinocytosis and not some other bulk form of endocytosis, we performed uptake assays in the presence or absence of two highly selective inhibitors of macropinocytosis, 5-(N-Ethyl-N-isopropyl) amiloride (EIPA) and the combination of jasplakinolide and blebbistatin (J/B). As described in **1.7**, EIPA inhibits macropinocytosis by blocking the Na^+/H^+ exchanger NHE-1 and impairing activation of actin-remodeling Rho

GTPases. The combination of jasplakinolide and blebbistatin, inhibitors of actin depolymerization and myosin II respectively, have also been shown to selectively inhibit macropinocytosis. We hypothesized that 37°C probe uptake in stimulated murine T cells would be blocked by both of these inhibitors but not by an inhibitor of CME, PitStop 2. Results from these experiments are summarized in **Figure 9**.

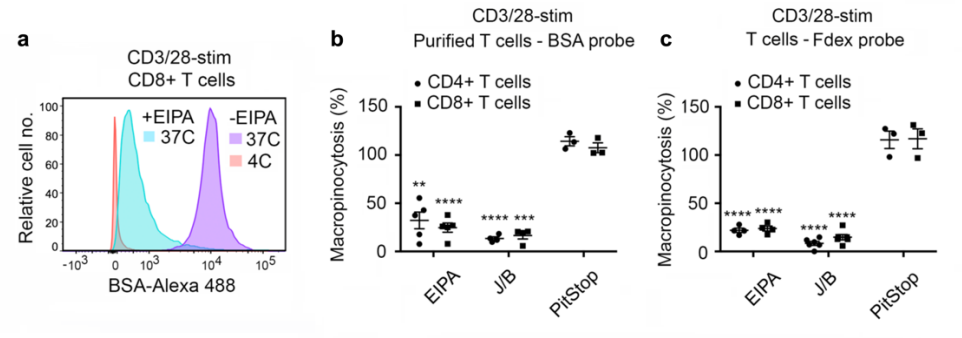

Figure 9 – Inhibitors of macropinocytosis block T cell uptake of macropinocytosis probes. **a** Murine splenocytes (**a, c**) or purified pan T cells (**b**) were stimulated with anti-CD3/28 mAbs for 12 hours before incubation with Alexa 488-BSA probe. (**a, b**) or 70 kDa Fdex (**c**) at 37°C or 4°C in the presence or absence of EIPA (**a-c**), J/B (**b, c**), and PitStop 2 (**b, c**) used at 50 μM, 1/75 μM, and 25 μM respectively for a further 8 h. **a** Representative flow cytometry plot showing the influence of EIPA upon probe uptake by $CD8^+$ T cells. **b, c** Mean ± 1 SEM of the percentage macropinocytosis relative to the positive control, calculated as indicated in Methods and Materials. **b** EIPA, n = 5; J/B, = 4, PitStop 2, n = 3 independent experiments. **c** EIPA, n = 4; J/B, = 6, PitStop 2, n = 3 independent experiments. **P* < 0.05, ***P* < 0.01, ****P* < 0.001, *****P* < 0.0001 by Student's 1-sample, 2-sided *t*-test.

Figure 9a shows the influence of EIPA on probe uptake at 37°C in stimulated and unstimulated murine splenocytes in a representative flow cytometry histogram. $CD8^+$ T cells stimulated at 37°C with anti-CD3/28 mAb for 12 hours before incubation with Alexa 488-BSA probe for an additional 8 hours readily ingested the probe (purple curve). By contrast, incubation with 50 μM EIPA for 15 minutes prior to addition of the probe dramatically impaired probe uptake as measured 8 hours later (light blue curve), and no probe was internalized by cells removed to 4°C during the period of probe incubation (red curve). **Figure 9b** shows data from repeated experiments in purified $CD4^+$ and $CD8^+$ T cells testing the influence of EIPA, J/B, and PitStop 2 on Alexa-488 BSA probe uptake as measured by flow cytometry in the period 12-20 hours post-stimulation. **Figure 9c** shows results from identical experiments in murine splenocytes and employing the Fdex probe. Results were broadly similar irrespective of which probe was employed or whether purified T cells were cultured in isolation or splenocytes were used. J/B exerted the most potent inhibitory effect on BSA and Fdex probe uptake, reliably reducing internalization (as measured by fluorescence) by 80-90%. EIPA inhibited slightly less, blocking BSA and Fdex probe uptake by 60-80%, with less inhibition in purified T cells (**b**) than in T cells co-cultured with splenocytes (**c**). By contrast incubation with the CME inhibitor PitStop 2 actually enhanced macropinocytosis of both probes by 110-120%.

To further support our contention that probe internalization in primary T cells occurs by macropinocytosis, we examined the dose-response relationship between macropinocytosis inhibitors and observed probe uptake by flow cytometry. Murine splenocytes were stimulated at 37°C with anti-CD3/28 mAb for 12 hours as before and incubated with EIPA at a range of concentrations for an additional 8 hours in the presence of Alexa 488-BSA probe. **Figure 10**

shows the percentage inhibition of macropinocytosis as measured by probe uptake for an increasing range of EIPA (**a**) and J/B (**b**) concentrations. At the lowest concentrations used, 2 μM EIPA or 0.04 μM jasplakinolide/3 μM blebbistatin, no significant inhibitory effect was observed. Incubation with 10 μM EIPA or 0.2 μM jasplakinolide/15 μM blebbistatin inhibited probe internalization significantly, approximately 20-30% and 30% respectively. The highest inhibitor concentrations used, 50 μM EIPA and 1/75 μM J/B, produced the most potent inhibition of macropinocytosis: >80% for EIPA and >90% for J/B.

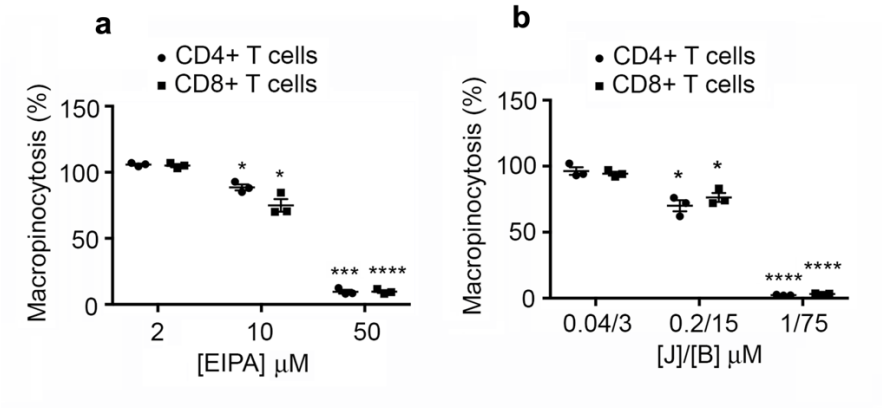

Figure 10 – Dose-response curves for EIPA and J/B inhibition of BSA probe uptake. **a, b** Murine splenocytes were stimulated with anti-CD3/28 mAbs for 12 hours before incubation with BSA-Alexa 488 at 37°C in the presence or absence of EIPA (**a**) and J/B (**b**) for a further 8 hours at the indicated concentrations. Mean ± 1 SEM of the percentage macropinocytosis relative to the positive control, calculated as indicated in Methods. **a, b** n = 3 independent experiments. **P* < 0.05, ***P*<0.01, ****P* < 0.001, *****P* < 0.0001 by Student's 1-sample, 2-sided *t*-test.

Effect of macropinocytosis inhibitors on probe uptake in human T cells

We next tested the influence of EIPA and J/B on human T cell ingestion of macropinocytosis probes. Human PBMCs were stimulated at 37°C or 4°C with anti-CD3/28 mAbs for 12 hours before incubation with Alexa 488-BSA probe for a further 8 hours in the presence or absence of EIPA or J/B, used at 50 μM and 1/75 μM respectively, prior to flow cytometry analysis. **Figure 11a** shows a representative flow cytometry histogram of probe internalization by human $CD8^+$ T cells in the presence and absence of EIPA at the indicated temperatures. At 37°C, $CD8^+$ T cells robustly took up the probe 12-20 hours post-stimulation (purple curve) but not at 4°C. Pre-incubation with 50 μM EIPA 15 minutes prior to the addition of the probe potently inhibited uptake, producing a curve (light blue) resembling the negative control. **Figure 11b** summarizes data from repeated experiments identical to that described for **Figure 11a**. Similar to results obtained with primary murine $CD4^+$ and $CD8^+$ T cells, EIPA and J/B potently inhibited human T cell macropinocytosis, by approximately 90% and 80% respectively.

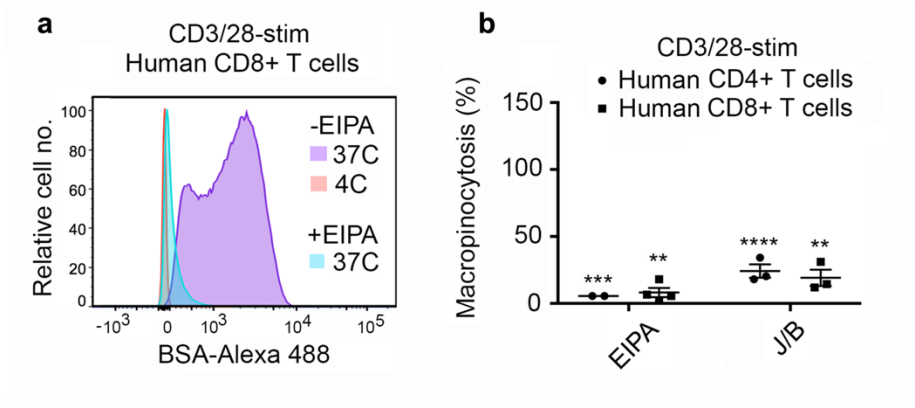

Figure 11 – EIPA inhibits BSA probe uptake in human cells. Human PBMC were stimulated with CD3/28 mAb for 12 hours before incubation with BSA-Alexa 488 at 37°C or 4°C in the presence or absence of the indicated inhibitors for a further 8 hours. EIPA and J/B were used at 50 μM and 1/75 μM respectively. **a** Representative flow cytometry plot showing the influence of EIPA upon probe uptake by human $CD8^+$ T cells. **b** Mean ± 1 SEM of the percentage macropinocytosis relative to the positive control, calculated as indicated in Methods and materials. (n = 2 and 4 independent experiments for $CD4^+$ and $CD8^+$, respectively, with EIPA and n = 3 independent experiments for J/B. *$P < 0.05$, **$P < 0.01$, ***$P < 0.001$, ****$P < 0.0001$ by Student's 1-sample, 2-sided *t*-test.

Confocal microscopy showing inhibition of probe uptake by EIPA

To confirm inhibition of probe uptake in EIPA-treated CD3/28-stimulated $CD4^+$ and $CD8^+$ murine T cells, we turned again to confocal microscopy. Purified pan-T cells were stimulated at 37°C with anti-CD3/28 mAbs for 12 hours then incubated with Alexa 488-BSA probe in the presence or absence of 50 μM EIPA. **Figure 12a** shows representative fields from the same experiment. In the absence of the inhibitor (left), fluorescent green probe can be seen accumulated in relatively large vesicles within $CD8^+$ T cells (outlined in red). By comparison, cells treated with EIPA 12-20 hours post-stimulation (right) show far fewer and smaller probe-positive vesicles within $CD8^+$ T cells. A manual quantitation of the number of macropinosomes per cell, displayed in **Figure 12b**, reveals a wide variation in stimulated, untreated cells (black bars). The majority of stimulated, EIPA-treated $CD8^+$ (**Figure 12b, left**) and $CD4^+$ (**Figure 12b, right**) T cells, however, show 2 or fewer macropinosomes per cell.

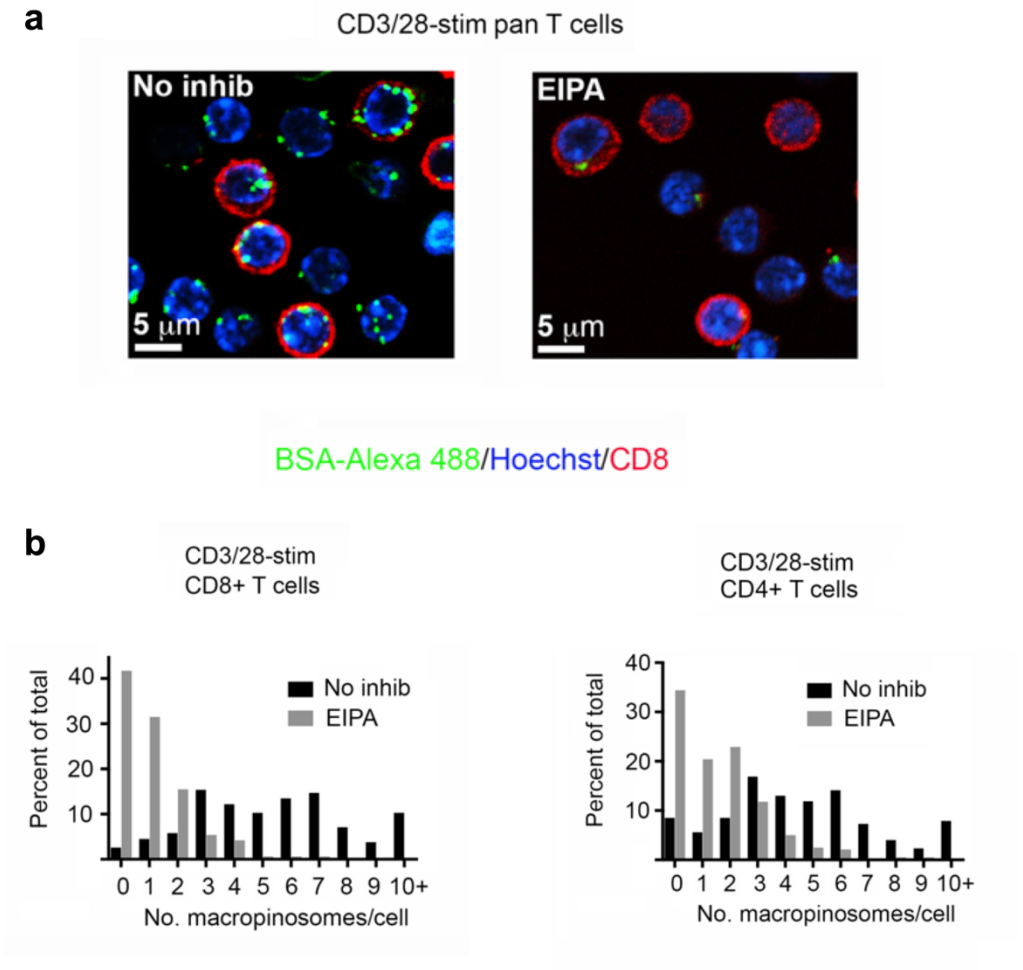

Figure 12 – Inhibition of BSA probe uptake by EIPA shown by confocal microscopy. a BSA-Alexa 488 uptake by CD3/28 mAb-stimulated purified murine T cells (probe incubation from 12 to 20 hours) in the absence and presence of EIPA at 37°C. Images are representative of five repeat experiments. **b** Quantitation of the number of macropinosomes per $CD8^+$ and $CD4^+$ T cell in the absence and presence of EIPA ($CD8^+$ n = 156 and 168 cells, respectively, $CD4^+$ n = 177 and 279 cells respectively).

2.6 DISCUSSION

To determine if primary murine and human $CD4^+/8^+$ T cells perform macropinocytosis we assessed their ability to internalize high molecular weight, fluorophore-conjugated macropinocytosis probes by flow cytometry. We found that both unstimulated and CD3/28-stimulated $CD4^+$ and $CD8^+$ T cells readily took up both the 70 kDa Fdex (**Figure 2**) and 67 kDa BSA probe (**Figure 3**) and that probe internalization was enhanced approximately 3-fold in stimulated cells (**Figure 2e**, **Figure 3e**). Probe uptake at 37°C in stimulated cells was accompanied by an increase in cell size as measured by FSC-A, irrespective of the probe used (**Figure 2b**,**d**, **Figure 3b**,**d**). By contrast, no probe internalization occurred in cells incubated at 4°C during the 12-24 (Fdex) or 12-20 (BSA) hour period post-stimulation (**Figure 2a-d**, **Figure 3a-d**).

BSA probe uptake at 37°C into primary murine $CD4^+$ T cells was confirmed by confocal microscopy of CD3/28-stimulated purified pan-T cells (**Figure 4a**). Imaging also recapitulated flow cytometry findings that no probe ingestion occurs at at 4°C, consistent with an energy-dependent process. A manual quantitation of the number of putative macropinosomes per cell, shown in **Figure 4b**, revealed that the majority of cells incubated at 37°C had 7 or fewer probe-positive vesicles per cell whereas the majority of cells incubated at 4°C had 0 probe-positive vesicles per cell.

Experiments employing adoptively-transferred OTII TCR Tg T cells permitted us to assess the ability of $CD4^+$ T cells stimulated with cognate peptide-MHC ligand to internalize macropinocytosis probes *in vivo*. As summarized in **Figure 5a**, 24 hours after adoptive transfer

of OTII TCR Tg T cells, recipient mice were immunized with whole OVA protein, then injected with Alexa 647-BSA probe 12 hours later. Lymph nodes were harvested 8 hours after probe injection and probe uptake in unstimulated and OVA-stimulated OTII TCR Tg cells was assessed by flow cytometry. OVA-stimulated OTII TCR Tg cells readily internalized the BSA probe coincident with an increase in cell size as measured by FSC-A (**Figure 5b**). We noted that unstimulated OTII TCR Tg cells also took up probe constitutively *in vivo* to an extent similar to that seen for *in vitro* experiments. Furthermore, the magnitude of uptake in stimulated vs. unstimulated cells *in vivo* was consistent with that seen for *in vitro* experiments (**Figure 5c**). These experiments confirmed that T cell uptake of macropinocytosis probes was not just an *in vitro* phenomenon and occurs under conditions of physiological T cell activation.

Primary human T cells, isolated from PBMCs also constitutively internalized the BSA probe at 37°C and upregulated probe uptake significantly upon stimulation with human anti-CD3/28 mAbs (**Figure 6a-b**). By contrast, no significant probe internalization occurred at at 4°C. The mean ratio of stimulated to unstimulated probe uptake was noticeably higher in these cells—approximately 5-6 compared to ~3 for previous experiments with murine cells—though these data were considerably more varied (**Figure 6c**). Similar results were obtained in experiments with primary human T cells, again isolated from PBMCs, but stimulated instead with the mitogenic lectin PHA (**Figure 7**). Low-level constitutive uptake was observed at 37°C in unstimulated cells, whereas no uptake occurred at at 4°C, while probe internalization was significantly enhanced in stimulated cells. The ratio of stimulated to unstimulated internalization in these experiments was a bit lower (3.5-4) compared to human T cells stimulated with anti-

CD3/28 mAbs, and these data were less varied than those as well (**Figure 7c**, compare **Figure 6c**).

SEM of both unstimulated and CD3/28-stimulated primary murine $CD4^+$ T cells revealed striking plasma membrane features consistent with macropinocytosis as observed in other cell types, such as macrophages. As **Figure 8a-b** shows, numerous protrusions and large, circularizing ruffles were seen projecting from the surface of $CD4^+$ T cells approximately 5-7 μm in diameter. Several of these structures displayed apparent concavity and strongly resembled macropinocytic cups at various stages of evolution (**Figure 8a-b**, arrows). While unstimulated cells also exhibited these features, they were much less commonly observed, consistent with the low-level constitutive macropinocytosis previously observed in these cells by flow cytometry and confocal microscopy. These plasma membrane ruffles and cups also bore a strong resemblance macropinocytic cups observed in bone marrow-derived macrophages stimulated with CSF1 for 15 (**Figure 8c**, arrows).

Given the actin-dependence of macropinocytosis, we assessed actin polymerization within these surface structures by confocal microscopy (**Figure 8d**). CD3/28-stimulated $CD4^+$ T cells stained with fluorescently-tagged phalloidin, a bicyclic heptapeptide that selectively stains F-actin, and imaged by confocal microscopy revealed enrichment of polymerized actin in ruffles and loops, coincident with plasma membrane CD4 staining, projecting from the cell surface 3 μm above the plane of cell adhesion to the substratum.

Taken together, our SEM and confocal microscopy studies suggested the existence in T cells of large, F-actin-rich plasma membrane structures consistent with CDRs and cups seen in other cell types performing macropinocytosis.

Experiments assaying the uptake of high molecular weight probes strongly suggested that both unstimulated and stimulated murine and human primary T cells perform macropinocytosis. To definitively determine if what we observed was bona fide macropinocytosis, we tested the sensitivity of both Fdex and BSA probe uptake to the "gold standard" inhibitors, 50 μM EIPA and 1/75 μM J/B. As **Figure 9a** shows, robust 37°C uptake of the BSA probe at 12-20 hours post-stimulation in $CD8^+$ T cells was potently inhibited by addition of EIPA prior to probe incubation. By comparison, no probe uptake occurred at 4°C. Similar results were obtained in repeated experiments using stimulated, purified $CD4^+$ and $CD8^+$ T cells treated with EIPA or J/B during incubation with the BSA probe (**Figure 9b**). This effect was reproduced in repeated experiments using stimulated splenocytes treated with either inhibitor prior to incubation with the Fdex probe (**Figure 9c**). EIPA blocked uptake by 70-80%, inhibiting slightly more effectively in experiments employing the Fdex probe for reasons that aren't clear. J/B was even more effective, blocking $CD4^+$ and $CD8^+$ T cell uptake of both probes in by 80-90%.

By comparison, addition of the CME inhibitor PitStop 2 to cultures prior to incubation with either the BSA or Fdex probe did not inhibit probe uptake (**Figure 9b-c**). In fact, a slight enhancement of uptake was seen with inhibition of CME, possibly as a consequence of a compensatory mechanism that upregulated macropinocytosis in the setting of CME blockade.

Inhibition of CME has been shown to induce compensatory CIE in some cell types, so this finding is not wholly without precedent.[246,247]

To more closely examine the effect of treatment with macropinocytosis inhibitors on probe BSA uptake in T cells, we performed experiments testing EIPA and J/B over a range of concentrations. **Figure 10** shows how increasing concentrations of EIPA (**a**) and J/B (**b**) produced progressive inhibition of T cell macropinocytosis; as inhibitor concentration increases by a factor of 5, a typical reverse sigmoid curve is produced. Notably, the effective inhibitory dose was the same as that shown to inhibit macropinocytosis in other cell types. This evidence further strengthened support for the conclusion that the observed uptake was genuine macropinocytosis.

On the basis of these results we predicted that EIPA and J/B would also inhibit BSA probe uptake in human cells stimulated *in vitro*. The representative flow cytometry histogram in **Figure 11a**, which shows probe internalization in human, CD3/28-stimulated $CD8^+$ T cells, shows this prediction was confirmed. At 12-20 hours post-stimulation, probe was ingested at a high rate in 37°C cultures, whereas addition of 50 μM EIPA prior to probe incubation at the same temperature produced potent inhibition of uptake. This effect was reproducible and comparable in magnitude in both $CD4^+$ and $CD8^+$ human T cells when 1/75 μM J/B was substituted for EIPA in identical uptake assays (**Figure 11b**).

Finally, we stimulated purified, murine pan-T cells *in vitro* with anti-CD3/28 mAbs for 12-20 hours in the presence or absence of 50 μM EIPA and assayed intracellular probe accumulation by

confocal microscopy. The representative fields in **Figure 12a** illustrate the profound inhibitory effect of EIPA treatment. In the absence of inhibitor, Alexa 488-BSA probe was seen within mostly peripheral vesicles within $CD8^+$ cells, with some cells harboring >10 vesicles. By contrast, the majority of $CD8^+$ cells treated with EIPA prior to probe addition showed few if any probe-positive intracellular vesicles. Given that our negative selection procedure for purifying T cells prior to the assay yields $CD4^+$ and $CD8^+$ T cells at very high purity, it's not unreasonable to presume that the non-$CD8^+$ cells in these fields are $CD4^+$ T cells, however we cannot be certain since an additional marker was not used. It is worth noting, however, that in these cells too there is a great accumulation of probe in apparently intracellular vesicles in the absence of inhibitor and very few apparent probe-containing vesicles among the unlabeled, EIPA-treated cells. **Figure 12b**, however, displays the results from a manual quantitation of probe positive vesicles per cell in each condition for specifically-labeled $CD8^+$ (left) and $CD4^+$ (right) T cells treated and untreated with EIPA. These data clearly confirm strong inhibition by EIPA, apparently due to a markedly lower rate of macropinosome formation in these cells.

Altogether, the highly reproducible uptake of macropinocytosis probes into vesicles resembling macropinosomes, along with its reliable inhibition by EIPA and J/B, led us to conclude that primary murine and human T cells perform macropinocytosis that is constitutive in unstimulated naïve cells and significantly enhanced in cells nascently-stimulated by various means.

The ubiquity and scale of macropinocytic uptake in primary T cells was an unexpected discovery for several reasons. Chief among these was the relative paucity of cytoplasmic volume in naïve and nascently-activated T cells; macropinosomes are relatively large vesicles and their

generation requires internalization of large patches of membrane. Compared to macrophages, which tend to have average diameters 2-3 times as large as T cells, the latter seemed unlikely candidates to perform macropinocytosis. Additionally, researchers have been visualizing lymphocytes by microscopy for well over a century so it is surprising that this activity had not been previously recognized.

In the next chapter we explore the mechanism of T cell macropinocytosis and compare our findings to those made in other macropinocytosing cell types.

CHAPTER III:

THE MECHANISM OF T CELL MACROPINOCYTOSIS[2]

3.1 ABSTRACT

Classical or canonical descriptions of macropinocytosis in most cell types suggest an integral role for the small GTPase Ras. Ras activation initiates a signaling cascade through phosphatidylinositol 3-kinases (PI3K) that activates Rho-family GTPases capable of site-specific remodeling of the actin cytoskeleton. The formation and closure of macropinocytic cups is orchestrated by these GTPases in conjunction with their downstream effectors such as WAVE, Arp2/3, and Pak1. To investigate the mechanism of T cell macropinocytosis, we tested the effect of inhibitors of these signaling molecules on probe uptake in murine T cells. Surprisingly, treatment with farnesyl thiosialicylic acid (FTS), which inhibits Ras signaling by displacing H-, N-, and K-Ras isoforms from cell membranes, had no effect on probe internalization in murine T cells stimulated with anti-CD3/28 mAbs. To further substantiate the apparent Ras-independence of stimulated T cell macropinocytosis, we tested the macropinocytic capacity of stimulated T cells from mice deficient in RasGRP1, the principle guanine nucleotide exchange factor (GEF) in this cell type. Loss of RasGRP1 had no impact on BSA probe uptake. Targeting molecules downstream of Ras, by contrast, did impair macropinocytosis: LY294002, EHT 1864, and IPA-3 each partially inhibited ingestion of the BSA probe. Together these findings suggested that, in

[2] The contents of this chapter were adapted and reproduced from the following publication: Charpentier, J. C. *et al.* Macropinocytosis drives T cell growth by sustaining the activation of mTORC1. *Nat Commun* **11**, 180 (2020).

contrast to classical macropinocytosis observed in other cell types, T cell macropinocytosis does not require Ras signaling, but is partially dependent on PI3K, Rac1, and Pak-1 activities. With the exception of LY294002, which had no significant effect, similar results were obtained in assays using unstimulated cells.

3.2 INTRODUCTION

To better understand the mechanism of T cell macropinocytosis, and to compare it to classical descriptions of macropinocytosis in other cell types, we first investigated its dependence on signaling by Ras. As reviewed in **Chapter 1.5**, numerous lines of evidence implicate Ras signaling in recruiting and coordinating the molecular machinery required to promote plasma membrane ruffling and macropinocytic cup formation. PMA or M-CSF-induced macropinocytosis in macrophages can be inhibited by treatment with farnesyl thiosalicylic acid (FTS).[201] As previously described, this compound inhibits farnesylation and membrane recruitment of H-, N-, and K-Ras isoforms, effectively preventing their activation and signaling.

We hypothesized that if T cell macropinocytosis was similarly Ras-dependent, stimulated T cells treated with FTS would exhibit impaired macropinocytosis in probe uptake assays. Given the demonstrated importance of Ras signaling in regulating the formation of macropinocytic cups and the size of macropinosomes, we expected that T cell macropinocytosis would likewise be highly dependent upon it.

The dissection of signaling pathways with the use of pharmacological inhibitors, as opposed to genetic methods, is hindered by the widely-recognized problem of drug and binding site

promiscuity (polypharmacology).[248,249] Another method for investigating the importance of Ras signaling to T cell macropinocytosis, one which obviates the necessity of using inhibitors with less than optimal selectivity, is to test the uptake of probes in $CD4^+/CD8^+$ T cells isolated from RAS guanyl releasing protein 1 (Rasgrp1)-deficient mice. Rasgrp1 is the principal Ras GEF involved in the activation of Ras in peripheral T cells, especially during TCR-induced Ras activation.[250] Other Ras GEFs expressed in T cells, such as RAS guanyl releasing protein 1 (Rasgrp4), son of sevenless homolog 1 (Sos1), and son of sevenless homolog 2 (Sos2) are also expressed in T cells and are important for thymocyte development but expendable for TCR signaling.[250–253] We predicted that T cells isolated from Rasgrp1-null mice would show defects in macropinocytosis consequent to impaired Ras activation.

Another way to investigate the signaling requirements for T cell macropinocytosis is to assess the impact of inhibiting class I PI3Ks. As previously described, modulation of membrane phosphoinositides and the generation of membranous PIP_3 by class I PI3Ks are essential events in macropinocytic signaling in many cell types. Inhibition of class I PI3Ks in stimulated T cells, then, should significantly impair probe internalization by macropinocytosis. As with Ras, constitutively active PI3K signaling is associated with a variety of oncological malignancies.[254–256] Consequently a number of PI3K inhibitors of variable selectivity have been developed and tested in clinical trials. One of these, LY294002, inhibits class I PI3Ks by competitive binding to the catalytic subunit's ATP-binding site and has been widely used in research studies.[257] We predicted that inhibition of class I PI3K signaling would also significantly impair T cell macropinocytosis.

Lastly, given the integral role of Rho GTPases and their effectors in producing the actin rearrangements necessary for macropinocytosis, we sought to test the effect of inhibiting Rac1 and its effector Pak1 in macropinocytosing T cells. GTP-bound Rac1 activates numerous actin-remodeling effectors, such as cortactin, an Arp2/3 activator and regulator of actomyosin contractility, IQGAP1, a scaffolding protein that binds both actin filaments and microtubules, and the WAVE regulatory complex, which also promotes Arp2/3-mediated actin polymerization.[258–260] Pak1 itself also activates or recruits an array of proteins that promote dynamic actin rearrangements. Reported Pak1 substrates include LIM kinases, which regulate actin-binding cofilin proteins, α/β-PIX, which are Rho GEFs, and filamin A, an actin-binding protein which anchors transmembrane proteins to the actin cytoskeleton and builds orthogonal networks of actin filaments.[261–264]

We predicted that inhibition of Rac1 with EHT 1864, a competitive inhibitor of Rac1 guanine nucleotide exchange, and inhibition of Pak1 with IPA-3, an isoform selective inhibitor that enhances the protein's autoinhibitory homodimerization, would produce significant but modest impairment of T cell macropinocytosis.[265,266]

3.3 MATERIALS AND METHODS

Animals. Wild-type mice were bred in house and were on a mixed 129S6/SvEv X C57BL/6 genetic background. Rasgrp1 mutant mice (JAX) were on a C57BL/6 genetic background. Mice ranged in age from 6 weeks to 3 months. Mice of both sexes were used in experiments. All experiments performed with mice were in compliance with University of Michigan guidelines and were approved by the University Committee on the Use and Care of Animals.

T cell macropinocytosis assays. Murine splenocytes were isolated from wild-type or Rasgrp1 mutant mice and prepared as previously described. The following additional pharmacological inhibitors were added to cultures 15 min prior to addition of macropinocytosis probes at the concentrations indicated or at the following final concentrations: FTS (Sigma), 25 μM; LY294002 (Cayman), 50 μM; EHT 1864 (Cayman), 10 μM; IPA-3 (Tocris), 20 μM.

Statistical analysis. *P* values were calculated using Student's 1-sample or 2-sample, 2-sided *t*-tests as appropriate for normally distributed data.

3.4 RESULTS

To determine if stimulated T cell macropinocytosis is dependent on activation and signaling of Ras isoforms, we performed probe uptake assays in the presence of the broad-spectrum Ras inhibitor, farnesylthiosalicylic acid (FTS, also known as salirasib). Murine splenocytes were stimulated with anti-CD3/28 mAbs for 12 hours and incubated with Alexa-488 BSA probe in the presence or absence of macropinocytosis inhibitors (EIPA, J/B), a CME inhibitor (PitStop 2), or an inhibitor of H-, N-, and K-Ras membrane recruitment (FTS). Results from these experiments, showing macropinocytosis in inhibitor-treated $CD4^+$ and $CD8^+$ T cells as a proportion of probe uptake in the absence of inhibitors, are summarized in **Figure 13a**. EIPA and J/B reliably and strongly inhibit T cell macropinocytosis while PitStop 2 moderately enhances it, recapitulating previous findings. Inhibition of Ras signaling by FTS, on the other hand, had no discernible impact on T cell macropinocytosis. To further dissect the signaling pathways associated with T cell macropinocytosis, we next tested the effect of inhibitors of PI3Ks (LY294002), Rac1 (EHT

1864), and Pak1 (IPA-3). Murine splenocytes were again stimulated at 37°C or 4°C with anti-CD3/28 mAbs for 12 hours. Alexa 488-BSA probe uptake in the hours 12-20 post-stimulation was then measured in the presence or absence of these inhibitors. Results from these experiments are shown in **Figure 13b**. As expected, inhibition of macropinocytosis-associated signaling and effector proteins all moderately impaired T cell macropinocytosis: LY294002 by ~30-40%, EHT 1864 by ~30%, and IPA-3 by ~40% compared to stimulated cells cultured in the absence of inhibitors.

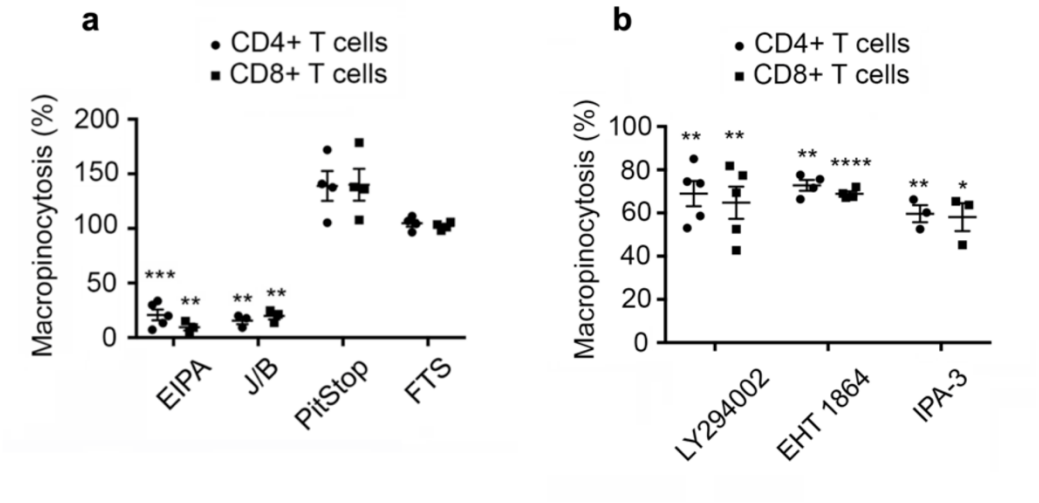

Figure 13 – T cell macropinocytosis is Ras independent. Murine splenocytes were stimulated with anti-CD3/28 mAbs for 12 hours before incubation with BSA-Alexa 488 at 37°C or 4°C in the presence or absence of the indicated inhibitors for a further 8 hours. Mean ± 1 SEM of the percentage macropinocytosis relative to the positive control, calculated as indicated in Materials and methods. **a** EIPA, n = 5 for $CD4^+$ and n = 3 for $CD8^+$; J/B, n = 3; Pitstop, n = 4; FTS. **b** LY294002, n = 5, EHT 1864, n = 4; IPA-3, n = 3 independent experiments.

To further examine the apparent Ras-independence of T cell macropinocytosis, we conducted flow cytometry probe uptake assays using T cells isolated from mice deficient in Rasgrp1. Rasgrp1 is the predominant Ras GEF expressed in T cells and deletion mutants largely lack the ability to activate Ras in T cells. The ability of unstimulated and anti-CD3/28 mAb-stimulated $CD4^+$ and $CD8^+$ T cells from homozygous Rasgrp1 deletion mutants (denoted -/-) and haplosufficient mice (+/-) were compared. The latter heterozygotes have one wild-type Rasgrp1 allele that is sufficient to reproduce the wild-type phenotype. Results from these experiments are summarized in **Figure 14**. **Figure 14a** shows representative flow cytometry histograms, all from the same experiment, displaying probe uptake 12-20 hours post-CD3/28 stimulation in Rasgrp1-deficient and -sufficient $CD4^+$ and $CD8^+$ T cells at 37°C or 4°C. At 37°C, probe internalization was comparable in both Rasgrp1-deficient (light blue curves) and -sufficient (violet curves) $CD4^+$ (top panels) and $CD8^+$ (bottom panels) T cells. No significant probe uptake occurred at the non-permissive temperature of 4°C (green and orange curves). **Figure 14b** shows the ratio of probe uptake in $CD4^+$ and $CD8^+$ T cells from Raspgrp1-deficient mice to that observed in Rasgrp1-sufficient mice. This ratio was nearly 1 for both cell populations, indicating that macropinocytosis is *not* significantly perturbed or impaired in murine T cells lacking an ability to activate Ras signaling.

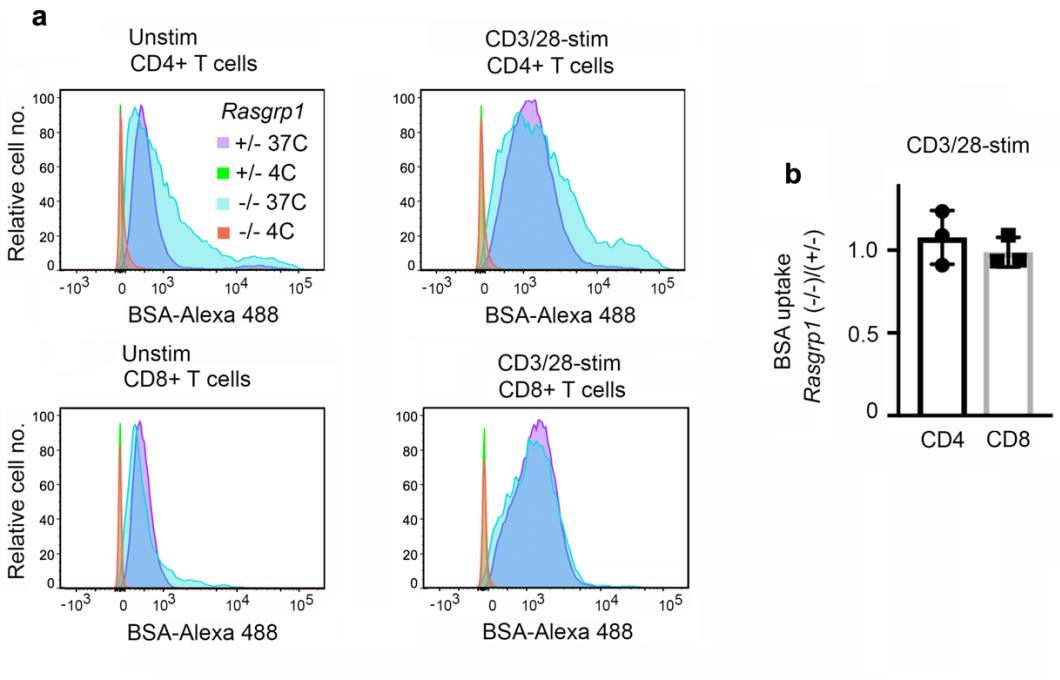

Figure 14 – T cell macropinocytosis is not impaired in Rasgrp1-deficient mice. Murine splenocytes from Rasgrp1 mutant mice were unstimulated or stimulated with CD3/28 mAb for 12 hours before incubation with BSA-Alexa 488 at 37°C or 4°C for a further 8 hours. a Representative flow cytometry histogram plots and mean ± SEM of the percentage macropinocytosis relative to the positive control.

Given that T cell macropinocytosis is constitutive in naïve, unstimulated $CD4^+$ and $CD8^+$ T cells, we repeatedly tested the ability of previously-used inhibitors to block probe ingestion in these cells. Unstimulated murine splenocytes were cultured for 12 hours at 37°C before addition of inhibitors at the highest concentrations previously used (listed in Methods and materials) for an additional 2 hours. Data from these experiments are summarized in **Figure 15**. EIPA and J/B nearly abolished all unstimulated T cell probe uptake, whereas PitStop 2 again had no effect. Surprisingly, inhibition of PI3K signaling by LY294002 had no measurable impact on probe uptake either. Inhibition of Rac1 and its effector Pak1, by EHT 1864 and IPA-3 respectively, moderately impaired probe internalization, with IPA-3 showing a more pronounced inhibition than EHT 1864.

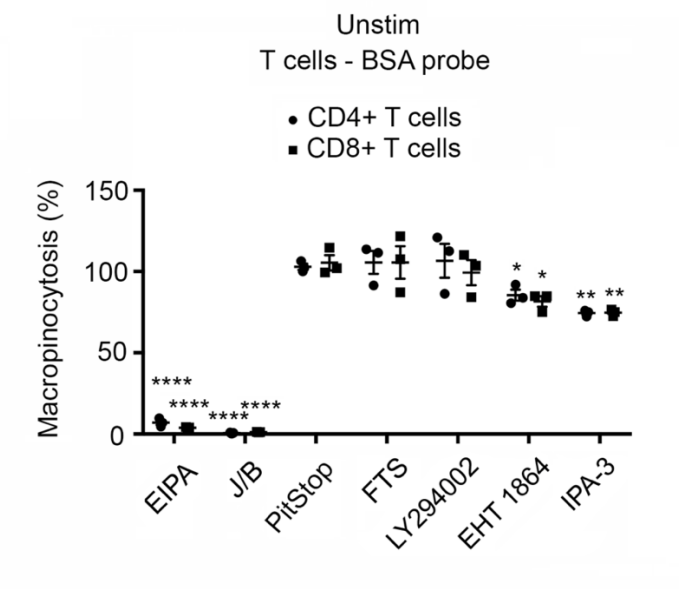

Figure 15 – Macropinocytosis inhibitors block BSA probe uptake in unstimulated cells but LY294002 does not. Unstimulated murine splenocytes were incubated for 12 hours at 37°C in the presence of the indicated inhibitors for a further 8 hours. Mean ± SEM of the percentage macropinocytosis relative to the positive control. n = 3 independent experiments for each inhibitor. **P*<0.05, ***P*<0.01, ****P*<0.001, *****P*<0.0001 by Student's 1-sample, 2-sided *t*-test.

3.5 DISCUSSION

Prior macropinocytosis studies, primarily in amoebae and macrophages, have revealed a great deal about the signaling and effector requirements for the generation of plasma membrane structures (protrusions, ruffles, cups, etc.) as well as the mechanisms of macropinosome generation. Sensitivity to the selective inhibitors EIPA and J/B suggests some of the requirements for T cell macropinocytosis by their individual mechanisms of action. As previously described, EIPA implicates plasma membrane NHEs, which are required to maintain relative alkalinization of the immediate submembranous region so that Rho GTPases function optimally. J/B inhibition points to requirements for dynamic actin remodeling and myosin contractility.

Beyond these rather obvious clues, we designed experiments to interrogate further the mechanism of T cell macropinocytosis using additional inhibitors targeting signaling proteins and effectors identified in previous macropinocytosis studies.

As detailed in **Chapter 1.6**, signaling by Ras GTPases is centrally important in classical descriptions of macropinocytosis. We predicted that Ras signaling would play a similar critical role in T cell macropinocytosis, however, experiments testing the influence of Ras inhibition by FTS (salirasib) showed no significant defects in macropinocytosis in either stimulated (**Figure 13a**) or unstimulated (**Figure 15**) murine $CD4^+$ or $CD8^+$ T cells. This was a surprising result but one that could potentially be explained by insufficient inhibition of Ras isoforms by FTS. As previously described, FTS inhibits the canonical Ras isoforms (H-, N-, and K-Ras) by competitive binding for associated Ras-escort proteins required for membrane association. But

other isoforms of Ras, such as R-Ras2 (TC21), are variably prenylated (R-Ras2 is geranylgeranylated), capable of activating class I PI3Ks in their active form, and may not depend on the same Ras-escort proteins for membrane tethering.[267,268] It's possible that variable expression and prenylation of Ras isoforms in T cells could preclude efficient inhibition of Ras signaling by FTS alone in these cells. PI3K-activating signals from non-H-, K-, or N- Ras isoforms could have compensated for FTS inhibition and perhaps that is why we saw no inhibition in FTS-treated cells.

Subsequent experiments examining macropinocytosis in murine $CD4^+$ and $CD8^+$ T cells specifically deleted of Rasgrp1, the predominant Ras GEF in T cells, suggested that this was not likely the explanation for the inhibitor's lack of effect. Complete abrogation of Ras signaling in these cells produced no impairment in T cell macropinocytosis (**Figure 14**). Since neither constitutive uptake in unstimulated nor CD3/28-stimulated uptake in Rasgrp1-deleted cells was significantly perturbed, we concluded that Ras signaling was not necessary for T cell macropinocytosis.

The most likely explanation for the observed Ras-independence is that co-stimulatory signals from activated CD28 receptors are sufficient to activate class I PI3Ks, rendering Ras-dependent activation unnecessary.[269,270] It's unclear, however, why constitutive macropinocytosis in unstimulated, Rasgrp1-deleted cells was not impaired, given that these cells are not performing co-stimulatory signaling and cannot activate Ras. One potential explanation comes from the observation that Rho family GEFs like Vav1/2 are recruited to the T cell signalasome by the adaptor proteins LAT and SLP-76. This would permit Ras and PI3K-independent Rac activation

in unstimulated cells in the presence of tonic, low-level recruitment of Vav proteins to membranes. Activation-induced enhancement of Vav-targeting and PI3K activation in stimulated cells, then, might explain their augmented uptake. This model is consistent with the observed lack of inhibitory effect produced by LY294002 in unstimulated $CD4^+/CD8^+$ murine T cells (**Figure 15**).

In CD3/28-stimulated murine $CD4^+$ and $CD8^+$ T cells, however, PI3K inhibition by LY294002 did significantly impair macropinocytosis (**Figure 12b**), as expected. The magnitude of inhibition was modest, approximately 30%, but there was considerable variation between experiments. This may be explained by the non-trivial, documented, off-target effects of LY294002, which has been shown to not only bind multiple classes of PI3Ks, but also unrelated targets such as protein kinase CK2, mTOR, and glycogen synthase kinase 3β (GSK3β).[257]

Inhibition of Rac1 by EHT 1864 significantly impaired macropinocytic uptake in both stimulated and unstimulated murine $CD4^+$ and $CD8^+$ T cells (**Figure 13b**, **Figure 15**). The magnitude of inhibition was modest, an approximate 25-30% reduction in both groups. With respect to off-target effects, EHT 1864 has been shown to inhibit other Rac isoforms in addition to Rac1, such as Rac1b, Rac2, and Rac3, as well as its effectors Pak1 and Pak2.[265,271] Since these reported effects are confined to Rac isoforms and their effectors, though, their influence is less likely to seriously confound interpretation. The relatively modest inhibitory effect exerted by EHT 1864 may be due to the dependence of T cell macropinocytosis on another Rho GTPase that is highly-expressed in T cells but uninhibited by EHT-1864, Cdc42. It's also possible that the signal seen

in these experiments is due to the combined effect of Rac1 and Pak1 inhibition, but that is contradicted by the greater inhibitory effect of IPA-3, the Pak1 inhibitor also tested.

p21-activated kinases (Paks) are effectors of Rho GTPases such as Rac1 and Cdc42. In 3T3 fibroblasts, Pak1 kinase activity induces actin polymerization and generation of lamellipodia.[218] It has also been shown to regulate macropinocytosis by phosphorylating a specific serine residue on CtBP1/BARS, an essential activity for macropinocytic cup closure and scission (as shown in A431 epidermoid carcinoma cells performing EGF-induced macropinocytosis).[218,219] IPA-3 is a sulfhydryl-containing compound that inhibits Pak1 by binding to its N-terminal regulatory domain and preventing GTPase docking.[272] Treatment of CD3/28-stimulated murine $CD4^+$ and $CD8^+$ T cells with IPA-3 inhibited T cell macropinocytosis by approximately 40%. Inhibition was slightly less pronounced (~30%) in unstimulated cells.

CHAPTER IV:

T CELL MACROPINOCYTOSIS AND G1 CELL GROWTH[3]

4.1. ABSTRACT

Activated T cells show substantial increases in cell size between 12-20 hours post-stimulation. This period of rapid growth corresponds to the G1 phase of the cell cycle in nascently-activated T cells. To determine whether macropinocytosis is required for G1 growth in these cells I added macropinocytosis inhibitors to cell cultures immediately prior to this period and examined their impacts on cell growth as measured by flow cytometry. The strongest inhibitors of T cell macropinocytosis, EIPA and J/B, were also potent inhibitors of G1 phase growth. Addition of inhibitors that partially inhibit T cell macropinocytosis also constrained growth but to a lesser extent. Importantly for these studies, addition of inhibitors resulted in minimal toxicity. Overall, a strong positive correlation was observed between inhibition of macropinocytosis and restriction of G1 phase growth. These findings support the hypothesis that macropinocytosis is required for the growth of activated T cells even under nutrient replete conditions.

[3] The contents of this chapter were adapted and reproduced from the following publication: Charpentier, J. C. *et al.* Macropinocytosis drives T cell growth by sustaining the activation of mTORC1. *Nat Commun* **11**, 180 (2020).

4.2 INTRODUCTION

Naïve T cells nascently-activated by antigen stimulation must quickly acquire biosynthetic precursors and accumulate biomass sufficient to roughly double in size within 24 hours in order to initiate clonal expansion. To do this they must transition from a quiescent metabolic program characterized by low nutrient uptake and catabolism sufficient to maintain housekeeping activities to one of high nutrient uptake and anabolism. Specifically this requires a shift from low-level oxidative phosphorylation and β-oxidation in naïve cells to aerobic glycolysis, glutaminolysis, and upregulation of the pentose phosphate pathway in activated T cells.

Like many rapidly proliferating cell types and cancer cells exhibiting the Warburg effect, nascently-activated T cells upregulate aerobic glycolysis. How and why this meets the bioenergetic demands of activated T cells better than what have been traditionally regarded as more efficient alternatives, such as oxidative metabolism, is still unclear. Some evidence suggests that when glucose uptake limits cell metabolic rate, oxidative phosphorylation is the most efficient means of ATP generation, but at high glucose uptake rates (as in activated T cells) cytoplasmic solvent capacity becomes limiting, and aerobic glycolysis generates the greatest ATP yield per volume density.[273] Furthermore, when glucose is abundant, as in commercial cell media (e.g., RPMI 1640 medium contains 11 mM glucose), the *rate* of ATP production is comparable between oxidative phosphorylation and aerobic glycolysis.[274] Accordingly, it seems unlikely that aerobic glycolysis is favored by activated T cells because it generates ATP more quickly, as many have suggested.[275] It is interesting to note that a number of glycolytic enzymes, such as 6-phosphofructo-2-kinase/fructose-2,6-biphosphatase 3 (PFKFB3), have been shown to interact with F-actin and localize to lamellipodia.[276] It's possible that wholly apart from any

advantage conferred with respect to bioenergetics the promotion of aerobic glycolysis in activated T cells *also* facilitates motility by the formation of a plasma membrane metabolon, as has been observed in erythrocytes.[277]

Activated T cells also increase glucose flux through the parallel pentose phosphate pathway.[278,279] Entry of glucose-6-phosphate into this pathway yields pentose sugars that combine with pyrimidines and purines to form nucleotides needed for proliferation. The pentose phosphate pathway also produces reduced nicotinamide adenine dinucleotide phosphate (NADPH), a redox cofactor needed for biosynthetic reductions.

Another metabolic pathway upregulated in activated T cells is the mevalonate pathway.[280] Acetyl-CoA condensed by 3-hydroxy-3-methylglutaryl CoA (HMG-CoA) synthase generates HMG-CoA. HMG-CoA conversion to mevalonate by HMG-CoA reductase initiates the first step in this highly conserved biosynthetic cascade that ultimately generates farnesyl pyrophosphate (FPP). FPP is the common substrate for various anabolic reactions that generate ubiquinones, sterols, and prenylated proteins. The latter are especially important for the post-translational modification of Ras, Rab, and Rho GTPases, which require isoprenylation (farnesylation or geranylgeranylation) for membrane association and full activation.[280]

Activated T cells also upregulate glucose and amino acid transporters. PI3K-Akt signaling, enhanced by CD28 co-stimulation, increases both expression and plasma membrane localization of the major glucose transporter in T cells, GLUT-1.[269,270,279] Also upregulated are Tfr (CD71),

and LAT1, a large neutral amino acid transporter consisting of SLC3A2 (CD98) and SLC7A5.[279,281]

As previously mentioned, glutaminolysis, which converts glutamine into TCA cycle intermediates, is upregulated in activated T cells. Expression of glutamine transporters, such as ASCT2, is also significantly enhanced upon activation.[281] In addition, glutamine has been shown in Jurkat T cells to promote activated T cell survival by upregulating glutathione and the anti-apoptotic Bcl-2 protein.[282]

Downstream of TCR and CD28 co-stimulation, the combinatorial action of the transcription factors NFAT, AP-1, and NFκB induces transcription of the cytokine IL-2 and the high affinity IL-2 receptor subunit IL-2Rα (CD25).[283] Autocrine and paracrine signaling by IL-2 *in vitro* promotes activated T cell survival, growth, and proliferation, though its *in vivo* functions are considerably more complicated.[283,284]

In addition to acquiring biosynthetic intermediates, reprogramming metabolism, and inducing expression of common γ chain cytokine receptors, activated T cells must also enter the cell cycle. Naïve T cells maintained in the quiescent G_0 state enter interphase, which is further divided into G_1, S, and G_2 phases. M phase and cytokinesis follow. Progression through these phases is mediated by cyclin-dependent kinases (CDKs) and their cyclin partners. Within 6-10 hours of TCR stimulation, the CDK4/6-cyclin D complex drives the transition of naïve T cells from G_0 to G_1 phase.[281] As T cells progress through G_1 phase in response to TCR and CD28 stimulation, activated Akt and Src kinases promote cyclin E expression.[281] Downregulation of CDK4/6-cyclin

D and upregulation of CDK2-cyclin E, which promotes S phase entry, follows. In the first cell cycle, G_1/S phase typically lasts from 10-24 hours post-stimulation.[285] G_2 phase is comparatively brief, occurring 24-26 hours post-stimulation, with mitosis (M phase) beginning at 26 hours post-stimulation.[285]

In initial experiments examining uptake of macropinocytosis probes by activated T cells, we examined the period from 12-20 or 12-24 hours post-stimulation, which correspond to G_1 and G_1/S phases, respectively, and noted coincident significant increases in cell size. This was seen *in vitro* in murine T cells internalizing the Fdex probe (**Figure 2b, d**) or BSA probe (**Figure 3 b, d**), *in vivo* in murine T cells internalizing the BSA probe (**Figure 5b**), and in human T cells *in vitro* internalizing the BSA probe (**Figure 6b**).

To investigate the possibility that macropinocytosis was required for G_1 phase growth, we tested the influence of macropinocytosis inhibitors on probe uptake in this period in flow cytometry assays. We predicted that addition of EIPA and J/B to cultures 15 minutes prior to the probe incubation period would restrict G1 growth as measured by FSC-A. We further predicted that partial inhibitors of macropinocytosis, such as those targeting PI3K, Rac1, and Pak1, would also impair G1 growth but likely to a lesser extent.

4.3 MATERIALS AND METHODS

Animals. Wild-type mice were bred in house and were on a mixed 129S6/SvEv X C57BL/6 genetic background. Mice ranged in age from 6 weeks to 3 months. Mice of both sexes were used in experiments. All experiments performed with mice were in compliance with University

of Michigan guidelines and were approved by the University Committee on the Use and Care of Animals.

T cell macropinocytosis assays. Murine splenocytes were isolated from wild-type mice and prepared as previously described. Incubation with probes was for the indicated times at 37°C or 4°C. In addition to the previously described inhibitors, Torin 1 (Tocris) was added to cultures 15 min prior to addition of macropinocytosis probes at a final concentration of 500 nM.

T cell growth. Murine splenocytes were stimulated with CD3/CD28 mAb as above at 37 °C for 12 or 20 h in the presence or absence of inhibitors that were added at 12 hours. Cells were harvested, washed, stained with APC-Cy7-CD4 and APC-CD8α mAb and analyzed by flow cytometry. Median FSC-A of $CD4^+$ and $CD8^+$ T cells was taken as a relative measure of cell size. In each experiment, the effect of inhibitors upon T cell growth between 12 and 20 hours was calculated as a percentage of T cell growth observed in the absence of inhibitor as follows: [(FSC-A in presence of inhibitor at 20 hours - FSC-A in absence of inhibitor at 12 hours)/(FSC-A in absence of inhibitor at 20 hours - FSC-A in absence of inhibitor at 12 hours)] × 100.

Statistical analysis. *P* values were calculated using Student's 1-sample or 2-sample 2-sided t-tests as appropriate for normally distributed data.

4.4 RESULTS

Inhibition of macropinocytosis significantly impairs activated cell growth

Activated $CD4^+$ and $CD8^+$ murine T cells significantly increase in size, as measured by FSC-A, in the period 12-20 hours post-stimulation. **Figure 16** shows a representative flow cytometry scatter plot comparing the size of unstimulated (top left), 12 hour-stimulated (top right), 20 hour-stimulated (bottom left), and stimulated $CD8^+$ T cells treated with EIPA during hours 12-20 post-stimulation (bottom right) with anti-CD3/28 mAbs. On average, $CD8^+$ T cells stimulated for 12 hours are larger than unstimulated cells, however they exhibit the greatest period of growth between hours 12-20 post-stimulation. Selective inhibition of macropinocytosis with EIPA largely blocks growth during this period. FSC-A is plotted against side scatter area (SSC-A), a measure of cell granularity or complexity. Similar results were obtained for $CD4^+$ T cells.

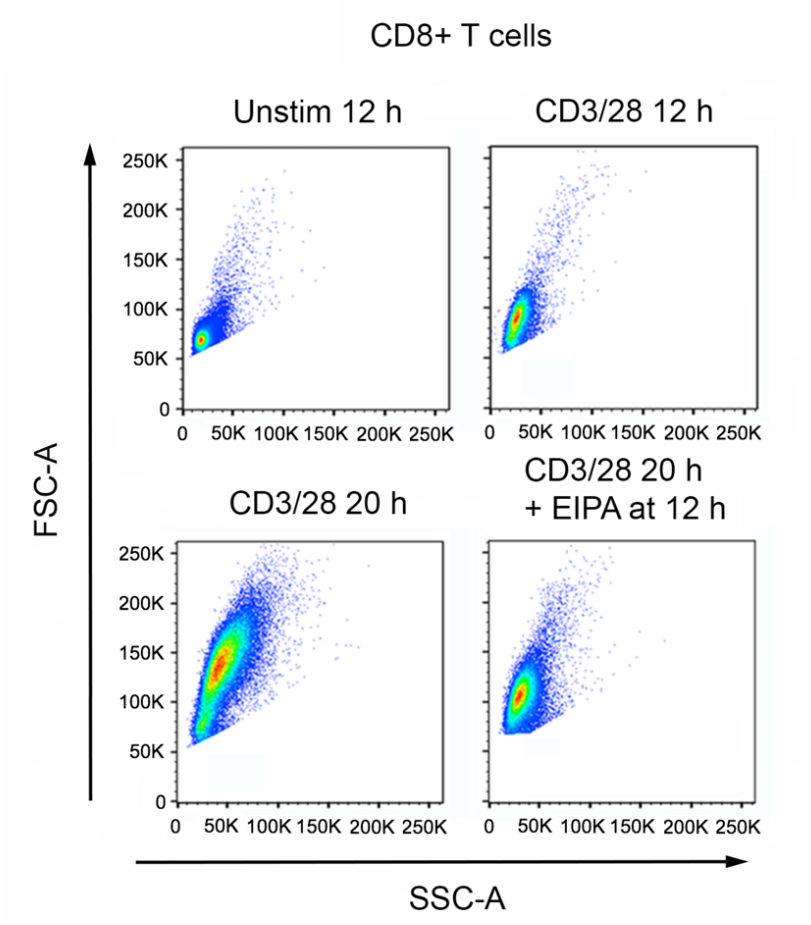

Figure 16 – Activated T cells significantly increase in size 12-20 hours post-stimulation. Murine splenocytes were unstimulated or stimulated with anti-CD3/28 mAbs for 12 or 20 hours. Shown are flow cytometry scatter plots of FSC-A versus SSC-A for $CD8^+$ T cells from a single experiment (representative of 8 performed with EIPA). Similar results were obtained with $CD4^+$ T cells.

Building on our observation that inhibition of macropinocytosis blocks increases in cell size 12-20 hours post-stimulation, we hypothesized that macropinocytosis was required for activated T cell growth. If this relationship was specific and direct, we would expect inhibition of 12-20 hour growth to closely mirror inhibition of macropinocytosis over a range of concentrations. **Figure 17** shows dose-response curves employing increasing concentrations of EIPA (**a**) and J/B (**b**) and their impacts on 12-20 hour growth post-stimulation. In both cases, impairment of 12-20 hour growth reliably and proportionally reflects the extent of macropinocytosis inhibition in this period (compare **Figure 13**).

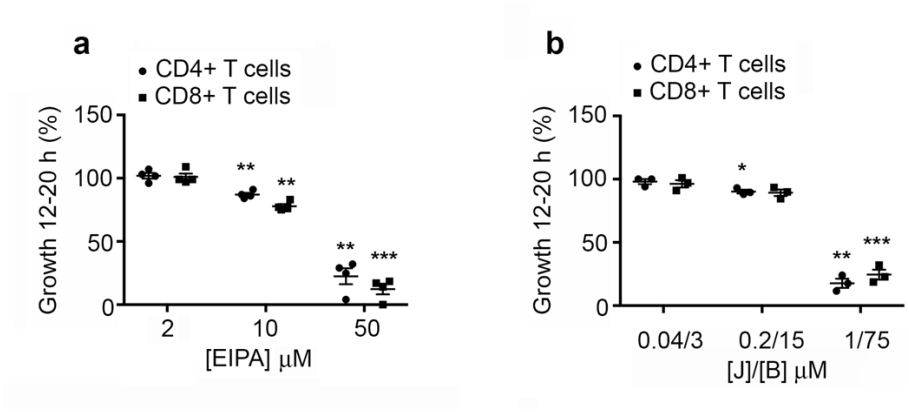

Figure 17 – G1 phase growth is restricted by inhibitors of macropinocytosis. Murine splenocytes were stimulated with CD3/28 mAb for 12 h before incubation with BSA-Alexa 488 at 37°C or 4°C in the presence or absence of the indicated inhibitors for a further 8 hours. **a, b** Mean ± 1 SEM of the percentage macropinocytosis relative to the positive control, calculated as indicated in Methods and materials (n = 3 independent experiments). **P* < 0.05, ***P* < 0.01, ****P* < 0.001, *****P* < 0.0001 by Student's 1-sample, 2-sided *t*-test.

Partial inhibitors of macropinocytosis moderately block activated cell growth

To further examine the relationship between T cell macropinocytosis and growth, we tested the effect of partial inhibitors of macropinocytosis on growth 12-20 hours post-stimulation with anti-CD3/28 mAbs. Results from these experiments are shown in **Figure 18**. In both $CD4^+$ (left) and $CD8^+$ (right) T cells, inhibition by EIPA and J/B produced the most pronounced growth defects, reducing growth in this period by more than 75%. As expected, inhibitors of CME (PitStop 2) and H-, N-, and K-Ras (FTS), neither of which block macropinocytosis, had no significant effect on 12-20 hour growth. By contrast, inhibition of PI3K, Rac1, and Pak1 by LY294002, EHT 1864, and IPA-3, respectively, all moderately blocked 12-20 hour post-stimulation growth by approximately 50%. Growth restriction imposed by these partial macropinocytosis inhibitors was comparable to that seen by inhibition of the mechanistic target of rapamycin complex 1 (mTORC1) by Torin 1.

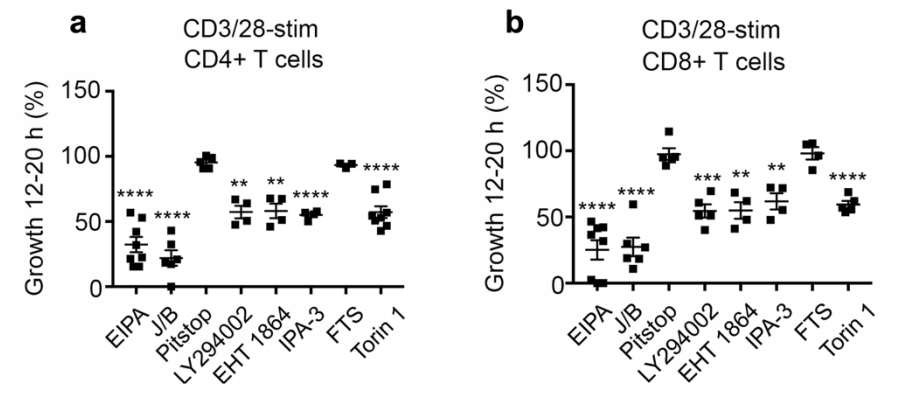

Figure 18 – Partial inhibitors of macropinocytosis also impair G1 phase growth. a, b Murine splenocytes were stimulated with CD3/28 mAb for 20 hours in the absence or presence of the indicated inhibitors that were added to cultures at 12 hours. For each inhibitor, the mean percentage ± 1 SEM of $CD4^+$ (**a**) $CD8^+$ (**b**) T cell growth between 12 and 20 hours relative to growth in the absence of inhibitor in the same experiment is shown (see Methods and materials) (**a** EIPA, n = 8; J/B, n = 6; PitStop, n = 5; LY294002, n = 5; EHT 1864, n = 4; IPA-3, n = 4; FTS, n = 4; Torin 1, n = 5 independent experiments. **b**). $^{**}P < 0.01$, $^{***}P < 0.001$, $^{****}P < 0.0001$ by Student's 1-sample, 2-sided *t*-test.

Growth as a function of macropinocytosis in activated T cells

Previous experiments suggested a direct relationship between inhibition of macropinocytosis and restriction of activated T cell growth 12-20 hours post-stimulation. This relationship became more apparent when 12-20 hour growth was plotted as a function of the percentage of macropinocytosis relative to controls. As **Figure 19** shows, $CD4^+$ and $CD8^+$ activated T cell growth in the period 12-20 hours post-stimulation is a nearly linear function of macropinocytic uptake. Irrespective of the specific inhibitor used and its mechanism of action, inhibition of growth was directly proportional to inhibition of macropinocytosis. Under no circumstances was inhibition of macropinocytosis not accompanied by a proportional reduction in cell growth in this period.

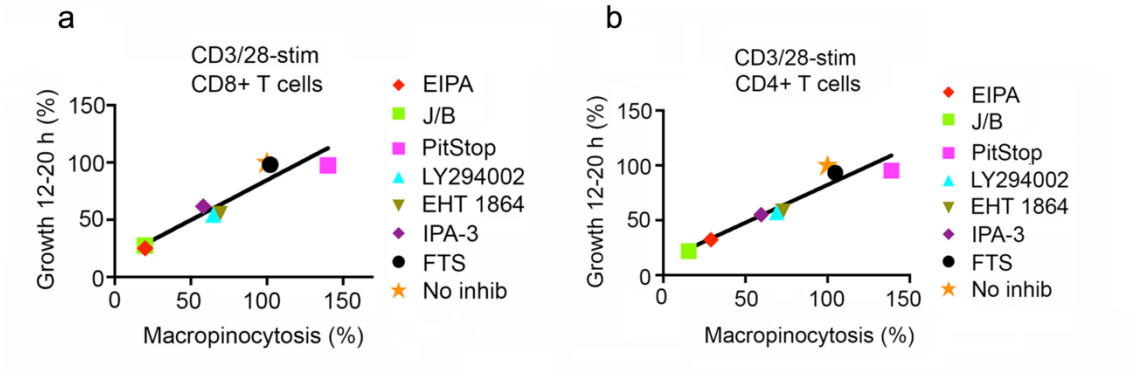

Figure 19 – Macropinocytosis inhibitors block G1 phase growth in CD8$^+$ and CD4$^+$ T cells. Graph shows mean percentage macropinocytosis (**Figure 12a, b**) vs. mean percentage growth (**Figure 18b**) for CD8$^+$ T cells (**a**) and CD4$^+$ T cells (**b**) for each inhibitor.

4.5 DISCUSSION

We began by considering the substantial anabolic burden activated T cells must meet as they progress through their first cell cycle post-stimulation. Noting that the period 12-20 hours post-stimulation, which corresponds to G1 phase, represented the period of greatest growth in our uptake assays, we hypothesized a relationship between macropinocytosis and activated T cell growth. If this relationship were direct (i.e., cell growth is proportional to macropinocytic uptake under nutrient-replete conditions), inhibition of macropinocytosis should produce a corresponding reduction in cell growth.

To test this we inhibited macropinocytosis in the 12-20 hour post-stimulation period using a range of concentrations of EIPA and J/B, then observed the impact on cell size by measuring FSC-A. As expected, progressive inhibition of macropinocytosis using increasing concentrations of either EIPA or J/B were correlated with proportional reductions in cell size (**Figure 17**). The strength of this relationship is underlined by comparing **Figure 17** to **Figure 10**, which show the same trends using the same concentrations of inhibitors.

Next we reasoned that if selective inhibition of macropinocytosis by EIPA and J/B produced proportional reductions in G1 phase cell growth, partial inhibitors of macropinocytosis should do the same. If inhibition of macropinocytosis by these inhibitors (LY294002, EHT 1864, and IPA-3) was not accompanied by a proportional reduction in growth, this would weaken support for the idea that there is a direct relationship between macropinocytosis and growth in activated T cells. On the other hand, if these inhibitors, which each have independent, unrelated mechanisms

of action, all produced reductions in cell growth proportional to the magnitude of their inhibition of macropinocytosis, this would be compelling evidence in favor of the hypothesis.

Figure 18 shows the impact of all tested inhibitors on G1 phase growth in $CD4^+$ (**a**) and $CD8^+$ T (**b**) cells. We noted that EIPA and J/B produced the most profound impairment (> 60% reduction in growth), as expected, whereas partial inhibitors of macropinocytosis produced less severe defects (≤ 50% reduction). Importantly, PitStop 2 and FTS, which do not significantly inhibit macropinocytosis in T cells, also do not impair growth post-stimulation.

These results confirmed our supposition of a direct relationship between macropinocytic uptake 12-20 hours post-stimulation and G1 phase growth. This strength of this association became undeniable when we plotted 12-20 hour growth as a function of the percentage of macropinocytosis observed after treatment with each inhibitor (**Figure 19**). On the basis of the obvious trend uncovered by these experiments we concluded that macropinocytosis directly and positively regulates T cell growth during post-stimulation G1 phase growth.

We did note, however, that the apparent compensatory enhancement of macropinocytosis reliably seen with CME inhibition by PitStop 2 (see **Figure 13a**) did not produce a corresponding increase in growth *beyond* that observed in positive controls. The most likely explanation for this is that macropinocytosis promotes growth only up to a certain threshold growth rate, after which other factors become limiting.

This raises the question of how exactly macropinocytosis contributes to G1 phase growth in activated T cells under conditions of nutrient optimality. One obvious explanation is that it

enables the bulk acquisition of precursors for biosynthesis, including amino acids and glucose obtained from the extracellular space. This requirement for macropinocytosis might be explained by a relative paucity of plasma membrane glucose and amino acid transporters in nascently-activated T cells. It may be the case that during the first cell cycle post-stimulation, T cells rely on macropinocytosis for rapid acquisition of nutrients to compensate for the delay in transcriptionally and translationally upregulating glucose and amino acid transporters.

Alternatively, macropinocytosis may be required for anabolic signaling functions instead of or in addition to provisioning substrates for biosynthesis from the extracellular space. Perhaps the most obvious way in which macropinocytosis may regulate cellular growth programs is by inducing activation of the mechanistic target of rapamycin complex 1 (mTORC1), a master regulator of cell growth and metabolism in eukaryotic cells. We will explore this possibility in the next chapter.

CHAPTER V:

T CELL MACROPINOCYTOSIS AND mTORC1[4]

5.1 ABSTRACT

The mechanistic target of rapamycin (mTOR) is a serine/threonine kinase that serves as the catalytic subunit of the mTOR 1 complex (mTORC1). mTORC1 nucleates a complex signaling network that detects and integrates environmental inputs such as growth factors, oxygen, amino acids, energetic stress signals, and others to regulate anabolism, catabolism, and growth. We hypothesized that in non-transformed primary T cells, macropinocytosis may be necessary for G1 phase growth, at least in part, because it delivers protein or free amino acids to the lysosome whereby they license mTORC1 activation and growth signaling. After confirming that macropinocytosis probes are targeted to lysosomes, we then demonstrated that mTORC1 signaling is sustained through 12 and 20 hours post-stimulation and abolished by treatment with the ATP-competitive mTOR inhibitor Torin 1. Addition of EIPA or J/B at 12 hours post-stimulation potently inhibited mTORC1 activation but not activation of the transcription factor NFkB. Additionally, inhibition of acute mTORC1 activation by EIPA in stimulated cells did not block activation of ERK/mitogen-activated protein kinases (MAPK). mTORC1 activation was also blocked by addition of the partial macropinocytosis inhibitors of macropinocytosis. Inhibition of lysosomal proteases had no effect on mTORC1 activation, suggesting protein

[4] The contents of this chapter were adapted and reproduced from the following publication: Charpentier, J. C. *et al.* Macropinocytosis drives T cell growth by sustaining the activation of mTORC1. *Nat Commun* **11**, 180 (2020).

degradation of macropinocytosed cargoes is not required for this event to occur. T cells stimulated for 12 hours, washed, and recultured for 2 hours in minimal medium with or without particular amino acids identified leucine and arginine as sufficient to sustain macropinocytosis-dependent mTORC1 activation. These findings suggested that under nutrient-replete conditions, macropinocytosis facilitates T cell growth, at least in part, by delivery of free amino acids to the lysosome, where they sustain the activation of mTORC1.

5.2 INTRODUCTION

mTORC1 is a multi-subunit protein complex that regulates metabolic homeostasis and cellular growth (accumulation of biomass) in response to diverse environmental and intracellular signals that converge on the lysosome. Aberrant mTORC1 signaling is associated with a range of human oncological malignancies and mTORC1 inhibitors are currently approved to treat some cancers.[286] Additionally, mTORC1 inhibition by rapamycin and other compounds produces potent immunosuppression, which has led to the use of these inhibitors in solid organ transplantation and autoimmune disease.[287]

The mTORC1 complex consists of the subunits mTOR, a serine/threonine kinase, mammalian lethal with SEC13 protein 8 (mLST8), an adaptor protein of unknown function thought to stabilize the active site of mTOR, the Tti1/Tel2 complex, a scaffolding protein important for complex assembly, and regulatory-associated protein of mTOR (Raptor), a subunit that rheostatically regulates the kinase activity of mTOR in response to growth factors, amino acids, energy, and other signals.[288,289] mTORC1 is inhibited by two endogenous proteins, DEP domain-containing mTOR-interacting protein (DEPTOR) and 40kDa Proline-rich Akt substrate (PRAS40).[290]

In the absence of PI3K signaling, the TSC complex, an oligomer consisting of tuberous sclerosis complex 1 (TSC1, hamartin), tuberous sclerosis complex 2 (TSC2, tuberin), and Tre2-Bub2-Cdc16-1 domain family member 7 (TBC1D7), represses mTORC1's catalytic activity.[291,292] Specifically, Rheb-GTP loading, required for mTORC1 kinase activation, is suppressed by the action of TSC2's GTPase-activating protein (GAP) domain.[292]

While mTORC1 integrates a wide variety of sensory inputs, it is especially sensitive to growth factor and amino acid signals. Growth factor binding to cell surface receptors activates a PI3K phosphorylation cascade that sequentially activates phosphoinositide-dependent kinase 1 (PDK1), then the serine/threonine kinase Akt (protein kinase B). Akt in turn phosphorylates and inhibits the TSC complex, relieving repression of Rheb GTP-loading. While GEFs for Rheb have yet to be discovered it is known that Rheb-GTP activates mTORC1 kinase activity allosterically, by interactions with mLST8 and the mTOR catalytic domain, whereas Rheb-GDP dissociates from the complex.[293,294] Some groups have noted that *in vivo* activation of cytotoxic T lymphocytes (CTLs) still occurs in the presence of pharmacological inhibitors of Akt, suggesting that PDK1 may signal to mTORC1 via other kinases in addition to Akt.[295]

Amino acids signal to mTORC1 through Rag GTPases. Under conditions of amino acid starvation or scarcity, mTORC1 is not enriched on the surface of lysosomes and is thought to be predominantly cytoplasmic.[296] The pentameric GEF Ragulator influences Rag heterodimers to mediate mTORC1 translocation to the surface of the lysosome, though how exactly this occurs is currently unclear. Historically it was thought to occur by GEF activity toward RagA/B, however a recent study as suggested it acts (along with SLC38A9) as an atypical GEF for RagC, inducing dissociation of GTP from RagC to promote activation.[297] SLC38A9 has also been suggested to exert GEF activity toward RagA/B, but a more recent cryo-electron microscopy study has reinforced the view that Rag dimer activation depends on modulation of RagC .[297,298]

Guanine nucleotide exchange in Rag GTPases is regulated by a variety of cytoplasmic amino acid sensors as well as by proteins resident in the lysosomal membrane. Cytoplasmic sensors include Sestrin1/2 and cytosolic arginine sensor for mTORC1 subunit 1 (CASTOR1). In the absence of leucine, Sestrin1/2 inhibit GTPase-activating protein (GAP) activity toward Rags-2 (GATOR2), a negative regulator of GTPase-activating protein (GAP) activity toward Rags-1 (GATOR1), a RagA/B GAP.[299,300] Upon binding leucine, Sestrin1/2-GATOR2 interaction is abolished, leading to inhibition of GATOR1.[299,300] Inhibition of GAP activity toward RagA/B induces lysosomal mTORC1 translocation where Rheb-GTP directly promotes mTORC1 activation. Additionally, Sestrin/2 show guanine dissociation inhibitor (GDI) activity for RagA/B.[301] Similarly, CASTOR1 homodimerizes to inhibit GATOR2 under conditions of arginine starvation, an interaction negated by CASTOR1 arginine binding.[302] At least one aminoacyl-tRNA synthetase also signals to mTORC1 as a moonlighting function: leucyl-tRNA synthetase (LARS1) promotes mTORC1 activation via GAP activity toward Rag GTPases and signaling through (Vps34)-phospholipase D1 (PLD1) in response to leucine binding.[303]

Genetic screens have also identified the proton-assisted amino acid transporter (PAT) or SLC36 family of amino acid transporters as having an especially strong influence on mTORC1 activation. PATs transport alanine, glycine, and proline by proton-coupled secondary active transport, are localized to late endosomes and lysosomes in a variety of cell types, and are thought to signal to mTORC1 by a transceptor mechanism.[304] It seems highly probable that additional mTORC1-regulating amino acid sensors will be discovered.

Amino acids within the lysosomal lumen can also signal to activate mTORC1. Lumenal amino acids have been shown to interact with the transmembrane V-ATPase, and a neutral amino acid transporter, Solute Carrier Family 38 Member 9 (SLC38A9), to influence Ragulator and Rag-GTP loading.[305] The ATPase activity of the V-ATPase has been shown to be necessary to communicate amino acid sufficiency signals to mTORC1, though it's not clear exactly how this occurs.[296] Also of note is SLC38A9's function as an intralysosomal cholesterol sensor; increases in lysosomal cholesterol are communicated by SLC38A9 to the Ragulator-Rag complex and this signal alone appears to be sufficient to promote mTORC1 translocation and activation at the lysosome.[306] Opposing this, the Niemann-Pick C1 (NPC1) protein binds the mTORC1 scaffolding complex directly and inhibits it in response to cholesterol depletion.[306]

Activation of mTORC1 promotes anabolism by directing the synthesis of nucleic acids, proteins, and lipids, and blocks catabolism by inhibiting autophagy, lipolysis, and β-oxidation.[296,307,308] mTORC1 kinase activity exerts its effects on cellular growth through its downstream effectors, such as ribosomal S6 kinase (S6K) and eukaryotic translation initiation factor 4E-binding protein (4E-BP). These proteins upregulate translation, splicing, proliferative signaling, and both ribosomal and mitochondrial biogenesis through multiple mechanisms.[309–311]

4E-BPs are translational repressors that in their unphosphorylated state sequester the eukaryotic translation initiation factor 4E (eIF4E). Upon 4E-BP phosphorylation by mTORC1, eIF4E binds another translation factor, eukaryotic translation initiation factor 4G (eIF4G), on the 5' end of mRNAs to promote cap-dependent translation.[312]

S6K is thought to promote translation by phosphorylating ribosomal S6 protein (rpS6), a protein component of the 40S eukaryotic ribosome, however, the exact role of rpS6 phosphorylation in promoting translation remains unclear after four decades of research.[313] S6K itself also influences translation by regulating transcription of ribosomal biogenesis genes.[314] rpS6 phosphorylation enhances the affinity of ribosomes for a particular class of mRNAs responsive to mTORC1-mediated nutrient signaling, those containing 5′-terminal oligopyrimidine tract structural motifs ('TOP mRNAs'), thereby promoting their translation.[315] In addition to its role in promoting translation, rpS6 also regulates glucose homeostasis and cell size.[316] mTORC1 signaling also enhances production of ATP and reducing equivalents by its regulation of mitochondrial biogenesis. It also promotes cell cycle progression by upregulating expression of cyclin D1 in a 4E-BP-dependent manner.[317,318]

mTORC1 exists in a double negative feedback loop with AMP activated protein kinase (AMPK), a cellular sensor of energy status. AMPK maintains energy homeostasis by regulation of the autophagy-initiating unc-51-like kinase 1 (ULK1) and antagonism of mTORC1 signaling.[319] Under conditions of glucose starvation, accumulation of AMP activates AMPK in a manner that depends on phosphorylation of the serine–threonine liver kinase B1 (LKB1).[320] Phosphorylated, activated AMPK then activates ULK1 to promote autophagy.[321] AMPK simultaneously inhibits mTORC1 signaling during energy stress by phosphorylation of its TSC2 and Raptor subunits.[322] LKB1-induced phosphorylation of TSC2 by AMPK enhances its Rheb-GAP activity, whereas phosphorylation of two conserved serine residues on Raptor inhibits mTORC1 activation.[322] Under nutrient-replete conditions, however, mTORC1 phosphorylation of ULK1 disrupts its interaction with AMPK, thereby inhibiting autophagy.[321]

mTORC1 in T cells

mTORC1 signaling in activated T cells integrates immunological, nutrient, and other environmental inputs to influence cell cycle progression, metabolic reprogramming, cell fate decisions, and effector functions.[323,324] Immunological inputs, chiefly cognate antigen recognition, co-stimulation of CD28 and OX40, and detection of inflammatory or homeostatic cytokines, all converge on the PI3K-Akt-TSC2 signaling axis and the activation of mTORC1.[325]

mTORC1 is activated in response to TCR ligation and this activity requires Rasgrp1.[326] Some evidence suggests that the magnitude of TCR signaling-induced activation of mTORC1 is directly proportional to the dose of cognate antigen and the duration of T cell-dendritic cell contact.[327,328] TCR-induced activation of mTORC1 is enhanced by CD28 co-stimulation and PI3K signaling. Its importance in T cell activation is highlighted by the phenotype of T cells with cell-specific knockout of mTOR or Raptor, which display growth and proliferation defects in response to CD3/28 stimulation.[329,330] mTORC1, along with PI3K and ERK (MAPK) signaling, significantly influences the metabolic reprogramming of nascently-activated T cells from oxidative phosphorylation to aerobic glycolysis and glutaminolysis chiefly through enhancing translation of the transcription factor c-Myc.[331] As previously discussed in **Chapter 4.2**, this metabolic switch is required to enable naïve T cells to become fully activated and to support subsequent proliferation to effector cells. In many cell types, mTORC1 activation upregulates mRNAs with particular features, such as 5' terminal oligopyrimidine tracts (5' TOPs), and transcriptomic profiles of different $CD4^+$ T cell populations reveal distinct translational

landscapes.[315,332] It's likely that mTORC1 signaling induced by TCR ligation also promotes the transition from a naïve cell translational program to an activated one.

mTORC1 also plays a critical role in $CD4^+$ and $CD8^+$ T cell differentiation. Genetic deletion of mTOR in the double-positive thymocyte stage profoundly impairs $CD4^+$ T cell differentiation and while TCR signaling appears unperturbed, mTOR-deficient T cells proliferate only slowly in response to stimulation and activation. Specifically, loss of mTOR signaling constrains $CD4^+$ lineage fate to $Foxp3^+$ regulatory T cells (Tregs), even under T_H1, T_H2, and T_H17-polarizing conditions.[329] Interestingly, deletion of Rheb in T cells does not preclude T_H2 differentiation but does preclude T_H1 and T_H17 differentiation under their respective polarizing conditions.[333] Deletion of other mTORC1 components in T cells produces even more puzzling defects: T cell-specific deletion of the Raptor subunit by generating mice with Raptor floxed alleles expressing Cre recombinase under the control of the Lck promoter produced $CD4^+$ T cells capable of differentiating into T_H1 cells but not T_H17 cells.[334] Another group used mice with Raptor floxed alleles expressing Cre under the control of the CD4 promoter and these mice were incapable of T_H1 or T_H2 differentiation.[335] mTOR signaling is also important for $CD8^+$ T cell differentiation: pharmacological inhibition of mTORC1 with rapamycin appears to paradoxically enhance $CD8^+$ T cell memory formation in the short-term, perhaps by upregulating lipid metabolism, but long-term blockade is associated with impaired memory cell formation.[336]

Clearly the relationship between mTORC1 signaling and T cell differentiation is complex and a thorough review of the topic is beyond the scope of this thesis. What this complexity underlines,

however, is the importance of mTORC1 for matching metabolic programs with developmental and differentiation ones.

The lysosome links macropinocytosis and mTORC1

Given the abundance of evidence from a variety of cell types documenting the trafficking to and fusion of mature macropinosomes with lysosomes, as well as the spatial regulation of mTORC1 by Rag-mediated lysosomal recruitment, we naturally posited that T cell macropinosomes are delivered to the lysosome where their cargoes promote growth by activating mTORC1. To investigate this we used an alternative BSA probe (DQ Red BSA) that is fluorogenic only when cleaved by lysosomal proteases, allowing us to test, using flow cytometry and confocal microscopy, the hypothesis that T cell macropinosomes are delivered to lysosomes.

Prior to this investigation little was known about mTORC1 kinetics in the first cell cycle of nascently-activated T cells. Considerable evidence has demonstrated the transduction of TCR and co-stimulatory signals to mTORC1, including by the CARMA1-Bcl10- MALT1 (CBM) signalosome, but it was unknown how long mTORC1 activation was sustained after TCR stimulation and co-stimulation.[337]

To investigate the kinetics of mTORC1 signaling in nascently-activated T cells we used phospho-flow cytometry, measuring the abundance of phosphorylated rpS6 as a downstream readout of mTORC1 activation. We predicted that mTORC1 signaling would be sustained through G1 phase and that its activation is required for the dramatic increases in growth in this period.

Given that input from multiple environmental sensors and several major signaling pathways all influence mTORC1 activation, it was conceivable that impairing the lysosomal delivery of macropinocytic cargoes would only modestly influence mTORC1 activation status. If, however, our hypothesis was correct—that macropinocytosis exerts such a profound effect on T cell growth primarily by influencing Rag-mediated mTORC1 recruitment and activation—then its inhibition by EIPA or J/B in the 12-20 hour period post-stimulation would be expected to terminate mTORC1 signaling. This is precisely what occurs when CSF1 or PMA-induced macropinocytosis in macrophages is inhibited by EIPA or J/B. We also expected that partial inhibitors of macropinocytosis would inhibit mTORC1 activation but perhaps to a lesser extent, given the less significant impacts these compounds had on 12-20 hour growth in prior experiments.

Furthermore, if mTORC1 inhibition occurs secondary to inhibition of macropinocytosis, it is important to ensure that this is not due to a general impairment or dysregulation of signaling through other T cell activation pathways, such as the MAPK and NFκB signaling pathways. Phospho-flow cytometry and Western blotting permits the monitoring of these pathways during G1 growth.

If delivery of macropinocytic cargoes to the lysosome sustains G1 phase mTORC1 activation, it's important to clarify the activating stimulus contained therein. One possibility is that, like oncogenic Ras-driven tumor cells, nascently-activated T cells use macropinocytosis to acquire extracellular protein, abundant in serum-supplemented growth media, and digest it in lysosomes

to yield amino acids that signal to the Ragulator-Rag complex to promote mTORC1 activation. Another possibility is that free amino acids or some other fluid-phase solute obtained by macropinocytosis is sufficient to activate mTORC1 and protein digestion is unnecessary. To test this we again utilized the DQ Red BSA probe, which functions as a lysosomal reporter, and a lysosomotropic agent, NH_4Cl, which at the appropriate concentration blocks acidification of the lysosome and thereby inhibits lysosomal proteolysis. Because free amino acids were abundant in the culture medium in addition to albumin and serum proteins, we predicted that macropinocytosis-dependent mTORC1 activation would not be impaired by inhibition of lysosomal protein digestion.

5.3 MATERIALS AND METHODS

Animals. Wild-type mice were bred in house and were on a mixed 129S6/SvEv X C57BL/6 genetic background. Mice ranged in age from 6 weeks to 3 months. Mice of both sexes were used in experiments. All experiments performed with mice were in compliance with University of Michigan guidelines and were approved by the University Committee on the Use and Care of Animals.

T cell macropinocytosis assays. Murine splenocytes or pan-T cells were isolated from wild-type mice and prepared as previously described except DQ Red BSA (Thermo Fisher) macropinocytosis probe was added to wells at final concentrations of 50μg/ml at the indicated times. Incubation with probes was for the indicated times at 37°C or 4°C. Pharmacological inhibitors were added to cultures 15 min prior to addition of macropinocytosis probes in a range of concentrations as indicated or at the following final concentration: NH_4Cl (Sigma), 10 mM.

Percentage inhibition of DQ Red BSA fluorescence in the presence of NH_4Cl was calculated as follows: [(Median fluorescence intensity (MFI) in absence of inhibitor at 37°C − MFI in presence of NH_4Cl at 37°C)/(MFI in absence of inhibitor at 37°C − MFI in absence of inhibitor at 4°C)] × 100.

Confocal microscopy. Murine pan-T cells were isolated and prepared as previously described except where noted they were also stained with rat anti-mouse LAMP-1 (eBioscience, clone 1D4B, cat. no. 14-1071-82, dilution 1:100), or LAMP-2 (Invitrogen, clone M3/84, cat. no. MA5–17861, dilution 1:100) mAb overnight at 4°C. For experiments testing inhibition of lysosomal proteolysis, cells were incubated in the presence or absence of DQ Red BSA (50 μg/ml) at 37°C or 4°C in the presence or absence of EIPA (50 μM) for a further 4 or 8 h post-stimulation.

Flow cytometric analysis of mTORC1 and NFκB activation. Murine splenocytes were stimulated as above for the indicated times in the presence or absence of inhibitors at concentrations indicated above. Cells were harvested, fixed in 4% paraformaldehyde for 20 min at room temperature, washed with PBS supplemented with 5% FCS, and permeabilized by drop-wise addition of ice-cold, 90% methanol with gentle vortexing. Cells were washed and stained with APC-Cy7- CD4, APC-CD8α and PE-Cy7-phospho-S6 mAb (Cell Signaling Technology, clone D57.2.2E, cat. no. 34411, dilution 1:50) or anti-phospho-NFκB p65 (pS356) (Cell Signaling Technology, clone 93H1, cat. no. 3033, dilution 1:100) followed by Alexa488-labeled donkey anti-rabbit secondary antibody (Jackson Immunoresearch, cat. no. 711-545-152, dilution 1:100) and analyzed by flow cytometry. The gating strategy is illustrated in the Appendix. In each experiment, the effect of inhibitors upon mTORC1 activation between 12 and 20 hours or

NFκB activation between 12 and 14 hours was calculated as a percentage of mTORC1 or NFκB activation observed in the absence of inhibitor as follows: [(MFI phospho-S6 or NFκB of CD3/28 stimulated T cells in presence of inhibitor - MFI phospho-S6 or NFκB of unstimulated T cells in absence of inhibitor)/(MFI phospho-S6 or NFκB of CD3/ 28 stimulated T cells in absence of inhibitor - MFI phospho-S6 or NFκB of unstimulated T cells in absence of inhibitor)] × 100.

For experiments that determined if AA were sufficient to sustain mTORC1 activation, splenocytes were stimulated for 12 h with CD3/28 mAb in RPMI 1640 with 10% FCS as above. Cells were then washed extensively in PBS and recultured in wells of 96 well U-bottomed plates at 1×10^6 cells per well in RPMI 1640 with 10% FCS, or with modified RPMI 1640 without AA (USBiological) to which different combinations of AA (Thermo Fisher or Sigma) had been added at the concentrations normally found in RPMI 1640. EIPA and J/B were added to some wells at the same concentrations indicated above. After 2 h, cells were harvested and analyzed for phospho-S6 by flow cytometry.

Western blotting. Purified splenic $CD4^+$ T cells were stimulated with Mouse T-Activator CD3/CD28 Dynabeads (Life Technologies) for the indicated times before cell disruption by boiling in reducing SDS-PAGE sample buffer. Activation of mTORC1, ERK MAPK and NFκB was determined by Western blotting using anti-phospho-S6 (Cell Signaling Technology, cat. no. 2211, dilution 1:1000), anti- p44/p42 MAPK (T202/Y204) (Cell Signaling Technology, clone E10, cat. no. 9106, dilution 1:1000), or anti-phospho IκBα (S32/36) (Cell Signaling Technology, clone 5A5, cat. no. 9246, dilution 1:1000) antibodies, respectively. Blots were stripped and

reprobed with antibodies against unphosphorylated MAPK (Cell Signaling Technology, clone 137F5, cat. no. 137F5, dilution 1:1000), S6 (Cell Signaling Technology, clone 54D2, cat. no. 2317, dilution 1:1000), or IκBα (Cell Signaling Technology, clone no. 9242, dilution 1:1000).

Statistical analysis. *P* values were calculated using Student's 1-sample or 2-sample 2-sided t-tests as appropriate for normally distributed data.

5.4 RESULTS

Macropinocytic cargoes are targeted to lysosomes

To determine if macropinosomes are trafficked to lysosomes, we performed uptake assays employing DQ Red BSA, a macropinocytosis probe of comparable size and mass to those previously used but one that that is fluorogenic only when cleaved by lysosomal proteases. **Figure 20a-b** displays representative flow cytometry histograms showing an increase in DQ Red BSA signal in CD3/28-stimulated murine $CD4^+$ (left) and $CD8^+$ (right) T cells between 12 and 18 hours post-stimulation. DQ Red BSA probe signal increased over the first four hours of probe incubation before reaching a steady-state at 16 hours post-stimulation. The mean ratio of DQ Red BSA fluorescence and SEM in DQ Red BSA probe signal in stimulated cells at 37°C vs. 4°C during hours 12-18 post-stimulation is shown in **Figure 20c**. For both $CD4^+$ and $CD8^+$ T cells, this ratio was approximately 3-4. To confirm lysosomal delivery of DQ Red BSA probe, we next incubated purified, CD3/28-stimulated, murine pan-T cells and $CD4^+$ T cells with DQ Red BSA probe during the period 12-16 hours post-stimulation, then imaged them by confocal microscopy per the method described in Methods and materials. Representative images from these experiments are shown in **Figure 20d**. In both purified pan-T cells (left) and $CD4^+$ T cells

(right), DQ Red BSA signal was detected (arrows) within lysosomes identified by co-staining for LAMP-1 (pan-T cells) or LAMP-2 ($CD4^+$ T cells), confirming macropinosome trafficking to lysosomes.

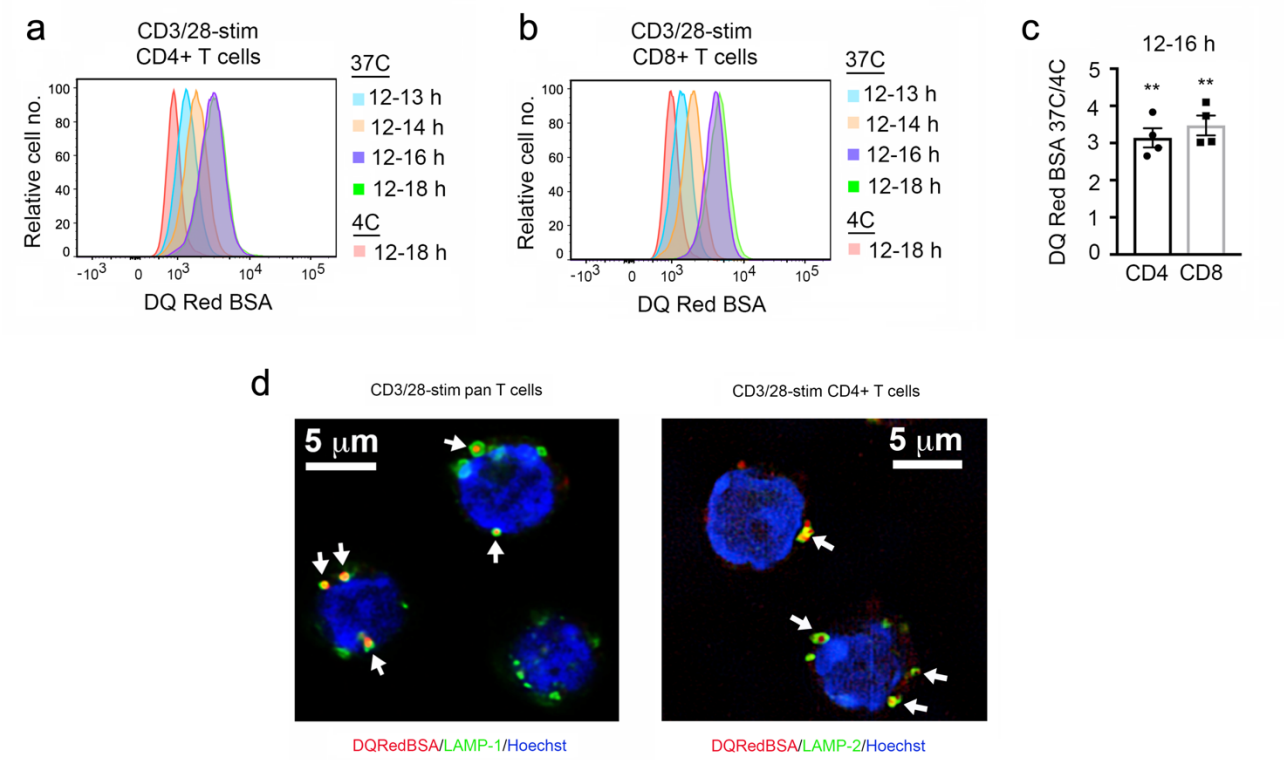

Figure 20 – DQ BSA is targeted to lysosomes in stimulated T cells. a-c Murine splenocytes were stimulated CD3/28 mAb for 12 hours before incubation with DQ Red BSA for the indicated times and at the indicated temperatures. Shown are representative flow cytometry histogram plots of DQ Red BSA fluorescence in $CD4^+$ (**a**) and $CD8^+$ T cells (**b**) and mean ± 1 SEM of the ratio of DQ Red BSA fluorescence in $CD4^+$ and $CD8^+$ T cells at 37°C or 4°C after probe incubation between 12 and 16 hours (**c**) (n = 4 independent experiments). $^{**}P < 0.01$ by Student's 1-sample, 2-sided *t*-test. **d** Purified pan T cells (left) or $CD4^+$ T cells (right) were stimulated with CD3/28 mAb for 12 hours before incubation with DQ Red BSA for 4 hours at 37°C. Traffic of DQ Red BSA to lysosomes was assessed by flow cytometry (**a-c**) and confocal microscopy (**d**). Flow cytometry data are representative of four independent experiments. Arrows in (**d**) show accumulation of DQ Red BSA in LAMP-1-positive or LAMP-2-positive lysosomes as determined by staining with respective antibodies. The mean percentage ± 1 SEM of LAMP-1-positive or LAMP-2-positive lysosomes that contained DQ Red BSA per cell was calculated at 77.3 ± 3.9 (n = 35 cells) and 84.9 ± 3.8 (n = 23 cells), respectively.

Activation of mTORC1 is dependent on macropinocytosis

Given the observed trafficking of macropinocytic cargoes to lysosomes (**Figure 20**) and the direct relationship between macropinocytosis and growth (**Figures 17-19**), we predicted that macropinocytosis drives growth in activated T cells by promoting activation of mTORC1. To test this prediction we first verified that mTORC1 is activated in nascently-activated T cells between 12 and 20 hours post-stimulation. To do this we measured fluorescence of phosphorylated ribosomal S6 protein (rpS6), a downstream effector of S6 kinase that is phosphorylated as a consequence of mTORC1 activation. As displayed in the representative flow cytometry histogram in **Figure 21**, unstimulated $CD4^+$ T cells do not exhibit mTORC1 activation (violet curve). In the absence of inhibitors, high levels of phosphorylated rpS6 is detected at 12 (green curve) and 20 hours (blue curve) post-stimulation, confirming sustained mTORC1 activation in this period. Addition of the selective mTORC1 inhibitor Torin 1 (500 nM) during hours 12-20 post-stimulation, however, abolishes mTORC1 activation as measured by phosphorylated rpS6 (red curve).

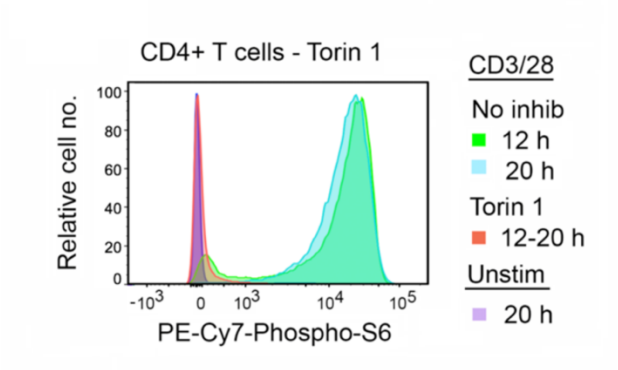

Figure 21 – Torin 1 inhibits ongoing G1 phase mTORC1 activation. Murine splenocytes were unstimulated or stimulated at 37°C with anti-CD3/28 mAbs for different times in the absence or presence of inhibitors added at 12 hours. The representative flow cytometry histogram shows relative amounts of phospho-S6 in $CD4^+$ T cells (n = 3 independent experiments).

We next sought to test the influence of macropinocytosis inhibitors on mTORC1 activation in primary $CD4^+$ and $CD8^+$ T cells. **Figure 22** shows representative flow cytometry histograms from experiments examining activation in $CD4^+$ T cells. $CD4^+$ T cells stimulated at 37°C by anti-CD3/28 mAbs recapitulated the robust mTORC1 activation 12 hours (red curve) and 20 hours (light blue curve) post-stimulation previously seen. Inhibition of macropinocytosis by addition of either 50 μM EIPA (top right) or 1/75 μM J/B (bottom left) at 12 hours post-stimulation, however, profoundly inhibits mTORC1 activation – an effect that increases over time but is apparent as soon as one hour after incubation with inhibitors. Inhibition of CME by incubation with PitStop 2 (bottom right) does not abolish mTORC1 activation but surprisingly enhances it by 20 hours post-stimulation.

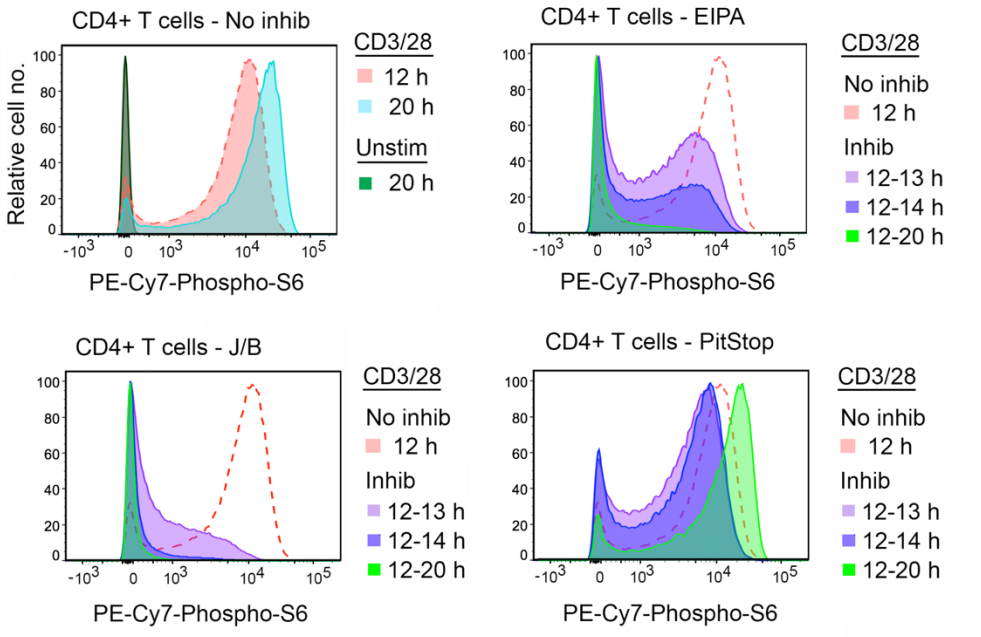

Figure 22 – Activation of mTORC1 is dependent on macropinocytosis in CD4$^+$ T cells. Murine splenocytes were unstimulated or stimulated at 37°C with CD3/28 mAb for different times in the absence or presence of inhibitors added at 12 hours. Relative amounts of phospho-S6 in CD4$^+$ T cells were determined by flow cytometry. All panels are from the same experiment. The red dashed line in each panel indicates the 12 hour positive control. Data are representative of 6 independent experiments performed with EIPA and three independent experiments performed with J/B and PitStop 2.

Similar results were obtained in experiments examining activation in $CD8^+$ T cells. **Figure 23** summarizes these results in representative flow cytometry histograms. $CD8^+$ T cells stimulated at 37°C by anti-CD3/28 mAbs also exhibit robust mTORC1 activation 12 hours post-stimulation (top left, red curve). As with $CD4^+$ T cells, activation was sustained and enhanced in the period from 12 to 20 hours post-stimulation and addition of either 50 μM EIPA (top right) or 1/75 μM J/B (bottom left) at hours post-stimulation similarly inhibited mTORC1 activation. Inhibition of CME in these cells did not block mTORC1 activation and, as with $CD4^+$ T cells, activation was not blocked but CME inhibition 20 hours post-stimulation, but was instead enhanced (bottom right).

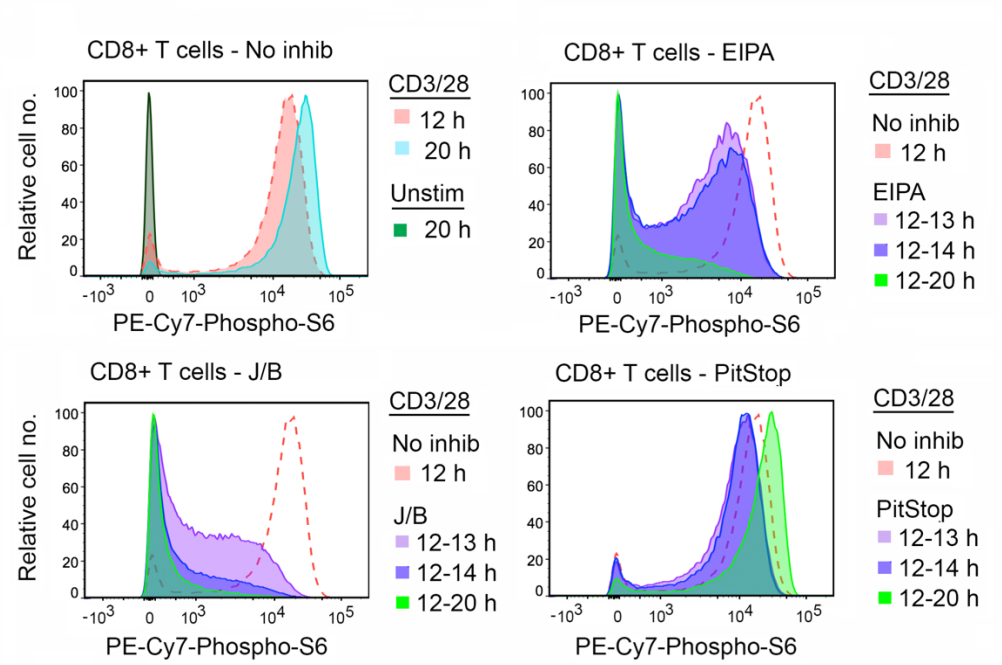

Figure 23 – Activation of mTORC1 is dependent on macropinocytosis in CD8$^+$ T cells. Murine splenocytes were unstimulated or stimulated at 37°C with CD3/28 mAb for different times in the absence or presence of inhibitors added at 12 hours. Relative amounts of phospho-S6 in CD4$^+$ T cells were determined by flow cytometry. All panels are from the same experiment. The red dashed line in each panel indicates the 12 hour positive control. Data are representative of 6 independent experiments performed with EIPA and three independent experiments performed with J/B and PitStop 2.

In both $CD4^+$ and $CD8^+$ T cells, inhibition of mTORC1 activation in the period 12-20 hours post-stimulation was directly proportional to the concentration of macropinocytosis inhibitors (EIPA and J/B) used. This reproducible dose-response relationship is summarized in **Figure 24**.

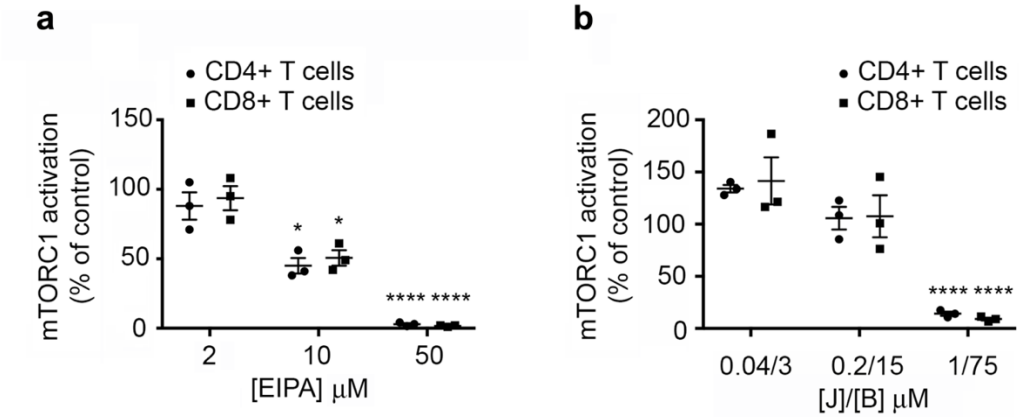

Figure 24 – Inhibition of macropinocytosis blocks mTORC1 activation in a dose-dependent manner. Murine splenocytes were stimulated at 37°C with CD3/28 mAb for 20 hours in the absence or presence of EIPA (**a**) and J/B (**b**) that were added to cultures at 12 hours. Mean percentage ± SEM of mTORC1 activation at 20 hours (n = 3 independent experiments). **P* < 0.05, ***P* < 0.01, ****P* < 0.001, *****P* < 0.0001 by Student's 1-sample, 2-sided *t*-test.

To examine mTORC1 signaling kinetics in acutely activated cells treated with macropinocytosis inhibitors, we performed experiments evaluating levels of phosphorylated rpS6 over time in the presence or absence of 50 μM EIPA. As the representative flow cytometry histograms in **Figure 25a** illustrate, after one hour of stimulation in the presence of EIPA (orange curves), mTORC1 activation in $CD4^+$ T cells is already significantly attenuated compared to the positive control condition (red curves) and is even lower than the signal measured in unstimulated cells (blue curves). By two hours post-stimulation, the phosphorylated rpS6 signal is nearly entirely abolished in EIPA-treated cells and remains so through three hours post-activation. **Figure 25b** shows a quantitation of repeated experiments in both $CD4^+$ and $CD8^+$ T cells confirming that mTORC1 signaling is immediately abolished by inhibition of macropinocytosis with EIPA.

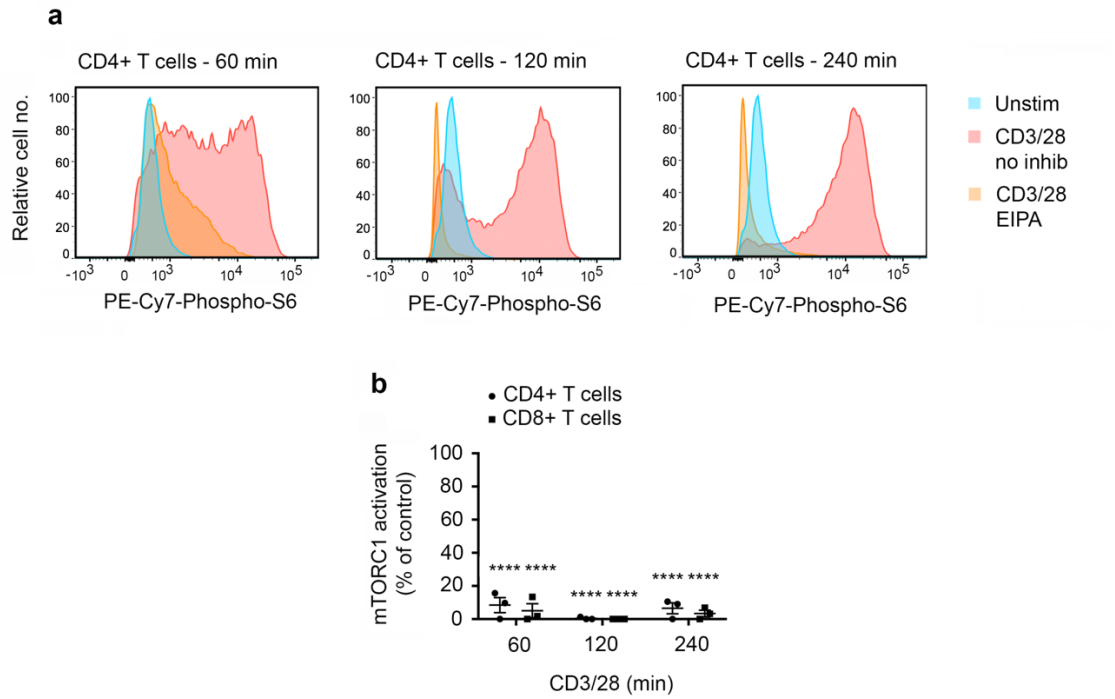

Figure 25 – EIPA inhibits mTORC1 in activated CD4$^+$ and CD8$^+$ T cells. Murine splenocytes were stimulated at 37°C with anti-CD3/28 mAbs for the indicated times in the presence or absence of EIPA added at culture initiation. Relative amounts of phospho-S6 in CD4$^+$ and CD8$^+$ T cells were determined by flow cytometry. **a** Shown are representative plots and mean ± SEM of the percentage of mTORC1 activation at each time point for CD4$^+$ and CD8$^+$ T cells (n = 3 independent experiments). **b** ****$P < 0.0001$ by Student's 1-sample, 2-sided *t*-test.

We next tested the influence of partial inhibitors of macropinocytosis on mTORC1 activation in the period 12-20 hours post-stimulation. $CD4^+$ and $CD8^+$ T cells stimulated for 12 hours were incubated with various inhibitors of macropinocytosis for additional 8 hours prior to analysis by flow cytometry. As shown in **Figure 26**, all inhibitors of macropinocytosis, including those with only a modest effect, potently inhibited mTORC1 activation, measured as a percentage of phosphorylated rpS6 signal detected in uninhibited controls. Nearly all of these inhibitors blocked mTORC1 activation as effectively as the selective mTORC1 inhibitor Torin 1 in both $CD4^+$ and $CD8^+$ T cells. Incubation with the CME inhibitor PitStop 2, however, had no significant effect.

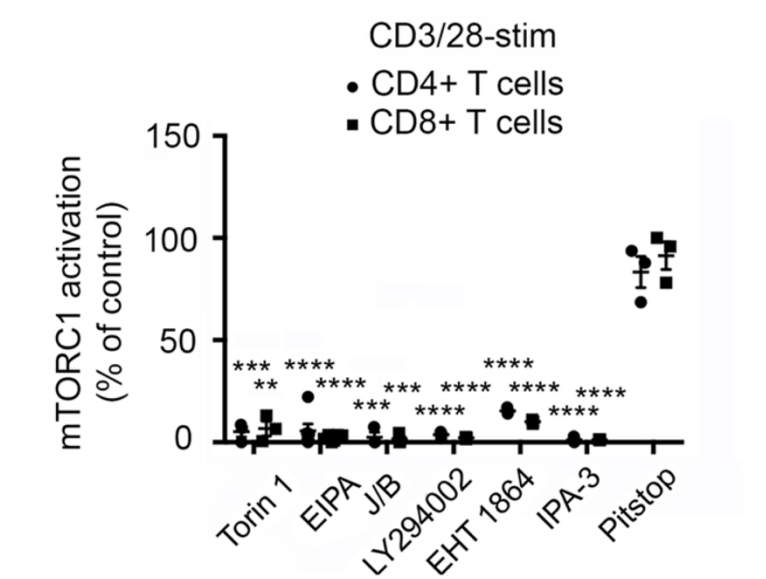

Figure 26 – Inhibition of macropinocytosis blocks mTORC1 activation. Murine splenocytes were stimulated with CD3/28 mAb at 37°C for 20 hours in the absence or presence of the indicated inhibitors that were added to cultures at the 12 hour time point. Mean ± SEM of the percentage of mTORC1 activation at 20 hours relative to the positive control following addition of inhibitors at 12 hours calculated as indicated in Methods and materials (EIPA, n = 6, all other inhibitors, n = 3). ***P* < 0.01, ****P* < 0.001, *****P* < 0.0001 by Student's 1-sample, 2-sided *t*-test.

Inhibition of macropinocytosis does not impair signaling through other T cell pathways

To ensure that the observed inhibition of mTORC1 signaling by macropinocytosis inhibitors was specific and not the consequence of interference and derangement of the activity of other signaling pathways required for T cell activation, we performed flow cytometry assays examining the impact of macropinocytosis inhibitors on activation of the transcription factor NFκB. **Figure 27a** and **c** display representative flow cytometry histograms showing the influence of EIPA and J/B, respectively, on phosphorylation of NFκB in $CD4^+$ (left) and $CD8^+$ (right) T cells. Cells stimulated with anti-CD3/28 mAbs for 12 hours were incubated an additional 2 hours in the presence or absence of 50 μM EIPA (**a**) or 1/75 μM J/B (**c**), then stained with a phospho-specific antibody to NFκB. Incubation with EIPA in this period did not impair NFκB activation and, in the case of $CD4^+$ T cells, significantly enhanced it. This can be seen in the quantitation shown in **c** expressing NFκB activation in the presence of EIPA as a percentage of the activation observed in uninhibited controls. The influence of EIPA on activation of NFκB in $CD8^+$ T cells was marginal. Similarly, treatment with J/B 12-14 hours post-stimulation did not decrease NFκB activation in $CD4^+$ (left) or $CD8^+$ (right) T cells either but instead significantly enhanced it in both, as can be seen in **c** and **d**.

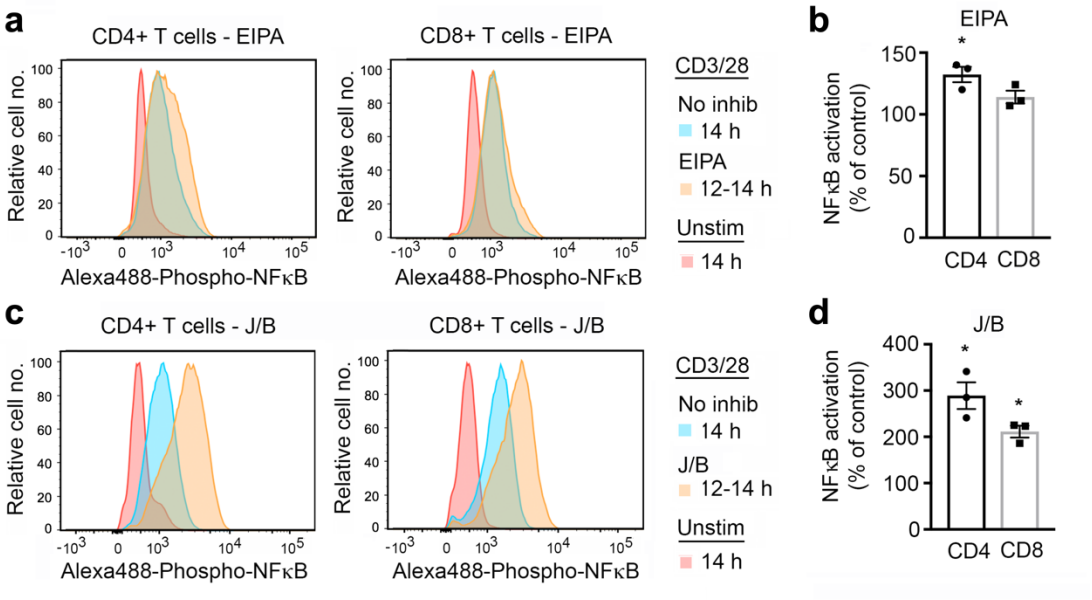

Figure 27 – Inhibition of macropinocytosis does not impair NFκB activation. Murine splenocytes were stimulated with anti-CD3/28 mAbs at 37°C for 14 hours in the absence or presence of the indicated inhibitors that were added to cultures at 12 hours. EIPA was used at 50 μM and J/B was used at 1/75 μM. Relative amounts of phosphorylated NFκB in $CD4^+$ and $CD8^+$ T cells at 14 hours were determined by flow cytometry. **a, c** Representative flow cytometry histograms showing effect of EIPA and J/B upon phosphorylated NFκB. **b, d** Mean ± 1 SEM of the percentage of NFκB activation 14 hours relative to the positive control (see Methods and materials). n = 3 independent experiments. **P* < 0.05, by Student's 1-sample, 2-sided *t*-test.

To confirm that inhibition of mTORC1 signaling secondary to inhibition of macropinocytosis is specific and does not impede signaling during the acute phase of T cell activation, we stimulated purified splenic $CD4^+$ T cells with anti-CD3/28 mAbs at 37°C in the presence and absence of EIPA, then analyzed the impact on mTORC, ERK (MAPK) and NFκB signaling in the first two hours post-stimulation by Western blot. Results from these experiments are shown in **Figure 28.**

Figure 28a shows results from two experiments (left, right) measuring the impact of EIPA on mTORC1 signaling in nascently-activated $CD4^+$ T cells after 10, 30, 60, and 120 minutes post-stimulation using a phospho-specific antibody to detect phosphorylated rpS6. The magnitude of phospho-specific signals as measured by densitometry were normalized to expression of the corresponding non-phosphorylated species (in this case rpS6) as measured following blot stripping and re-probing with specific antibodies to the non-phosphorylated species. Below the EIPA tracks are calculated ratios of normalized phospho-signals in EIPA-treated to non-treated T cells for each time point. These panels corroborate flow cytometry studies demonstrating inhibition of mTORC1 activation by EIPA.

Figure 28b shows two similar experiments (left, right) examining the impact of EIPA on ERK (MAPK) signaling in nascently activated $CD4^+$ T cells. Addition of EIPA to these cultures did not inhibit ERK (MAPK) phosphorylation and in one experiment (left) markedly enhanced it within the first hour post-stimulation.

Lastly, **Figure 28c** shows two experiments (left, right) measuring the influence of EIPA on NFκB signaling in nascently-activated $CD4^+$ T cells. Phosphorylation of IκBα, a readout of

NFκB activation, was not impaired by addition of EIPA to cultures, but was instead enhanced. Taken together, results from experiments summarized in **Figure 27** and **Figure 28** suggest that selective inhibition of activated T cell macropinocytosis significantly impairs mTORC1 signaling but not other major signaling pathways necessary for full T cell activation.

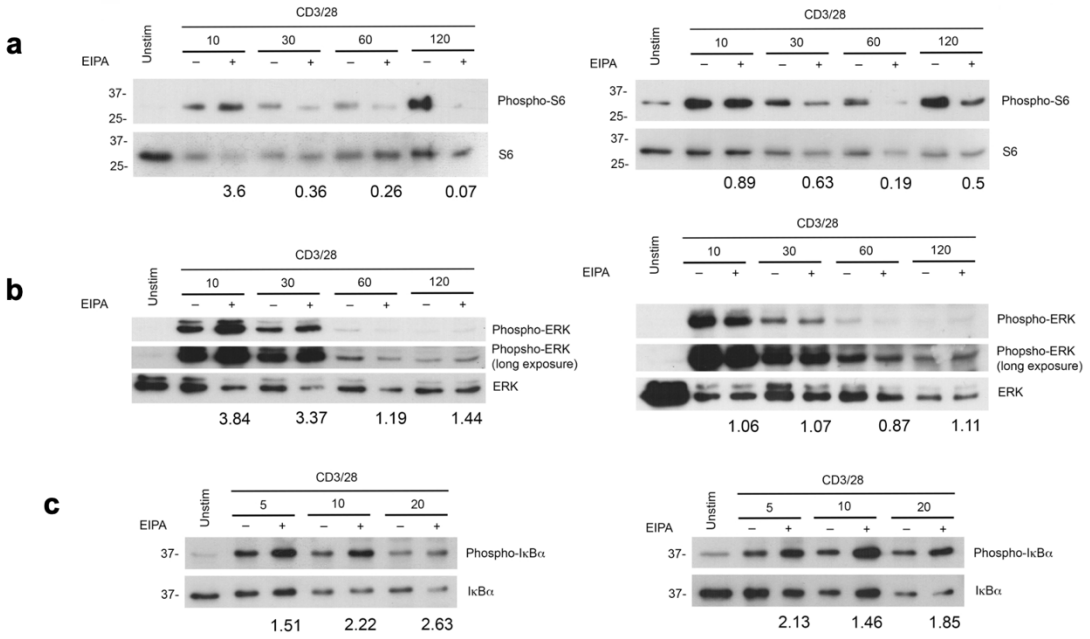

Figure 28 – Macropinocytosis inhibitors block mTORC1 activation but do not impair acute ERK (MAPK) or NFκB signaling in activated CD4$^+$ T cells. Purified splenic CD4$^+$ T cells were stimulated with anti-CD3/28 mAbs at 37°C for the indicated times (in min) in the presence or absence of EIPA added at culture initiation. Activation of mTORC1 (**a**), ERK (MAPK) (**b**) and NFκB (**c**) was determined by Western blotting using phospho-specific-S6, -ERK, and -IκBα antibodies respectively. The magnitude of phospho-signals was normalized to the amounts of corresponding non-phosphorylated species following blot stripping and re-probing with specific antibodies. Numbers below EIPA tracks represent the ratio of normalized phospho signals of EIPA-treated to non-treated T cells at each time point of anti-CD3/28 mAbs stimulation. Shown are repeat experiments for each molecular species.

NH_4Cl inhibits lysosomal digestion of DQ Red BSA probe

We next sought to understand whether proteolysis of macropinocytic cargoes being delivered to lysosomes was necessary to activate mTORC1 during G1 growth in murine T cells. First we used flow cytometry to demonstrate that the lysosomotropic agent NH_4Cl effectively inhibits lysosomal proteases at a concentration of 10 mM. To test this, we stimulated murine splenocytes with anti-CD3/28 mAbs for 12 hours at 37°C or 4°C followed by incubation with DQ Red BSA probe for an additional 4 hours in the presence or absence of NH_4Cl. **Figure 29a-b** shows representative flow cytometry histograms from experiments with stimulated $CD4^+$ (left) and $CD8^+$ (right) T cells. At 4°C no probe is internalized but at 37°C it is ingested by macropinocytosis, trafficked to lysosomes, and degraded by proteases to generate a strong fluorescent signal. Addition of NH_4Cl to cultures prior to probe incubation, on the other hand, results in a negligible fluorescent signal, confirming inhibition of lysosomal proteases. **Figure 29c** displays a quantitation of the nearly complete inhibition of DQ Red BSA fluorescence by NH_4Cl in $CD4^+$ and $CD8^+$ T cells.

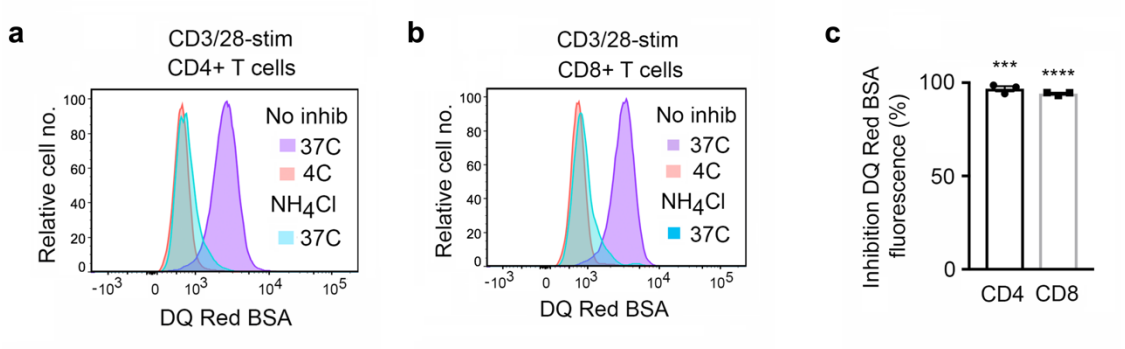

Figure 29 – NH_4Cl potently inhibits DQ Red BSA fluorescence. Murine splenocytes were stimulated with CD3/28 mAb at 37°C for 12 hours followed by incubation with DQ Red BSA for 4 hours at the indicated temperatures in the presence or absence of NH_4Cl. **a, b** Representative flow cytometry histograms of DQ Red BSA fluorescence in $CD4^+$ (**a**) and $CD8^+$ (**b**) T cells. **c** Mean percentage ± 1 SEM of inhibition of DQ Red BSA fluorescence in $CD4^+$ and $CD8^+$ T cells in the presence of NH_4Cl calculated as described in Methods and materials (n = 3 independent experiments). ***$P < 0.001$, ****$P < 0.0001$ by Student's 1-sample, 2-sided *t*-test.

Lysosomal proteolysis is not required for macropinocytosis-dependent mTORC1 activation

To determine if lysosomal proteolysis is required for macropinocytic cargoes to activate mTORC1 in stimulated murine $CD4^+$ and $CD8^+$ T cells, we stimulated murine splenocytes at 37°C with anti-CD3/28 mAbs for 12 hours then incubated them for an additional 8 hours in the presence or absence of EIPA or NH_4Cl. **Figure 30** shows results from these experiments. **Figure 30a-b** shows representative flow cytometry histograms displaying phosphorylated rpS6 signals from these experiments in $CD4^+$ (left) and $CD8^+$ (right) T cells. Addition of NH_4Cl had no significant impact on phosphorylated rpS6 levels, suggesting the activity of lysosomal proteases is not necessary for macropinocytic cargoes to activate mTORC1 (purple, violet curves). By contrast, addition of EIPA in the period 12-20 hours post-stimulation dramatically impaired mTORC1 signaling as measured by phosphorylated rpS6 (green curves). **Figure 30c** shows the percentage of mTORC1 activation at 20 hours relative to the no inhibitor positive control following addition of NH_4Cl at 12 hours. As can be seen, 12-20 hour inhibition of lysosomal proteolysis by NH_4Cl had no significant impact on mTORC1 activation.

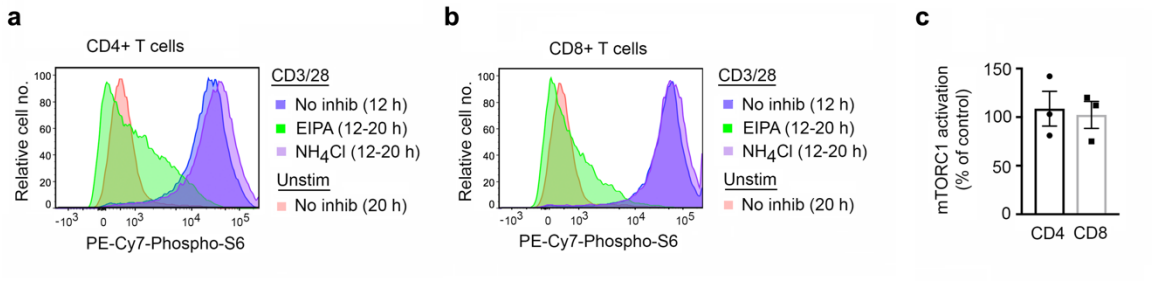

Figure 30 – Lysosomal proteolysis is not required for macropinocytosis-dependent mTORC1 activation. Murine splenocytes were stimulated with anti-CD3/28 mAbs for 12 hours followed by incubation for 8 hours at 37°C in the presence or absence of EIPA or NH_4Cl. **a, b** Representative flow cytometry histogram of phospho-S6 levels in $CD4^+$ (**a**) and $CD8^+$ (**b**) T cells. **c** Mean ± 1 SEM of the percentage of mTORC1 activation at 20 hours relative to the positive control following addition of NH_4Cl at 12 hours calculated as indicated in Methods and materials (n = 3 independent experiments).

Given that lysosomal protein degradation was not necessary for macropinocytic cargoes to activate mTORC1, we hypothesized that they contained free amino acids that are both necessary and sufficient to promote mTORC1 activation in $CD4^+$ and $CD8^+$ T cells. To investigate this we stimulated murine splenocytes (in complete medium; RPMI plus FCS) with anti-CD3/28 mAbs at 37 C for 12 hours, then thoroughly washed them prior to reculturing in minimal RPMI media containing 1) all 20 proteinogenic amino acids, 2) the four amino acids leucine, glutamine, arginine, and serine (LQRS), and 3) no amino acids. In addition, 50 μM EIPA was added to or absented from the cultures and they were allowed to grow for an additional two hours in the amino acid-supplemented (or not) minimal media. At 14 hours post-stimulation, phosphorylated rbS6 was measured by flow cytometry.

Figure 31a shows representative flow cytometry histograms from one experiment with stimulated $CD4^+$ T cells. Reculture for two additional hours in the same complete medium as was used for the first 12 hours resulted in sustained mTORC1 activation (top, middle), as expected, and this signal was significantly inhibited by EIPA administration in the 12-14 hour post-stimulation period. Absenting serum (FCS) from the medium did not impair mTORC1 signaling in this period either, so long as all amino acids were present (top, right; violet curve). mTORC1 signaling in these cells remained sensitive to EIPA treatment (top, right; blue curve). In splenocytes re-cultured for two additional hours in serum-free minimal medium containing no amino acids, mTORC1 signaling fell dramatically compared to hour 12 levels (bottom, right; violet curve). Reculture for hours 12-14 post-stimulation in serum-free minimal medium containing only LQRS at the same concentrations they appear in commercial RPMI media, was

sufficient to sustain mTORC1 activation (bottom, left; violet curve). This signal was also inhibited by treatment with EIPA (bottom, left; blue curve).

Parallel experiments showed that mTORC1 activation in these minimal, amino acid-containing media was also sensitive to inhibition by J/B. **Figure 31b** shows data from many experiments showing the ability of 20 amino acid- and LQRS-supplemented media preparations to significantly sustain mTORC1 activation in stimulated $CD4^+$ T cells, as well as the inhibitory effect of macropinocytosis inhibitors on it.

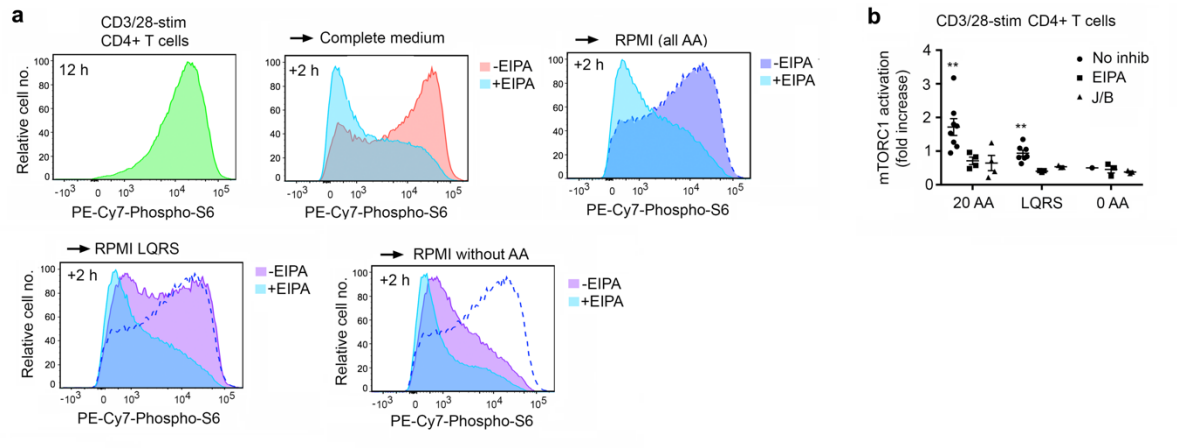

Figure 31 – Macropinocytosis delivers to CD4$^+$ T cells free amino acids necessary for the sustained activation of mTORC1. Murine splenocytes were stimulated at 37°C with anti-CD3/28 mAbs in complete medium (RPMI plus FCS) for 12 hours, washed, and recultured in the indicated media for 2 hours in the presence or absence of EIPA. **a** Representative flow cytometry histograms show phosphorylated rpS6 levels in CD4$^+$ T cells. All panels are from the same experiment. The mid-blue-dashed line indicates all amino acids in the absence of EIPA. **b** Mean ± 1 SEM of the fold increase in mTORC1 activation in CD4$^+$ T cells at 14 hours relative to the 0 amino acid control in the absence of inhibitors (n = 8 and 7 independent experiments for 20 amino acids and LQRS, respectively, in the absence of inhibitors; n = 4 for 20 amino acids and n = 3 independent experiments for LQRS and 0 amino acids in the presence of inhibitors). $^{**}P < 0.01$ by Student's 1-sample, 2-sided *t*-test.

Similar results were obtained with $CD8^+$ T cells stimulated for 12 hours with anti-CD3/28 mAbs in complete medium, then cultured in the same serum-free minimal media containing custom amino acid formulations. As **Figure 32a** shows, reculture for hours 12-14 in minimal medium with all 20 amino acids sustains mTORC1 activation as measured by phosphorylated rpS6 (left, violet curve) and this signal was inhibited by EIPA treatment (left, blue curve). The mTORC1 signal could not be maintained by reculture for two hours in minimal medium containing no amino acids (right, violet curve), and was as low as that seen in EIPA-treated cells (right, blue curve). Reculture in medium containing only LQRS did significantly sustain mTORC1 activation (middle, violet curve), an effect that was inhibited by EIPA (middle, blue curve). **Figure 32b** shows data from many experiments demonstrating the ability of 20 amino acid- and LQRS-supplemented media preparations to significantly activate mTORC1 in stimulated $CD8^+$ T cells relative to zero amino acid negative controls. The reproducible inhibitory effect of EIPA and J/B is also shown.

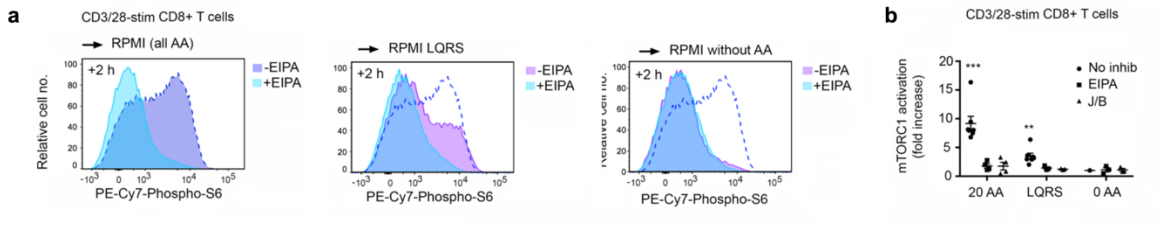

Figure 32 – Macropinocytosis delivers to CD8$^+$ T cells free amino acids necessary for the sustained activation of mTORC1. Murine splenocytes were stimulated at 37°C with CD3/28 mAb in complete medium (RPMI plus FCS) for 12 hours, washed, and recultured in the indicated media for 2 hours in the presence or absence of EIPA. **a** Representative flow cytometry histograms show phosphorylated rpS6 levels in CD8$^+$ T cells. All panels are from the same experiment. The mid-blue-dashed line indicates all amino acids in the absence of EIPA. **b** Mean ± 1 SEM of the fold increase in mTORC1 activation in CD8$^+$ T cells at 14 hours relative to the 0 amino acid control in the absence of inhibitors (n = 8 and 7 independent experiments for 20 amino acids and LQRS, respectively, in the absence of inhibitors; n = 4 for 20 amino acids and n = 3 independent experiments for LQRS and 0 amino acids in the presence of inhibitors). $^{**}P < 0.01$ by Student's 1-sample, 2-sided *t*-test.

mTORC1 activation is most sensitive to leucine and arginine detection

Experimental results suggested that, in stimulated $CD4^+/CD8^+$ T cells, macropinocytosis delivers the amino acids L, Q, R, and S to lysosomes. There they signal in an inside-out fashion to the Ragulator-Rag complex to promote the activation of mTORC1. To better understand if mTORC1 activation was dependent on and sensitive to particular amino acids we conducted similar 12-14 hour post-stimulation reculture experiments using minimal media preparations and custom amino acid formulations. Each formulation contained all 20 amino acids except one, to test the sensitivity of mTORC1 to its absence. Murine splenocytes were stimulated for 12 hours at 37°C with anti-CD3/28 mAbs, washed thoroughly, and recultured for an additional two hours in the serum-free minimal media preparations indicated in **Figure 33a**. In these cultures, absenting serine (S) and glutamine (Q) did not significantly impair mTORC1 activation. By contrast, mTORC1 activation was substantially impaired in cells recultured in minimal media lacking arginine (R) or leucine (L). Results from multiple experiments demonstrated this finding was reproducible in $CD4^+$ and $CD8^+$ T cells, and these data are summarized in **Figure 33b**. Taken together, these experiments suggested that G1 phase mTORC1 activation in stimulated T cells is most sensitive to arginine (R) and leucine (L) amino acid inputs.

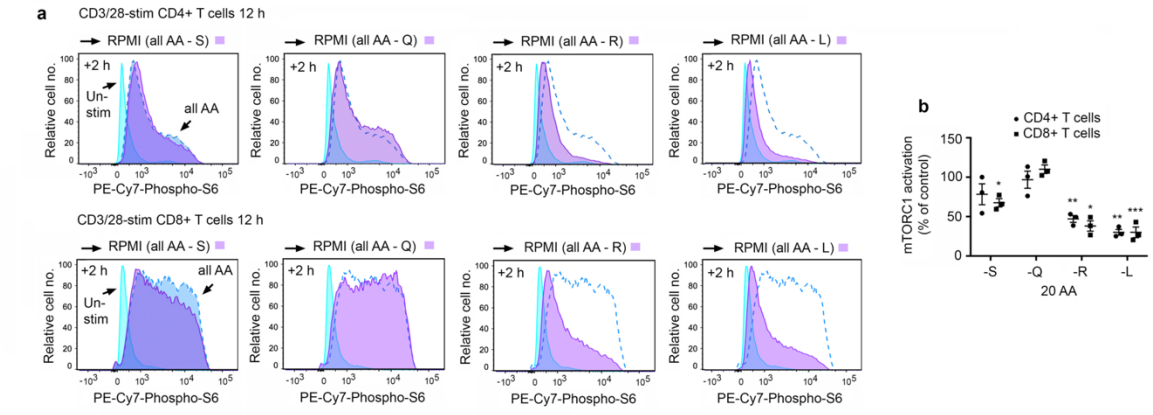

Figure 33 – Leucine or arginine are sufficient to sustain mTORC1 signaling in activated T cells. a, b Murine splenocytes were stimulated at 37°C with anti-CD3/28 mAbs in complete medium (RPMI plus FCS) for 12 hours, washed, and recultured in the indicated media for two additional hours. a Representative flow cytometry histograms show phosphorylated rpS6 levels in $CD4^+$ and $CD8^+$ T cells. All panels are from the same experiment. The mid-blue-dashed line indicates all amino acids. The light blue histogram indicates negative control unstimulated T cells at 12 hours. b Mean ± 1 SEM of the percentage mTORC1 activation in $CD4^+$ and $CD8^+$ T cells at 14 hours relative to the all 20 amino acids control (n = 3 independent experiments). $*P < 0.05$, $**P < 0.01$, $***P < 0.001$ by Student's 1-sample, 2-sided *t*-test.

A model of mTORC1 activation in nascently-activated T cells

Figure 34 shows a model of mTORC1 activation in nascently-activated T cells. Multiple signals are required for full activation of mTORC1. One set of signals, from immunological inputs such as the TCR, co-stimulatory receptors, and cytokine receptors, converge on activation of the PI3K-Akt-TSC2 pathway to promote Rheb-GTP-loading. Another is the set of amino acid sensors converging on the Ragulator-Rag complex to promote translocation of mTORC1 to the lysosome and Rag heterodimer guanine nucleotide exchange. Macropinosomes are critical components of the amino acid sensing machinery in activated T cells, reporting on amino acid sufficiency in the extracellular space and sustaining the activation of mTORC1.

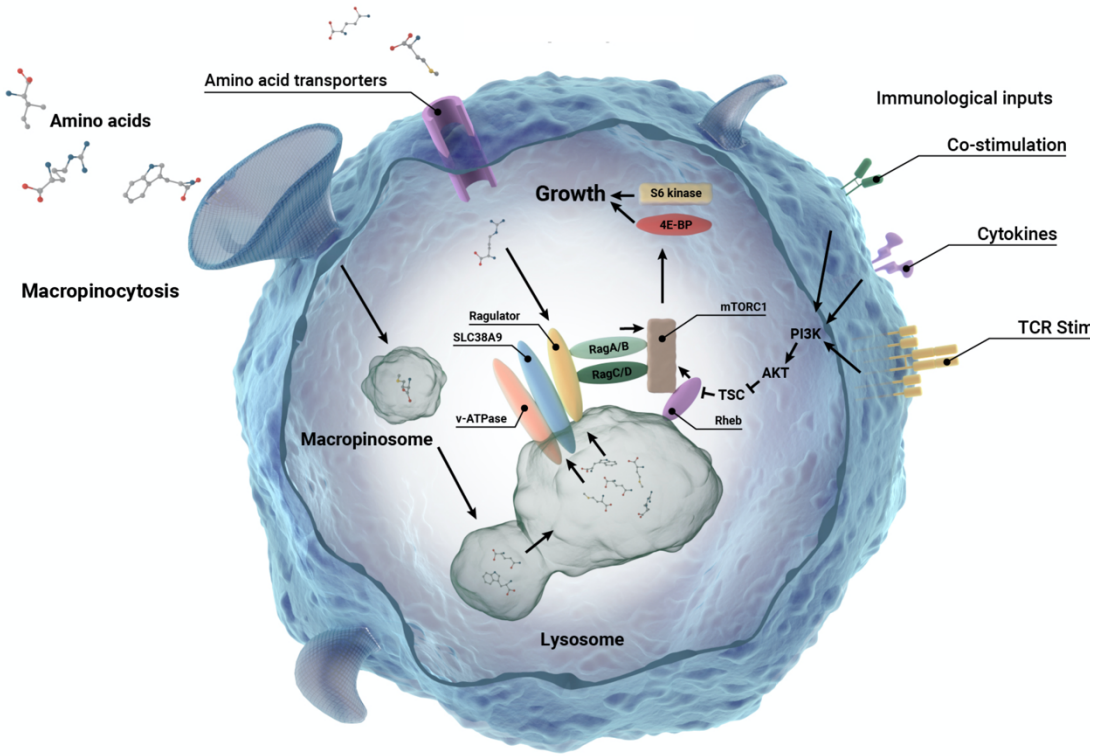

Figure 34 – Model of mTORC1 activation in stimulated T cells. Macropinocytosis delivers free amino acids from the extracellular space to lysosomes in T cells where they modulate the activity of the Ragulator complex, resulting in recruitment of mTORC1 to the lysosomal membrane. PI3K signals emanating from cell surface receptors lead to activation of the Rheb small GTPase on lysosomes, which, in turn, activates localized mTORC1. mTORC1 phosphorylates, among other targets, p70 S6 kinase and 4E-BP, which promotes anabolic processes and T cell growth. Amino acid transporters in T cells permit entry of amino acids into the cytosol where they are detected by cytosolic amino acid sensors that provide additional necessary signals for mTORC1 activation. Figure illustration by Shaun Donnelly.

5.5 DISCUSSION

As with many other eukaryotic cell types, T cell macropinosomes are delivered to lysosomes. As **Figure 21** shows, lysosomal DQ Red BSA fluorescence increased in both stimulated $CD4^+$ (**a**) and $CD8^+$ T (**b**) cells in the period 12-16 hours post-stimulation until reaching a steady state at 16 hours. At 16 hours post-stimulation the rate of probe delivery to and degradation within lysosomes appears to have equalized. Confocal microscopy of purified pan-T cells and $CD4^+$ T cells (**d**) confirmed delivery of probe to perinuclear organelles delimited by the lysosomal markers LAMP-1 and LAMP-2.

Phospho-flow cytometry monitoring phosphorylated rpS6 showed that mTORC1 is activated in $CD4^+$ and $CD8^+$ T cells at 12 hours post-stimulation and that activation is sustained through 20 hours post-stimulation (**Figures 21-23**). Crucially, mTORC1 activation was inhibited by addition of macropinocytosis inhibitors at 12 hours post-stimulation (**Figures 22-23**). mTORC1 inhibition by EIPA and J/B was profound, producing dramatic reductions in phosphorylated rpS6 within 1 hour and increasing in effect through 20 hours post-stimulation. Testing a range of EIPA and J/B concentrations for their impact on mTORC1 activation in this interval revealed a strong dose-response relationship where increasing concentration of inhibitor(s) produced corresponding reductions in mTORC1 activation (**Figure 24**). This trend closely resembled those seen when the same range of inhibitor concentrations were tested for their impacts on probe internalization (**Figure 10**) and 12-20 hour growth in stimulated cells (**Figure 17**).

As expected, mTORC1 signaling is strongly activated in the setting of acute stimulation. Levels of phosphorylated rpS6 are elevated in $CD4^+$ and $CD8^+$ T cells within one hour of stimulation

with anti-CD3/28 mAbs, increase over two hours, and remain high 4 hours post-stimulation (**Figure 25a**). Addition of EIPA 15 minutes prior to stimulation, however, profoundly impairs mTORC1 activation one hour later and by two hours post-stimulation the activation signal in EIPA-treated cells is essentially abolished (**Figure 25a-b**). We noted that inhibition of macropinocytosis blocks mTORC1 activation even more profoundly than the low level of activation seen in unstimulated, quiescent cells. It's possible that the marginal mTORC1 activation seen in unstimulated cells is related to their low-level, constitutive macropinocytosis, though this is not a possibility we investigated further.

Consistent with the observed effect of EIPA on mTORC1 activation, partial inhibitors of macropinocytosis also profoundly inhibited mTORC1 activation in CD3/28-stimulated $CD4^+$ and $CD8^+$ T cells (**Figure 26**), most as effectively as the selective inhibitor of mTOR Torin 1. At first glance this result may seem surprising. After all, inhibition of PI3K, Rac1, and Pak1 produced only modest reductions in macropinocytosis and G1 phase growth impairment. However mTORC1 is directly regulated by PI3K-Akt signaling, so inhibition by LY294002 is expected independently of its influence on macropinocytosis. Off-target inhibitor effects may also contribute: LY294002 is thought to bind and modulate the activity of mTORC1 directly.[257] It has also been shown in HeLa cells that mTORC1 lysosomal translocation is directly regulated by Rac1, independently of PI3K.[338] Consequently it's possible that EHT 1864 interferes with mTORC1 signaling independently of its influence on macropinocytosis.

Inhibition of macropinocytosis by EIPA or J/B did not inhibit NFκB signaling 20 minutes (**Figure 28c**) or 12-14 hours (**Figure 27**) post-stimulation. Phosphorylation of NFκB and IκBα

was actually significantly enhanced, especially in $CD4^+$ T cells and with J/B treatment. Mechanosensitive mechanisms of transcriptional control are well documented in the literature and disruption of cytoskeletal dynamics has been shown to enhance NFκB activation in mammalian cell types, including myelomonocytic and epithelial cells.[339,340] This may explain the enhancement seen with EIPA and J/B in these experiments.

Importantly, phosphorylation of ERK in the first two hours post-stimulation was also not inhibited by EIPA (**Figure 28b**). Significant enhancement was seen in some experiments but this effect was not reproducible. Signaling by other MAP kinases, such as p38 and JNK, is also important in T cell activation, but these were not examined.[341]

Acute mTORC1 activation, however was blocked by EIPA, as expected (**Figure 28a**). Together with results from flow cytometry experiments, these data suggest that inhibition of macropinocytosis by EIPA or J/B blocks mTORC1 activation without inhibiting acute NFκB or ERK signaling, or G1 phase NFκB signaling.

To determine if macropinocytosis is required to deliver protein or amino acids to the lysosome in order to activate mTORC1, we first showed that DQ Red BSA fluorescence could be abolished by alkalinization of the lysosome with NH_4Cl (**Figure 29**). After demonstrating inhibition of lysosomal proteases, we then showed that their activity was not required for mTORC1 activation (**Figure 30**).

We wanted to better understand the requirements for macropinocytosis-mediated mTORC1 activation, so we sought to identify the components in growth media essential for it. All of the

experiments thus far were conducted using RPMI 1640 medium supplemented with FCS. RPMI 1640 contains an abundance of amino acids, glucose, vitamins, and inorganic salts at concentrations that may not accurately reflect the typical *in vivo* nutrient milieu of cells and which may be responsible for macropinocytosis-mediated mTORC1 activation. Compared to animal plasma, RPMI 1640 contains an extremely high concentration of glucose (11 mM), comparatively low levels of certain electrolytes (calcium, sulfate, and magnesium), and high levels of others (phosphate).[342] Serum is even more heterogenous: the cell-free fraction of blood left after coagulation contains thousands of proteins (including enzymes), lipids (including hormones), carbohydrates and undefined components.

We stimulated $CD4^+$ and $CD8^+$ T cells for 12 hours than recultured them for two additional hours in custom, serum-free minimal media preparations after extensive washing. These media were supplemented with various combinations of (or no) amino acids to test whether macropinocytosed amino acids alone or in combination were sufficient to activate mTORC1.

As **Figure 31** and **Figure 32** show for $CD4^+$ and $CD8^+$ T cells respectively, reculture in minimal medium with all 20 amino acids was sufficient to sustain mTORC1 activation in the 12-14 hour period post-stimulation, whereas medium containing no amino acids was not. We next tested the combination of L, Q, R, and S, all amino acids previously linked to mTORC1 activation in prior studies, and found these alone were sufficient to sustain activation in this period. Most importantly, pre-treatment with EIPA or J/B blocked activation in every case, demonstrating that these mTORC1-activating amino acids were acquired by macropinocytosis. We then asked which of these amino acids (L, Q, R, and S) is most important for mTORC1 activation 12-14

hours post-stimulation. We tested this by preparing minimal media containing all 20 amino acids except L, Q, R, or S, then measuring the impact on mTORC1 activation. As **Figure 33** shows, loss of either Q (arginine) or L (leucine) caused the greatest impairment in the ability to sustain mTORC1 activation. Serine deficiency also significantly impaired mTORC1 activation in stimulated $CD8^+$ T cells. This suggests mTORC1 is most sensitive to levels of these amino acids in nascently-activated T cells.

Leucine is an essential amino acid and also the most common proteinogenic one. An increasing body of evidence attests to an additional role for leucine in regulating protein metabolism.[343,344] mTORC1 is especially sensitive to leucine activation, and the attenuation of activation seen when leucine is absented from the serum-free minimal medium is consistent with this (**Figure 33**). As reviewed in the introduction to this chapter, Sestrin2 binding of leucine indirectly promotes Rheb-GTP-loading, licensing one arm of mTORC1 activation. Importantly, leucine is transported into the cell by LAT1, a branched-chain amino acid transporter negligibly expressed in naïve T cells but induced and substantially upregulated in response to T cell activation.[345,346] It's possible that mTORC1 activation in stimulated T cells requires the macropinocytic uptake of leucine because low-level LAT1 expression at this time—and therefore LAT1-mediated leucine uptake—is insufficient to sustain activation at necessary levels.

Arginine is a conditionally-essential amino acid that also regulates metabolism but in ways that are less understood. Deficiency of arginine can selectively alter expression of metabolic genes and elevated concentrations have been shown to promote oxidative phosphorylation over glycolysis in activated T cells.[347] Arginine deficiency also promotes cell cycle arrest in T cells,

and its depletion in tumor microenvironments by arginase-expressing myeloid-derived suppressor cells (MDSCs) promotes T cell anergy.[348] Arginine activates mTORC1 by multiple mechanisms: by dedicated cytoplasmic sensors (CASTOR proteins), by inhibition of TSC complex translocation to the lysosome, and by the intralysosomal SLC38A9 transporter.[302,349,350]

Serine is a non-essential amino acid that plays an important role in regulating methyl group transfer reactions (such as generation of *S*-adenosylmethionine) by donating one-carbon units to tetrahydrofolate.[351] Serine has been shown to activate rapamycin-resistant mTORC1 signaling in HCT116 colorectal cancer cells in a manner that depends on the expression of amino acid transporter PAT4 (SLC36A4), but it is not typically thought of as a major mTORC1 activator.[352] Some have posited a role for it as a "priming" amino acid that sensitizes mTORC1 to "activating" amino acids like leucine.[353]

Glutamine has a well-appreciated role in activating mTORC1 and is capable of doing so independently of the Rag GTPases, by a mechanism requiring phospholipase D.[354] It is thought to be mostly transported into cells by SLC38-family transporters, which are also upregulated in response to T cell activation, however this appears to occur rapidly by relocation of intracellular vesicles to the plasma membrane.[355] Rapid surface expression of these transporters may explain why glutamine acquisition by macropinocytosis is not as critical for mTORC1 activation as it is for other amino acids.

Our identification of these amino acids as necessary for sustained mTORC1 activation allowed us to develop a model for how macropinocytosis regulates the growth of activated T cells

(**Figure 34**). Activation of mTORC1 is sustained at high levels through the first cell cycle post-stimulation by constant macropinocytosis-mediated delivery of amino acids to the lysosome, by cytoplasmic amino acid sensing, and by TCR and co-stimulatory signals converging on PI3K.

CHAPTER VI:

CONCLUSION

In recent decades it has come to be appreciated that endocytic mechanisms underly diverse, specialized functions in eukaryotic cells—and metazoan cells in particular. Macropinocytosis has been adapted for various cell-specific functions in animals but prior to this investigation had only been shown to facilitate feeding in Ras-transformed tumor cells starved of amino acids.

This thesis reports the discovery that primary murine and human TCR αβ T cells perform macropinocytosis constitutively under nutrient-replete conditions and upregulate this behavior 3-4 fold in response to TCR triggering and co-stimulation. In activated T cells, bulk, non-selective uptake of fluid phase contents from the extracellular space provisions free amino acids (and in particular the amino acids leucine and arginine) to the lysosomal lumen where they provide a necessary signal to activate mTORC1. In this way, macropinocytosis sustains mTORC1 activation through the G1 phase of the cell cycle, which is required for metabolic reprogramming and the rapid growth needed to drive clonal expansion.

Our work suggests that macropinocytosis may well be a more common process in highly proliferative eukaryotic cells than is currently appreciated and its role in licensing mTORC1

activation by communicating amino acid sufficiency signals may not be limited to nascently-activated T cells.

Preliminary studies examining macropinocytosis in differentiating thymocytes show that these cells macropinocytose at increasing rates as they progress to the intermediate single positive (ISP) stage, then dramatically downregulate macropinocytosis at the double-positive (DP) stage (unpublished data). After positive selection, the rate of constitutive macropinocytosis increases through successive stages of thymocyte development until it reaches the level shown previously in peripheral naïve T cells. These same studies suggest that memory T cells also perform macropinocytosis but at different rates relative to one another: effector memory T cells (T_{EM}) exhibit reduced macropinocytosis compared to central memory T cells (T_{CM}), which macropinocytose at about the same level as naïve T cells. Future research will clarify the role of macropinocytosis in these cells, which may or may not relate to growth regulation and mTORC1 signaling.

It's interesting to speculate on the reasons why TCR-stimulated macropinocytosis is required for optimal activation of naïve $CD4^+$ and $CD8^+$ T cells. After all, most of the forms of endocytosis previously described are capable of transporting amino acids and a wide variety of amino acid transporters are expressed in these cells. Transport through other endocytic pathways does not necessarily result in lysosomal delivery of cargoes as macropinocytosis does, or at least not as efficiently. Some pathways clearly are competent for this purpose, though: the IL-2Rβ pathway has been shown to deliver IL-2 to primary T cell lysosomes, albeit with a required stopover at the proteasome beforehand.[140]

A more likely explanation is that while naïve T cells express abundant plasma membrane amino acid transporters, their flux capacity is insufficient to meet the exceptionally high demand for amino acids during T cell activation. Activation requires and drives dramatic increases in amino acid and glucose uptake but while TCR signaling and co-stimulation substantially upregulates the glucose transporter GLUT1 and amino acid transporters like LAT1, SNAT-1/2, and ASCT2, their expression is secondary to induction of transcription factors like HIF1α and Myc.[356–358] Consequently, the expression of these transporters is delayed. Perhaps macropinocytosis enables T cells to more rapidly or efficiently activate mTORC1 than the transcription, translation, and membrane-targeting of activation-induced transporters will permit. In support of this, naïve human T cells express nearly indetectable levels of LAT1 protein.[359]

Alternatively, it's possible that cytoplasmic amino acid pools are sufficient but intralysosomal signaling is also required. Lysosomal import of cytoplasmic amino acids may require an adaptor that is not abundantly expressed in naïve or nascently-activated T cells, making them reliant on macropinocytic amino acid uptake to transduce that signal. This is the function of the adaptor LAPTM4b, which recruits LAT1 to the lysosomal compartment and is required for mTORC1 activation in HeLa cells.[360] It would be valuable to assay LAPTM4b expression and co-localization, if any, with LAT1 in activated T cells.

A last (and not mutually exclusive) possibility is that maximal mTORC1 activation in these cells requires not only an intralysosomal amino acid sufficiency signal but *also* a second signal conveyed by cytoplasmic amino acid sensors—Sestrin2 and CASTOR1 for example. In this way,

mTORC1 may function like a logical AND gate sensitive to both intracellular and extracellular amino acid availability where a concentration gradient exists between lysosomal and cytoplasmic amino acid pools. If this were the case, maximal mTORC1 activation would not occur if macropinocytosis were inhibited, even if cytoplasmic sufficiency signals were present. Note that this is consistent with our experimental results (see **Figures 22-26**, **30-32**).

It's also interesting to speculate on the reason for constitutive macropinocytosis in peripheral naïve T cells. One possibility is that it may serve to "arm" the lysosome with mTORC1-activating amino acids in the absence of TCR ligation. This may facilitate a more rapid response when TCR and co-stimulatory signals *are* received. Alternatively (or additionally), constitutive uptake and lysosomal amino acid delivery in these cells could be required to maintain low-level, tonic mTORC1 activation in these cells.

Another question that remains to be addressed is why pharmacological inhibition of macropinocytosis produces greater growth impairment than inhibition of mTORC1 with Torin 1 (**Figure 18**). This may be explained by a dual use for amino acids acquired by macropinocytosis: sustaining mTORC1 activation but also supplying substrates for biosynthesis. Indeed, it would have been useful to conduct ^{13}C metabolic flux analysis to trace the likely incorporation of amino acids obtained by macropinocytosis into central metabolism.

The role of mTORC1 signaling in regulating the utilization of extracellular nutrients, anabolism, and cell survival also appears to depend on environmental context. A study by Palm, et al. (2015) demonstrated that, in contrast to cells grown in amino acid-replete conditions, mTORC1

activation actually suppresses (and inhibition promotes) lysosomal catabolism of endocytosed protein and proliferation of amino acid-starved mouse embryonic fibroblasts (MEFs) *in vitro*.[361] Similar results were obtained in experiments using hypoxic, pancreatic cancer cells bearing oncogenic Ras mutations *in vivo*.[361] These data suggest that anabolic mTORC1 signaling is conditional and coupled to extracellular availability of free amino acids, and contrast with the findings of our studies conducted under amino acid-replete conditions.

The search for macropinocytosis-specific genes continues, though it is hindered by the pleiotropic nature of the actin interactome. While it is likely that most of the proteins that cooperate to generate macropinosomes are involved in many other cellular processes, it's possible that unique macropinocytosis genes will eventually be identified. It’s also likely that additional selective pharmacological inhibitors of macropinocytosis will be developed, and that we will gain further insight into the mechanisms of action of the selective inhibitors we have, making finer dissection and understanding of macropinocytosis-related signaling pathways possible. The discovery that oncogenic Ras-driven tumor cells catabolize extracellular protein obtained by macropinocytosis to sustain their growth and survival does raise the consideration of inhibiting macropinocytosis as a therapeutic strategy for targeting these tumors. Our findings, however, strongly suggest that successful intratumoral targeting would also likely impair macropinocytosis in tumor-infiltrating lymphocytes (TILs), which may be needed to sustain their growth and generate effector (i.e. anti-tumor) responses.

By the same token, inhibition of macropinocytosis may constitute an effective strategy for curtailing aberrant T cell reactivity *in vivo* in the setting or allergic hypersensitivity or

autoimmune diseases. Oral amiloride is generally well-tolerated as a diuretic, suggesting its derivative EIPA might exhibit favorable pharmacodynamic and pharmacokinetic properties and warrant preclinical study as a therapeutic candidate for this purpose. Other novel, putative macropinocytosis inhibitors identified through screens, such as imipramine and vinblastine, may also be suitable for this repurposing, though we did not find them to be effective inhibitors of T cell macropinocytosis in preliminary studies.[362]

The central outstanding question to be answered by future investigators of macropinocytosis is how pervasive of a phenomenon it is: which cells perform it constitutively or conditionally, and how commonly does it occur *in vivo*? Is macropinocytosis a common behavior of most highly proliferative metazoan cells under nutrient-replete conditions? If so, does it function in these cells to sustain mTORC1 activation, as it does in stimulated T cells and macrophages, or does it serve other purposes? These and related questions we leave to future investigations.

APPENDIX

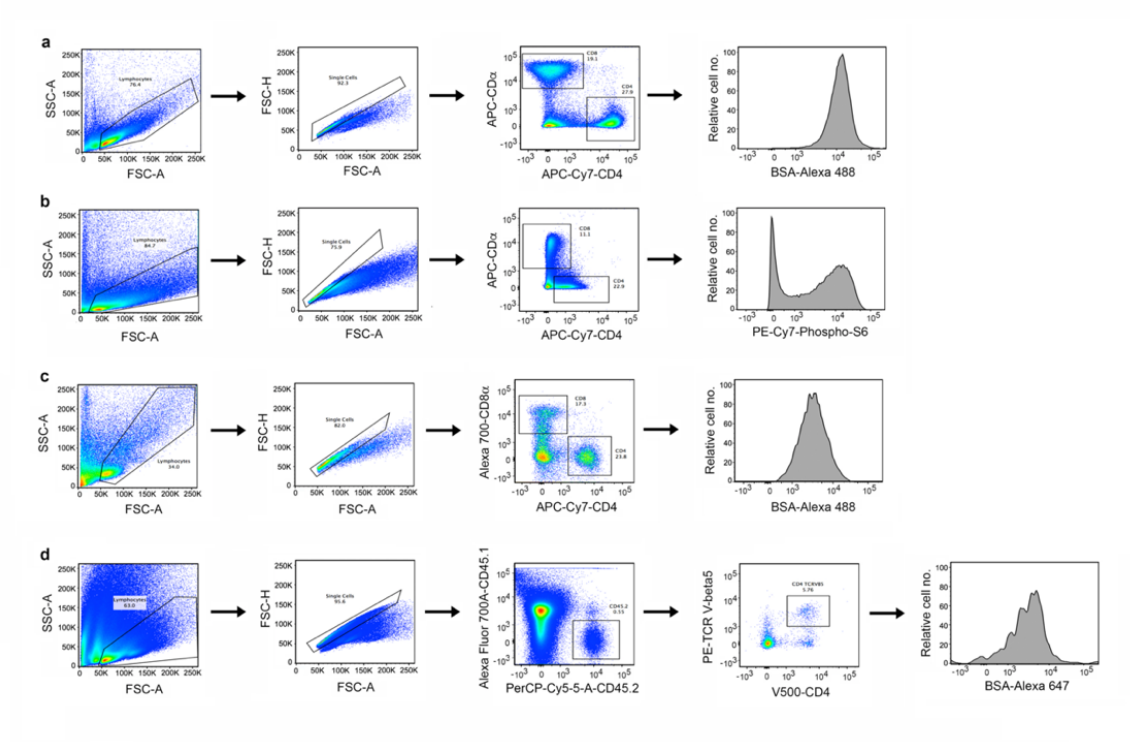

Figure 35 – Flow cytometry gating strategies. Gating strategies used to determine: **a** T cell uptake of macropinocytosis probes in murine splenocyte cultures; **b** Phosphorylated rpS6 or phosphorylated NFκB staining of fixed and permeabilized T cells in murine splenocyte cultures; **c** T cell uptake of macropinocytosis probes in human PBMC cultures; **d** OTII TCR Tg T cell uptake of macropinocytosis probes *in vivo*.

BIBLIOGRAPHY

1. Duve, C. de. The origin of eukaryotes: a reappraisal. *Nat Rev Genet* 8, 395–403 (2007).

2. Hartman, H. & Fedorov, A. The origin of the eukaryotic cell: A genomic investigation. *Proc National Acad Sci* 99, 1420–1425 (2002).

3. Stenbeck, G. & Horton, M. A. Endocytic trafficking in actively resorbing osteoclasts. *J Cell Sci* 117, 827–836 (2004).

4. Saheki, Y. & Camilli, P. D. Synaptic Vesicle Endocytosis. *Csh Perspect Biol* 4, a005645 (2012).

5. Cavalli, V., Corti, M. & Gruenberg, J. Endocytosis and signaling cascades: a close encounter. *Febs Lett* 498, 190–196 (2001).

6. Pearse, B. M. Clathrin: a unique protein associated with intracellular transfer of membrane by coated vesicles. *Proc National Acad Sci* 73, 1255–1259 (1976).

7. Thottacherry, J. J., Sathe, M., Prabhakara, C. & Mayor, S. Spoiled for Choice: Diverse Endocytic Pathways Function at the Cell Surface. *Annu Rev Cell Dev Bi* 35, 1–30 (2019).

8. Kaksonen, M. & Roux, A. Mechanisms of clathrin-mediated endocytosis. *Nat Rev Mol Cell Bio* 19, 313–326 (2018).

9. Rusk, N. *et al.* Synaptojanin 2 Functions at an Early Step of Clathrin-Mediated Endocytosis. *Curr Biol* 13, 659–663 (2003).

10. Taylor, M. J., Perrais, D. & Merrifield, C. J. A High Precision Survey of the Molecular Dynamics of Mammalian Clathrin-Mediated Endocytosis. *Plos Biol* 9, e1000604 (2011).

11. Bitsikas, V., Corrêa, I. R. & Nichols, B. J. Clathrin-independent pathways do not contribute significantly to endocytic flux. *Elife* 3, e03970 (2014).

12. Mathew, M. P. & Donaldson, J. G. Distinct cargo-specific response landscapes underpin the complex and nuanced role of galectin–glycan interactions in clathrin-independent endocytosis. *J Biol Chem* 293, 7222–7237 (2018).

13. Doherty, G. J. & McMahon, H. T. Mechanisms of Endocytosis. *Biochemistry-us* 78, 857–902 (2009).

14. Mooren, O. L., Galletta, B. J. & Cooper, J. A. Roles for Actin Assembly in Endocytosis. *Annu Rev Biochem* 81, 661–686 (2012).

15. McMahon, H. T. & Boucrot, E. Molecular mechanism and physiological functions of clathrin-mediated endocytosis. *Nat Rev Mol Cell Bio* 12, 517–533 (2011).

16. Mayle, K. M., Le, A. M. & Kamei, D. T. The intracellular trafficking pathway of transferrin. *Biochimica Et Biophysica Acta Bba - Gen Subj* 1820, 264–281 (2012).

17. Subtil, A. *et al.* Acute cholesterol depletion inhibits clathrin-coated pit budding. *Proc National Acad Sci* 96, 6775–6780 (1999).

18. Bliek, A. van der *et al.* Mutations in human dynamin block an intermediate stage in coated vesicle formation. *J Cell Biology* 122, 553–563 (1993).

19. Damke, H., Baba, T., Warnock, D. E. & Schmid, S. L. Induction of mutant dynamin specifically blocks endocytic coated vesicle formation. *J Cell Biology* 127, 915–934 (1994).

20. Roth, T. F. & Porter, K. R. YOLK PROTEIN UPTAKE IN THE OOCYTE OF THE MOSQUITO AEDES AEGYPTI. L. *J Cell Biology* 20, 313–332 (1964).

21. Echarri, A. & Pozo, M. A. D. Caveolae – mechanosensitive membrane invaginations linked to actin filaments. *J Cell Sci* 128, 2747–2758 (2015).

22. Echarri, A. *et al.* Caveolar domain organization and trafficking is regulated by Abl kinases and mDia1. *J Cell Sci* 125, 3097–3113 (2012).

23. Stoeber, M. *et al.* Oligomers of the ATPase EHD2 confine caveolae to the plasma membrane through association with actin. *Embo J* 31, 2350–2364 (2012).

24. Pelkmans, L. & Helenius, A. Endocytosis Via Caveolae. *Traffic* 3, 311–320 (2002).

25. Nabi, I. R. & Le, P. U. Caveolae/raft-dependent endocytosis. *J Cell Biology* 161, 673–677 (2003).

26. Henley, J. R., Krueger, E. W. A., Oswald, B. J. & McNiven, M. A. Dynamin-mediated Internalization of Caveolae. *J Cell Biology* 141, 85–99 (1998).

27. Yamada, E. THE FINE STRUCTURE OF THE GALL BLADDER EPITHELIUM OF THE MOUSE. *J Biophysical Biochem Cytol* 1, 445–458 (1955).

28. Chadda, R. *et al.* Cholesterol-Sensitive Cdc42 Activation Regulates Actin Polymerization for Endocytosis via the GEEC Pathway. *Traffic* 8, 702–717 (2007).

29. Sathe, M. *et al.* Small GTPases and BAR domain proteins regulate branched actin polymerisation for clathrin and dynamin-independent endocytosis. *Nat Commun* 9, 1835 (2018).

30. Lundmark, R. *et al.* The GTPase-Activating Protein GRAF1 Regulates the CLIC/GEEC Endocytic Pathway. *Curr Biol* 18, 1802–1808 (2008).

31. Chaudhary, N. *et al.* Endocytic Crosstalk: Cavins, Caveolins, and Caveolae Regulate Clathrin-Independent Endocytosis. *Plos Biol* 12, e1001832 (2014).

32. Kirkham, M. *et al.* Ultrastructural identification of uncoated caveolin-independent early endocytic vehicles. *J Cell Biology* 168, 465–476 (2005).

33. Sabharanjak, S., Sharma, P., Parton, R. G. & Mayor, S. GPI-Anchored Proteins Are Delivered to Recycling Endosomes via a Distinct cdc42-Regulated, Clathrin-Independent Pinocytic Pathway. *Dev Cell* 2, 411–423 (2002).

34. Langhorst, M. F., Solis, G. P., Hannbeck, S., Plattner, H. & Stuermer, C. A. O. Linking membrane microdomains to the cytoskeleton: Regulation of the lateral mobility of reggie-1/flotillin-2 by interaction with actin. *Febs Lett* 581, 4697–4703 (2007).

35. Ge, L. *et al.* Flotillins play an essential role in Niemann-Pick C1-like 1-mediated cholesterol uptake. *Proc National Acad Sci* 108, 551–556 (2011).

36. Glebov, O. O., Bright, N. A. & Nichols, B. J. Flotillin-1 defines a clathrin-independent endocytic pathway in mammalian cells. *Nat Cell Biol* 8, 46–54 (2006).

37. Basquin, C. *et al.* Membrane protrusion powers clathrin-independent endocytosis of interleukin-2 receptor. *Embo J* 34, 2147–2161 (2015).

38. Grassart, A., Dujeancourt, A., Lazarow, P. B., Dautry-Varsat, A. & Sauvonnet, N. Clathrin-independent endocytosis used by the IL-2 receptor is regulated by Rac1, Pak1 and Pak2. *Embo Rep* 9, 356–362 (2008).

39. Matkó, J. *et al.* GPI-microdomains (membrane rafts) and signaling of the multi-chain interleukin-2 receptor in human lymphoma/leukemia T cell lines. *Eur J Biochem* 269, 1199–1208 (2002).

40. Vereb, G. *et al.* Cholesterol-dependent clustering of IL-2Rα and its colocalization with HLA and CD48 on T lymphoma cells suggest their functional association with lipid rafts. *Proc National Acad Sci* 97, 6013–6018 (2000).

41. Sauvonnet, N., Dujeancourt, A. & Dautry-Varsat, A. Cortactin and dynamin are required for the clathrin-independent endocytosis of γc cytokine receptor. *J Cell Biology* 168, 155–163 (2005).

42. Hémar, A., Lieb, M., Subtil, A., Disanto, J. P. & Dautry-Varsat, A. Endocytosis of the β chain of interleukin-2 receptor requires neither interleukin-2 nor the γ chain. *Eur J Immunol* 24, 1951–1955 (1994).

43. Radhakrishna, H. & Donaldson, J. G. ADP-Ribosylation Factor 6 Regulates a Novel Plasma Membrane Recycling Pathway. *J Cell Biology* 139, 49–61 (1997).

44. Naslavsky, N., Weigert, R. & Donaldson, J. G. Characterization of a Nonclathrin Endocytic Pathway: Membrane Cargo and Lipid Requirements. *Mol Biol Cell* 15, 3542–3552 (2004).

45. D'Souza-Schorey, C., Li, G., Colombo, M. & Stahl, P. A regulatory role for ARF6 in receptor-mediated endocytosis. *Science* 267, 1175–1178 (1995).

46. KAPLAN, G. Differences in the Mode of Phagocytosis with Fc and C3 Receptors in Macrophages. *Scand J Immunol* 6, 797–807 (1977).

47. Botelho, R. J. & Grinstein, S. Phagocytosis. *Curr Biol* 21, R533–R538 (2011).

48. Pratten, M. K. & Lloyd, J. B. Pinocytosis and phagocytosis: the effect of size of a particulate substrate on its mode of capture by rat peritoneal macrophages cultured in vitro. *Biochimica Et Biophysica Acta Bba - Gen Subj* 881, 307–313 (1986).

49. Tabata, Y. & Ikada, Y. Effect of the size and surface charge of polymer microspheres on their phagocytosis by macrophage. *Biomaterials* 9, 356–362 (1988).

50. Koval, M., Preiter, K., Adles, C., Stahl, P. D. & Steinberg, T. H. Size of IgG-Opsonized Particles Determines Macrophage Response during Internalization. *Exp Cell Res* 242, 265–273 (1998).

51. Champion, J. A., Walker, A. & Mitragotri, S. Role of Particle Size in Phagocytosis of Polymeric Microspheres. *Pharmaceut Res* 25, 1815–1821 (2008).

52. Churchward, M. A. & Todd, K. G. Statin treatment affects cytokine release and phagocytic activity in primary cultured microglia through two separable mechanisms. *Mol Brain* 7, 85 (2014).

53. Bryan, A. M., Farnoud, A. M., Mor, V. & Poeta, M. D. Macrophage Cholesterol Depletion and Its Effect on the Phagocytosis of Cryptococcus neoformans. *J Vis Exp* (2014) doi:10.3791/52432.

54. Gold, E. S. *et al.* Dynamin 2 Is Required for Phagocytosis in Macrophages. *J Exp Medicine* 190, 1849–1856 (1999).

55. Metchnikoff, E. Untersuchungen über die mesodermalen Phagocyten einiger Wirbeltiere. *Biologisches centralblatt* 560–565 (1883).

56. Boucrot, E. *et al.* Endophilin marks and controls a clathrin-independent endocytic pathway. *Nature* 517, 460–465 (2015).

57. Casamento, A. & Boucrot, E. Molecular mechanism of Fast Endophilin-Mediated Endocytosis. *Biochem J* 477, 2327–2345 (2020).

58. Clayton, E. L. & Cousin, M. A. The molecular physiology of activity-dependent bulk endocytosis of synaptic vesicles. *J Neurochem* 111, 901–914 (2009).

59. Kokotos, A. C. & Low, D. W. Myosin II and Dynamin Control Actin Rings to Mediate Fission during Activity-Dependent Bulk Endocytosis. *J Neurosci* 35, 8687–8688 (2015).

60. Nicholson-Fish, J. C., Kokotos, A. C., Gillingwater, T. H., Smillie, K. J. & Cousin, M. A. VAMP4 Is an Essential Cargo Molecule for Activity-Dependent Bulk Endocytosis. *Neuron* 88, 973–984 (2015).

61. Bonanomi, D. *et al.* Identification of a developmentally regulated pathway of membrane retrieval in neuronal growth cones. *J Cell Sci* 121, 3757–3769 (2008).

62. Clayton, E. L. *et al.* The Phospho-Dependent Dynamin–Syndapin Interaction Triggers Activity-Dependent Bulk Endocytosis of Synaptic Vesicles. *J Neurosci* 29, 7706–7717 (2009).

63. Marxen, M., Volknandt, W. & Zimmermann, H. Endocytic vacuoles formed following a short pulse of K+-stimulation contain a plethora of presynaptic membrane proteins. *Neuroscience* 94, 985–996 (1999).

64. Watanabe, S. *et al.* Ultrafast endocytosis at mouse hippocampal synapses. *Nature* 504, 242–247 (2013).

65. Watanabe, S. & Boucrot, E. Fast and ultrafast endocytosis. *Curr Opin Cell Biol* 47, 64–71 (2017).

66. Yue, H. & Xu, J. Cholesterol regulates multiple forms of vesicle endocytosis at a mammalian central synapse. *J Neurochem* 134, 247–260 (2015).

67. Watanabe, S. *et al.* Ultrafast endocytosis at Caenorhabditis elegans neuromuscular junctions. *Elife* 2, e00723 (2013).

68. Hilgemann, D. W., Lin, M.-J., Fine, M. & Deisl, C. On the existence of endocytosis driven by membrane phase separations. *Biochimica Et Biophysica Acta Bba - Biomembr* 1862, 183007 (2019).

69. Fine, M. *et al.* Massive endocytosis driven by lipidic forces originating in the outer plasmalemmal monolayer: a new approach to membrane recycling and lipid domainsAmphipath-activated massive endocytosis. *J Gen Physiology* 137, 137–154 (2011).

70. Hilgemann, D. W., Fine, M., Linder, M. E., Jennings, B. C. & Lin, M.-J. Massive endocytosis triggered by surface membrane palmitoylation under mitochondrial control in BHK fibroblasts. *Elife* 2, e01293 (2013).

71. Lariccia, V. *et al.* Massive calcium–activated endocytosis without involvement of classical endocytic proteins. *J Gen Physiology* 137, 111–132 (2011).

72. Kerr, M. C. & Teasdale, R. D. Defining Macropinocytosis. *Traffic* 10, 364–371 (2009).

73. Lim, J. P. & Gleeson, P. A. Macropinocytosis: an endocytic pathway for internalising large gulps. *Immunol Cell Biol* 89, 836–843 (2011).

74. Cardarelli, F., Pozzi, D., Bifone, A., Marchini, C. & Caracciolo, G. Cholesterol-Dependent Macropinocytosis and Endosomal Escape Control the Transfection Efficiency of Lipoplexes in CHO Living Cells. *Mol Pharmaceut* 9, 334–340 (2012).

75. Grimmer, S., Deurs, B. van & Sandvig, K. Membrane ruffling and macropinocytosis in A431 cells require cholesterol. *J Cell Sci* 115, 2953–62 (2002).

76. Lewis, W. H. Pinocytosis. *Johns Hopkins Hosp. Bull.* 17–27 (1931).

77. Cheng, Z.-J. *et al.* Distinct Mechanisms of Clathrin-independent Endocytosis Have Unique Sphingolipid Requirements. *Mol Biol Cell* 17, 3197–3210 (2006).

78. Kovtun, O., Tillu, V. A., Ariotti, N., Parton, R. G. & Collins, B. M. Cavin family proteins and the assembly of caveolae. *J Cell Sci* 128, 1269–1278 (2015).

79. Chidlow, J. H. & Sessa, W. C. Caveolae, caveolins, and cavins: complex control of cellular signalling and inflammation. *Cardiovasc Res* 86, 219–225 (2010).

80. McMahon, K.-A. *et al.* Identification of intracellular cavin target proteins reveals cavin-PP1alpha interactions regulate apoptosis. *Nat Commun* 10, 3279 (2019).

81. Ostrom, R. S. & Insel, P. A. The evolving role of lipid rafts and caveolae in G protein-coupled receptor signaling: implications for molecular pharmacology. *Brit J Pharmacol* 143, 235–245 (2004).

82. Schnitzer, J. E., Oh, P. & McIntosh, D. P. Role of GTP Hydrolysis in Fission of Caveolae Directly from Plasma Membranes. *Science* 274, 239–242 (1996).

83. Mayor, S., Parton, R. G. & Donaldson, J. G. Clathrin-Independent Pathways of Endocytosis. *Csh Perspect Biol* 6, a016758 (2014).

84. Gupta, G. D. *et al.* Analysis of Endocytic Pathways in Drosophila Cells Reveals a Conserved Role for GBF1 in Internalization via GEECs. *Plos One* 4, e6768 (2009).

85. Rivera-Milla, E., Stuermer, C. A. O. & Málaga-Trillo, E. Ancient origin of reggie (flotillin), reggie-like, and other lipid-raft proteins: convergent evolution of the SPFH domain. *Cell Mol Life Sci Cmls* 63, 343–357 (2006).

86. Liu, J., DeYoung, S. M., Zhang, M., Dold, L. H. & Saltiel, A. R. The Stomatin/Prohibitin/Flotillin/HflK/C Domain of Flotillin-1 Contains Distinct Sequences That Direct Plasma Membrane Localization and Protein Interactions in 3T3-L1 Adipocytes. *J Biol Chem* 280, 16125–16134 (2005).

87. Morrow, I. C. *et al.* Flotillin-1/Reggie-2 Traffics to Surface Raft Domains via a Novel Golgi-independent Pathway IDENTIFICATION OF A NOVEL MEMBRANE TARGETING DOMAIN AND A ROLE FOR PALMITOYLATION. *J Biol Chem* 277, 48834–48841 (2002).

88. Solis, G. P. *et al.* Reggie/flotillin proteins are organized into stable tetramers in membrane microdomains. *Biochem J* 403, 313–322 (2007).

89. Frick, M. *et al.* Coassembly of Flotillins Induces Formation of Membrane Microdomains, Membrane Curvature, and Vesicle Budding. *Curr Biol* 17, 1151–1156 (2007).

90. Otto, G. P. & Nichols, B. J. The roles of flotillin microdomains – endocytosis and beyond. *J Cell Sci* 124, 3933–3940 (2011).

91. Schweitzer, J. K., Sedgwick, A. E. & D'Souza-Schorey, C. ARF6-mediated endocytic recycling impacts cell movement, cell division and lipid homeostasis. *Semin Cell Dev Biol* 22, 39–47 (2011).

92. Honda, A. *et al.* Phosphatidylinositol 4-Phosphate 5-Kinase α Is a Downstream Effector of the Small G Protein ARF6 in Membrane Ruffle Formation. *Cell* 99, 521–532 (1999).

93. Donaldson, J. G., Johnson, D. L. & Dutta, D. Rab and Arf G proteins in endosomal trafficking and cell surface homeostasis. *Small Gtpases* 7, 247–251 (2016).

94. Lau, A. W. & Chou, M. M. The adaptor complex AP-2 regulates post-endocytic trafficking through the non-clathrin Arf6-dependent endocytic pathway. *J Cell Sci* 121, 4008–4017 (2008).

95. Okada, R. *et al.* Activation of the Small G Protein Arf6 by Dynamin2 through Guanine Nucleotide Exchange Factors in Endocytosis. *Sci Rep-uk* 5, 14919 (2015).

96. Rosales, C. & Uribe-Querol, E. Phagocytosis: A Fundamental Process in Immunity. *Biomed Res Int* 2017, 1–18 (2017).

97. Yutin, N., Wolf, M. Y., Wolf, Y. I. & Koonin, E. V. The origins of phagocytosis and eukaryogenesis. *Biol Direct* 4, 9 (2009).

98. Shi, H. Eosinophils function as antigen-presenting cells. *J Leukocyte Biol* 76, 520–527 (2004).

99. Andrews, T. & Sullivan, K. E. Infections in Patients with Inherited Defects in Phagocytic Function. *Clin Microbiol Rev* 16, 597–621 (2003).

100. Galloway, D. A., Phillips, A. E. M., Owen, D. R. J. & Moore, C. S. Phagocytosis in the Brain: Homeostasis and Disease. *Front Immunol* 10, 790 (2019).

101. Tohyama, Y. & Yamamura, H. Protein Tyrosine Kinase, Syk: A Key Player in Phagocytic Cells. *J Biochem* 145, 267–273 (2009).

102. Gillooly, D. J., Simonsen, A. & Stenmark, H. Phosphoinositides and phagocytosis. *J Cell Biology* 155, 15–18 (2001).

103. Campbell-Valois, F.-X. *et al.* Quantitative Proteomics Reveals That Only a Subset of the Endoplasmic Reticulum Contributes to the Phagosome. *Mol Cell Proteomics* 11, M111.016378 (2012).

104. Nair-Gupta, P. *et al.* TLR Signals Induce Phagosomal MHC-I Delivery from the Endosomal Recycling Compartment to Allow Cross-Presentation. *Cell* 158, 506–521 (2014).

105. Ndjamen, B., Kang, B., Hatsuzawa, K. & Kima, P. E. Leishmania parasitophorous vacuoles interact continuously with the host cell's endoplasmic reticulum; parasitophorous vacuoles are hybrid compartments. *Cell Microbiol* 12, 1480–1494 (2010).

106. Potter, N. S. & Harding, C. V. Neutrophils Process Exogenous Bacteria Via an Alternate Class I MHC Processing Pathway for Presentation of Peptides to T Lymphocytes. *J Immunol* 167, 2538–2546 (2001).

107. Oliveira, C. C. & Hall, T. van. Alternative Antigen Processing for MHC Class I: Multiple Roads Lead to Rome. *Front Immunol* 6, 298 (2015).

108. Sönnichsen, B., Renzis, S. D., Nielsen, E., Rietdorf, J. & Zerial, M. Distinct Membrane Domains on Endosomes in the Recycling Pathway Visualized by Multicolor Imaging of Rab4, Rab5, and Rab11. *J Cell Biology* 149, 901–914 (2000).

109. Kinchen, J. M. & Ravichandran, K. S. Phagosome maturation: going through the acid test. *Nat Rev Mol Cell Bio* 9, 781–795 (2008).

110. Harrison, R. E., Bucci, C., Vieira, O. V., Schroer, T. A. & Grinstein, S. Phagosomes Fuse with Late Endosomes and/or Lysosomes by Extension of Membrane Protrusions along Microtubules: Role of Rab7 and RILP. *Mol Cell Biol* 23, 6494–6506 (2003).

111. Jordens, I. *et al.* The Rab7 effector protein RILP controls lysosomal transport by inducing the recruitment of dynein-dynactin motors. *Curr Biol* 11, 1680–1685 (2001).

112. Antonin, W. *et al.* A SNARE complex mediating fusion of late endosomes defines conserved properties of SNARE structure and function. *Embo J* 19, 6453–6464 (2000).

113. Ferreira, A. P. A. *et al.* Cdk5 and GSK3β inhibit Fast Endophilin-Mediated Endocytosis. *Biorxiv* 2020.04.11.036863 (2020) doi:10.1101/2020.04.11.036863.

114. Matta, S. *et al.* LRRK2 Controls an EndoA Phosphorylation Cycle in Synaptic Endocytosis. *Neuron* 75, 1008–1021 (2012).

115. Wu, X., Gan, B., Yoo, Y. & Guan, J.-L. FAK-Mediated Src Phosphorylation of Endophilin A2 Inhibits Endocytosis of MT1-MMP and Promotes ECM Degradation. *Dev Cell* 9, 185–196 (2005).

116. Kaneko, T. *et al.* Rho mediates endocytosis of epidermal growth factor receptor through phosphorylation of endophilin A1 by Rho-kinase. *Genes Cells* 10, 973–987 (2005).

117. Milosevic, I. *et al.* Recruitment of Endophilin to Clathrin-Coated Pit Necks Is Required for Efficient Vesicle Uncoating after Fission. *Neuron* 72, 587–601 (2011).

118. Kessels, M. M. & Qualmann, B. Syndapins integrate N-WASP in receptor-mediated endocytosis. *Embo J* 21, 6083–6094 (2002).

119. Tan, T. C. *et al.* Cdk5 is essential for synaptic vesicle endocytosis. *Nat Cell Biol* 5, 701–710 (2003).

120. Chanaday, N. L., Cousin, M. A., Milosevic, I., Watanabe, S. & Morgan, J. R. The Synaptic Vesicle Cycle Revisited: New Insights into the Modes and Mechanisms. *J Neurosci* 39, 8209–8216 (2019).

121. Watanabe, S. *et al.* Synaptojanin and Endophilin Mediate Neck Formation during Ultrafast Endocytosis. *Neuron* 98, 1184-1197.e6 (2018).

122. Bacia, K., Schwille, P. & Kurzchalia, T. Sterol structure determines the separation of phases and the curvature of the liquid-ordered phase in model membranes. *P Natl Acad Sci Usa* 102, 3272–3277 (2005).

123. Qureshi, O. S. *et al.* Trans-Endocytosis of CD80 and CD86: A Molecular Basis for the Cell-Extrinsic Function of CTLA-4. *Science* 332, 600–603 (2011).

124. Qureshi, O. S. *et al.* Constitutive Clathrin-mediated Endocytosis of CTLA-4 Persists during T Cell Activation. *J Biological Chem* 287, 9429–9440 (2012).

125. Monjas, A., Alcover, A. & Alarcón, B. Engaged and Bystander T Cell Receptors Are Down-modulated by Different Endocytotic Pathways. *J Biol Chem* 279, 55376–55384 (2004).

126. Crotzer, V. L., Mabardy, A. S., Weiss, A. & Brodsky, F. M. T Cell Receptor Engagement Leads to Phosphorylation of Clathrin Heavy Chain during Receptor Internalization. *J Exp Medicine* 199, 981–991 (2004).

127. Łyszkiewicz, M. *et al.* Human FCHO1 deficiency reveals role for clathrin-mediated endocytosis in development and function of T cells. *Nat Commun* 11, 1031 (2020).

128. Rossatti, P. *et al.* Cdc42 Couples T Cell Receptor Endocytosis to GRAF1-Mediated Tubular Invaginations of the Plasma Membrane. *Cells* 8, 1388 (2019).

129. Compeer, E. B. *et al.* A mobile endocytic network connects clathrin-independent receptor endocytosis to recycling and promotes T cell activation. *Nat Commun* 9, 1597 (2018).

130. Lamaze, C. *et al.* Interleukin 2 Receptors and Detergent-Resistant Membrane Domains Define a Clathrin-Independent Endocytic Pathway. *Mol Cell* 7, 661–671 (2001).

131. Johnson, D. L., Wayt, J., Wilson, J. M. & Donaldson, J. G. Arf6 and Rab22 mediate T cell conjugate formation by regulating clathrin-independent endosomal membrane trafficking. *J Cell Sci* 130, jcs.200477 (2017).

132. Wu, Y. *et al.* Human γδ T Cells: A Lymphoid Lineage Cell Capable of Professional Phagocytosis. *J Immunol* 183, 5622–5629 (2009).

133. Zhu, Y. *et al.* Human γδ T Cells Augment Antigen Presentation in Listeria Monocytogenes Infection. *Mol Med* 22, 737–746 (2016).

134. Martínez-Martín, N. *et al.* T Cell Receptor Internalization from the Immunological Synapse Is Mediated by TC21 and RhoG GTPase-Dependent Phagocytosis. *Immunity* 35, 208–222 (2011).

135. Charpentier, J. C. *et al.* Macropinocytosis drives T cell growth by sustaining the activation of mTORC1. *Nat Commun* 11, 180 (2020).

136. Yellin, M. J. *et al.* CD40 molecules induce down-modulation and endocytosis of T cell surface T cell-B cell activating molecule/CD40-L. Potential role in regulating helper effector function. *J Immunol Baltim Md 1950* 152, 598–608 (1994).

137. Yu, A., Olosz, F., Choi, C. Y. & Malek, T. R. Efficient Internalization of IL-2 Depends on the Distal Portion of the Cytoplasmic Tail of the IL-2R Common γ-Chain and a Lymphoid Cell Environment. *J Immunol* 165, 2556–2562 (2000).

138. Basquin, C. *et al.* The signalling factor PI3K is a specific regulator of the clathrin-independent dynamin-dependent endocytosis of IL-2 receptors. *J Cell Sci* 126, 1099–1108 (2013).

139. Rocca, A., Lamaze, C., Subtil, A. & Dautry-Varsat, A. Involvement of the Ubiquitin/Proteasome System in Sorting of the Interleukin 2 Receptor β Chain to Late Endocytic Compartments. *Mol Biol Cell* 12, 1293–1301 (2001).

140. Yu, A. & Malek, T. R. The Proteasome Regulates Receptor-mediated Endocytosis of Interleukin-2. *J Biol Chem* 276, 381–385 (2001).

141. Hsu, H. *et al.* WC1 Is a Hybrid γδ TCR Coreceptor and Pattern Recognition Receptor for Pathogenic Bacteria. *J Immunol* 194, 2280–2288 (2015).

142. Hsu, H., Baldwin, C. L. & Telfer, J. C. The Endocytosis and Signaling of the γδ T Cell Coreceptor WC1 Are Regulated by a Dileucine Motif. *J Immunol* 194, 2399–2406 (2015).

143. José, E. S., Borroto, A., Niedergang, F., Alcover, A. & Alarcón, B. Triggering the TCR Complex Causes the Downregulation of Nonengaged Receptors by a Signal Transduction-Dependent Mechanism. *Immunity* 12, 161–170 (2000).

144. D'Oro, U., Vacchio, M. S., Weissman, A. M. & Ashwell, J. D. Activation of the Lck Tyrosine Kinase Targets Cell Surface T Cell Antigen Receptors for Lysosomal Degradation. *Immunity* 7, 619–628 (1997).

145. Lauritsen, J. P. *et al.* Two distinct pathways exist for down-regulation of the TCR. *J Immunol Baltim Md 1950* 161, 260–7 (1998).

146. Calzoni, E. *et al.* F-BAR domain only protein 1 (FCHO1) deficiency is a novel cause of combined immune deficiency in humans. *J Allergy Clin Immun* 143, 2317-2321.e12 (2019).

147. McGavin, M. K. H. *et al.* The Intersectin 2 Adaptor Links Wiskott Aldrich Syndrome Protein (WASp)-mediated Actin Polymerization to T Cell Antigen Receptor Endocytosis. *J Exp Medicine* 194, 1777–1787 (2001).

148. Willinger, T., Staron, M., Ferguson, S. M., Camilli, P. D. & Flavell, R. A. Dynamin 2-dependent endocytosis sustains T-cell receptor signaling and drives metabolic reprogramming in T lymphocytes. *Proc National Acad Sci* 112, 4423–4428 (2015).

149. Prieto-Sánchez, R. M., Berenjeno, I. M. & Bustelo, X. R. Involvement of the Rho/Rac family member RhoG in caveolar endocytosis. *Oncogene* 25, 2961–2973 (2006).

150. Liu, H., Rhodes, M., Wiest, D. L. & Vignali, D. A. A. On the Dynamics of TCR:CD3 Complex Cell Surface Expression and Downmodulation. *Immunity* 13, 665–675 (2000).

151. D'Oro, U. *et al.* Regulation of Constitutive TCR Internalization by the ζ-Chain. *J Immunol* 169, 6269–6278 (2002).

152. Bras, S. L. *et al.* Recruitment of the Actin-binding Protein HIP-55 to the Immunological Synapse Regulates T Cell Receptor Signaling and Endocytosis. *J Biol Chem* 279, 15550–15560 (2004).

153. Iseka, F. M. *et al.* Role of the EHD Family of Endocytic Recycling Regulators for TCR Recycling and T Cell Function. *J Immunol* 200, 483–499 (2018).

154. Rajendran, L. *et al.* Asymmetric localization of flotillins/reggies in preassembled platforms confers inherent polarity to hematopoietic cells. *Proc National Acad Sci* 100, 8241–8246 (2003).

155. Redpath, G. M. I. *et al.* Flotillins promote T cell receptor sorting through a fast Rab5–Rab11 endocytic recycling axis. *Nat Commun* 10, 4392 (2019).

156. Ahmed, K. A., Munegowda, M. A., Xie, Y. & Xiang, J. Intercellular Trogocytosis Plays an Important Role in Modulation of Immune Responses. *Cell Mol Immunol* 5, 261–269 (2008).

157. Rosenits, K., Keppler, S. J., Vucikuja, S. & Aichele, P. T cells acquire cell surface determinants of APC via in vivo trogocytosis during viral infections. *Eur J Immunol* 40, 3450–3457 (2010).

158. Reed, J. & Wetzel, S. A. Trogocytosis-Mediated Intracellular Signaling in CD4 + T Cells Drives T H 2-Associated Effector Cytokine Production and Differentiation. *J Immunol* 202, 2873–2887 (2019).

159. Dhainaut, M. & Moser, M. Regulation of Immune Reactivity by Intercellular Transfer. *Front Immunol* 5, 112 (2014).

160. Miyake, K. *et al.* Trogocytosis of peptide–MHC class II complexes from dendritic cells confers antigen-presenting ability on basophils. *Proc National Acad Sci* 114, 1111–1116 (2017).

161. Mao, Y. & Finnemann, S. C. Regulation of phagocytosis by Rho GTPases. *Small Gtpases* 6, 89–99 (2015).

162. Chaudhri, G. *et al.* T cell receptor sharing by cytotoxic T lymphocytes facilitates efficient virus control. *Proc National Acad Sci* 106, 14984–14989 (2009).

163. Swanson, J. A. & Yoshida, S. Encyclopedia of Cell Biology. 758–765 (2016) doi:10.1016/b978-0-12-394447-4.20084-9.

164. Cao, H., Chen, J., Awoniyi, M., Henley, J. R. & McNiven, M. A. Dynamin 2 mediates fluid-phase micropinocytosis in epithelial cells. *J Cell Sci* 120, 4167–4177 (2007).

165. King, J. S. & Kay, R. R. The origins and evolution of macropinocytosis. *Philosophical Transactions Royal Soc B* 374, 20180158 (2019).

166. Lewis, W. H. Pinocytosis by malignant cells. *Cancer Research* 29, (1937).

167. Chapman-Andresen, C. The early days of pinocytosis. *Carlsberg Res Commun* 49, 179–186 (1984).

168. EDWARDS, J. G. FORMATION OF FOOD-CUPS IN AMŒBA INDUCED BY CHEMICALS. *Biological Bulletin* 48, 236–239 (1925).

169. Mast, S. O. & Doyle, W. L. Ingestion of fluid by Amoeba. *Protoplasma* 20, 555–560 (1933).

170. Sussman, R. & Sussman, M. Cultivation of Dictyostelium discoideum in axenic medium. *Biochem Bioph Res Co* 29, 53–55 (1967).

171. Hoon, J.-L., Wong, W.-K. & Koh, C.-G. Functions and Regulation of Circular Dorsal Ruffles. *Mol Cell Biol* 32, 4246–4257 (2012).

172. Racoosin, E. L. & Swanson, J. A. Macropinosome maturation and fusion with tubular lysosomes in macrophages. *J Cell Biology* 121, 1011–1020 (1993).

173. Moreau, H. D. *et al.* Macropinocytosis Overcomes Directional Bias in Dendritic Cells Due to Hydraulic Resistance and Facilitates Space Exploration. *Dev Cell* 49, 171-188.e5 (2019).

174. Li, Y. *et al.* Macropinocytosis-mediated membrane recycling drives neural crest migration by delivering F-actin to the lamellipodium. *Proc National Acad Sci* 117, 27400–27411 (2020).

175. Freeman, S. A. *et al.* Lipid-gated monovalent ion fluxes regulate endocytic traffic and support immune surveillance. *Science* 367, 301–305 (2020).

176. Buckley, C. M. *et al.* WASH drives early recycling from macropinosomes and phagosomes to maintain surface phagocytic receptors. *Proc National Acad Sci* 113, E5906–E5915 (2016).

177. Kay, R. R., Williams, T. D., Manton, J. D., Traynor, D. & Paschke, P. Living on soup: macropinocytic feeding in amoebae. *Int J Dev Biol* 63, 473–483 (2019).

178. Wadia, J. S., Schaller, M., Williamson, R. A. & Dowdy, S. F. Pathologic Prion Protein Infects Cells by Lipid-Raft Dependent Macropinocytosis. *Plos One* 3, e3314 (2008).

179. Fehlinger, A. *et al.* Prion strains depend on different endocytic routes for productive infection. *Sci Rep-uk* 7, 6923 (2017).

180. Yerbury, J. J. Protein aggregates stimulate macropinocytosis facilitating their propagation. *Prion* 10, 119–126 (2016).

181. Zeineddine, R. & Yerbury, J. J. The role of macropinocytosis in the propagation of protein aggregation associated with neurodegenerative diseases. *Front Physiol* 6, 277 (2015).

182. Zeineddine, R. *et al.* SOD1 protein aggregates stimulate macropinocytosis in neurons to facilitate their propagation. *Mol Neurodegener* 10, 57 (2015).

183. Nara, A., Aki, T., Funakoshi, T., Unuma, K. & Uemura, K. Hyperstimulation of macropinocytosis leads to lysosomal dysfunction during exposure to methamphetamine in SH-SY5Y cells. *Brain Res* 1466, 1–14 (2012).

184. Sánchez, E. G. *et al.* African Swine Fever Virus Uses Macropinocytosis to Enter Host Cells. *Plos Pathog* 8, e1002754 (2012).

185. Krzyzaniak, M. A., Zumstein, M. T., Gerez, J. A., Picotti, P. & Helenius, A. Host Cell Entry of Respiratory Syncytial Virus Involves Macropinocytosis Followed by Proteolytic Activation of the F Protein. *Plos Pathog* 9, e1003309 (2013).

186. Mercer, J. & Helenius, A. Virus entry by macropinocytosis. *Nat Cell Biol* 11, 510–520 (2009).

187. Vries, E. de *et al.* Dissection of the Influenza A Virus Endocytic Routes Reveals Macropinocytosis as an Alternative Entry Pathway. *Plos Pathog* 7, e1001329 (2011).

188. Rasmussen, I. & Vilhardt, F. Macropinocytosis Is the Entry Mechanism of Amphotropic Murine Leukemia Virus. *J Virol* 89, 1851–1866 (2015).

189. Ghosh, S. *et al.* β-Coronaviruses Use Lysosomes for Egress Instead of the Biosynthetic Secretory Pathway. *Cell* 183, 1520-1535.e14 (2020).

190. Wu, P.-H. *et al.* Lysosomal trafficking mediated by Arl8b and BORC promotes invasion of cancer cells that survive radiation. *Commun Biology* 3, 620 (2020).

191. Veithen, A., Cupers, P., Baudhuin, P. & Courtoy, P. J. v-Src induces constitutive macropinocytosis in rat fibroblasts. *J Cell Sci* 109 (Pt 8), 2005–12 (1996).

192. Commisso, C. *et al.* Macropinocytosis of protein is an amino acid supply route in Ras-transformed cells. *Nature* 497, 633–637 (2013).

193. Lee, S.-W. *et al.* EGFR-Pak Signaling Selectively Regulates Glutamine Deprivation-Induced Macropinocytosis. *Dev Cell* 50, 381-392.e5 (2019).

194. Kim, S. M. *et al.* PTEN deficiency and AMPK activation promote nutrient scavenging and anabolism in prostate cancer cells. *Cancer Discov* 8, CD-17-1215 (2018).

195. Commisso, C. The pervasiveness of macropinocytosis in oncological malignancies. *Philosophical Transactions Royal Soc B* 374, 20180153 (2019).

196. Nagano, T. *et al.* LY6D-induced macropinocytosis as a survival mechanism of senescent cells. *J Biol Chem* 296, 100049 (2021).

197. Williams, T. D. & Kay, R. R. The physiological regulation of macropinocytosis during Dictyostelium growth and development. *J Cell Sci* 131, jcs213736 (2018).

198. Bar-Sagi, D. & Feramisco, J. Induction of membrane ruffling and fluid-phase pinocytosis in quiescent fibroblasts by ras proteins. *Science* 233, 1061–1068 (1986).

199. Veltman, D. M. *et al.* A plasma membrane template for macropinocytic cups. *Elife* 5, e20085 (2016).

200. Swanson, J. A. Shaping cups into phagosomes and macropinosomes. *Nat Rev Mol Cell Bio* 9, 639–649 (2008).

201. Yoshida, S. *et al.* Differential signaling during macropinocytosis in response to M-CSF and PMA in macrophages. *Front Physiol* 6, 8 (2015).

202. Buckley, C. M. *et al.* Co-ordinated Ras and Rac activity shapes macropinocytic cups and enables phagocytosis of geometrically diverse bacteria. *Biorxiv* 763748 (2019) doi:10.1101/763748.

203. Marinović, M. *et al.* IQGAP-related protein IqgC suppresses Ras signaling during large-scale endocytosis. *Proc National Acad Sci* 116, 201810268 (2019).

204. Rásó, E. Splice variants of RAS—translational significance. *Cancer Metast Rev* 39, 1039–1049 (2020).

205. Ahearn, I. M., Haigis, K., Bar-Sagi, D. & Philips, M. R. Regulating the regulator: post-translational modification of RAS. *Nat Rev Mol Cell Bio* 13, 39–51 (2012).

206. Simanshu, D. K., Nissley, D. V. & McCormick, F. RAS Proteins and Their Regulators in Human Disease. *Cell* 170, 17–33 (2017).

207. Jura, N., Scotto-Lavino, E., Sobczyk, A. & Bar-Sagi, D. Differential Modification of Ras Proteins by Ubiquitination. *Mol Cell* 21, 679–687 (2006).

208. Zheng, Z.-Y., Xu, L., Bar-Sagi, D. & Chang, E. C. Escorting Ras. *Small Gtpases* 3, 236–239 (2012).

209. Baines, A. T., Xu, D. & Der, C. J. Inhibition of Ras for cancer treatment: the search continues. *Future Med Chem* 3, 1787–1808 (2011).

210. Rotblat, B., Ehrlich, M., Haklai, R. & Kloog, Y. The Ras Inhibitor Farnesylthiosalicylic Acid (Salirasib) Disrupts The Spatiotemporal Localization Of Active Ras: A Potential Treatment For Cancer. *Methods Enzymol* 439, 467–489 (2008).

211. Elad, G. *et al.* Targeting of K-Ras 4B by S-trans,trans-farnesyl thiosalicylic acid. *Biochimica Et Biophysica Acta Bba - Mol Cell Res* 1452, 228–242 (1999).

212. Geering, B., Cutillas, P. R., Nock, G., Gharbi, S. I. & Vanhaesebroeck, B. Class IA phosphoinositide 3-kinases are obligate p85-p110 heterodimers. *Proc National Acad Sci* 104, 7809–7814 (2007).

213. Vanhaesebroeck, B., Guillermet-Guibert, J., Graupera, M. & Bilanges, B. The emerging mechanisms of isoform-specific PI3K signalling. *Nat Rev Mol Cell Bio* 11, 329–341 (2010).

214. McDonald, C. B., Seldeen, K. L., Deegan, B. J., Bhat, V. & Farooq, A. Assembly of the Sos1–Grb2–Gab1 ternary signaling complex is under allosteric control. *Arch Biochem Biophys* 494, 216–225 (2010).

215. Castellano, E. & Downward, J. RAS Interaction with PI3K: More Than Just Another Effector Pathway. *Genes Cancer* 2, 261–274 (2011).

216. Swanson, J. A. & Yoshida, S. Macropinosomes as units of signal transduction. *Philosophical Transactions Royal Soc B* 374, 20180157 (2019).

217. Valdivia, A., Goicoechea, S. M., Awadia, S., Zinn, A. & Garcia-Mata, R. Regulation of circular dorsal ruffles, macropinocytosis, and cell migration by RhoG and its exchange factor, Trio. *Mol Biol Cell* 28, 1768–1781 (2017).

218. Sells, M. A., Boyd, J. T. & Chernoff, J. p21-Activated Kinase 1 (Pak1) Regulates Cell Motility in Mammalian Fibroblasts. *J Cell Biology* 145, 837–849 (1999).

219. Liberali, P. *et al.* The closure of Pak1-dependent macropinosomes requires the phosphorylation of CtBP1/BARS. *Embo J* 27, 970–981 (2008).

220. Maxson, M. E., Sarantis, H., Volchuk, A., Brumell, J. H. & Grinstein, S. Rab5 regulates macropinosome closure through recruitment of the inositol 5-phosphatases OCRL/Inpp5b and the hydrolysis of PtdIns(4,5)P2. *Biorxiv* 2020.06.08.139436 (2020) doi:10.1101/2020.06.08.139436.

221. Yamazaki, D., Fujiwara, T., Suetsugu, S. & Takenawa, T. A novel function of WAVE in lamellipodia: WAVE1 is required for stabilization of lamellipodial protrusions during cell spreading. *Genes Cells* 10, 381–392 (2005).

222. Singla, B., Lin, H.-P., Ghoshal, P., Cherian-Shaw, M. & Csányi, G. PKCδ stimulates macropinocytosis via activation of SSH1-cofilin pathway. *Cell Signal* 53, 111–121 (2018).

223. Haga, Y., Miwa, N., Jahangeer, S., Okada, T. & Nakamura, S. CtBP1/BARS is an activator of phospholipase D1 necessary for agonist-induced macropinocytosis. *Embo J* 28, 1197–1207 (2009).

224. Williamson, C. D. & Donaldson, J. G. Arf6, JIP3, and dynein shape and mediate macropinocytosis. *Mol Biol Cell* 30, 1477–1489 (2019).

225. Frittoli, E. *et al.* The Primate-specific Protein TBC1D3 Is Required for Optimal Macropinocytosis in a Novel ARF6-dependent Pathway. *Mol Biol Cell* 19, 1304–1316 (2008).

226. Buckley, C. M. & King, J. S. Drinking problems: mechanisms of macropinosome formation and maturation. *Febs J* 284, 3778–3790 (2017).

227. Dolat, L. & Spiliotis, E. T. Septins promote macropinosome maturation and traffic to the lysosome by facilitating membrane fusionSeptins promote macropinosome maturation. *J Cell Biology* 214, 517–527 (2016).

228. Yao, W. *et al.* Syndecan 1 is a critical mediator of macropinocytosis in pancreatic cancer. *Nature* 568, 410–414 (2019).

229. Brooks, R., Williamson, R. & Bass, M. Syndecan-4 independently regulates multiple small GTPases to promote fibroblast migration during wound healing. *Small Gtpases* 3, 73–79 (2012).

230. Ramirez, C., Hauser, A. D., Vucic, E. A. & Bar-Sagi, D. Plasma membrane V-ATPase controls oncogenic RAS-induced macropinocytosis. *Nature* 576, 477–481 (2019).

231. Tejeda-Muñoz, N., Albrecht, L. V., Bui, M. H. & Robertis, E. M. D. Wnt canonical pathway activates macropinocytosis and lysosomal degradation of extracellular proteins. *Proc National Acad Sci* 116, 201903506 (2019).

232. Aderem, A. & Underhill, D. M. Mechanisms of Phagocytosis in Macrophages. *Annu Rev Immunol* 17, 593–623 (1999).

233. Cendrowski, J., Mamińska, A. & Miaczynska, M. Endocytic regulation of cytokine receptor signaling. *Cytokine Growth F R* 32, 63–73 (2016).

234. West, M. A., Bretscher, M. S. & Watts, C. Distinct endocytotic pathways in epidermal growth factor-stimulated human carcinoma A431 cells. *J Cell Biology* 109, 2731–2739 (1989).

235. Koivusalo, M. *et al.* Amiloride inhibits macropinocytosis by lowering submembranous pH and preventing Rac1 and Cdc42 signaling. *J Cell Biology* 188, 547–563 (2010).

236. Lou, J., Low-Nam, S. T., Kerkvliet, J. G. & Hoppe, A. D. Delivery of CSF-1R to the lumen of macropinosomes promotes its destruction in macrophages. *J Cell Sci* 127, 5228–5239 (2014).

237. Yoshida, S., Pacitto, R., Yao, Y., Inoki, K. & Swanson, J. A. Growth factor signaling to mTORC1 by amino acid–laden macropinosomesAmino acid signaling to mTORC1 by macropinocytosis. *J Cell Biology* 211, 159–172 (2015).

238. Huang, S. & Huang, G. The dextrans as vehicles for gene and drug delivery. *Future Med Chem* 11, 1659–1667 (2019).

239. Chen, F., Huang, G. & Huang, H. Preparation and application of dextran and its derivatives as carriers. *Int J Biol Macromol* 145, 827–834 (2019).

240. Mehvar, R. Dextrans for targeted and sustained delivery of therapeutic and imaging agents. *J Control Release* 69, 1–25 (2000).

241. He, H., Liu, D. & Ince, C. Colloids and the Microcirculation. *Anesthesia Analgesia* 126, 1747–1754 (2018).

242. Li, L. *et al.* The effect of the size of fluorescent dextran on its endocytic pathway. *Cell Biol Int* 39, 531–539 (2015).

243. Rothschild, M. A., Oratz, M. & Schreiber, S. S. Serum albumin. *Hepatology* 8, 385–401 (1988).

244. Davis, M. J., Gregorka, B., Gestwicki, J. E. & Swanson, J. A. Inducible Renitence Limits Listeria monocytogenes Escape from Vacuoles in Macrophages. *J Immunol* 189, 4488–4495 (2012).

245. O'Flynn, K., Krensky, A. M., Beverley, P. C. L., Burakoff, S. J. & Linch, D. C. Phytohaemagglutinin activation of T cells through the sheep red blood cell receptor. *Nature* 313, 686–687 (1985).

246. Damke, H., Baba, T., Bliek, A. M. van der & Schmid, S. L. Clathrin-independent pinocytosis is induced in cells overexpressing a temperature-sensitive mutant of dynamin. *J Cell Biology* 131, 69–80 (1995).

247. Vercauteren, D. *et al.* The Use of Inhibitors to Study Endocytic Pathways of Gene Carriers: Optimization and Pitfalls. *Mol Ther* 18, 561–569 (2010).

248. Cerisier, N. *et al.* High Impact: The Role of Promiscuous Binding Sites in Polypharmacology. *Molecules* 24, 2529 (2019).

249. Haupt, V. J., Daminelli, S. & Schroeder, M. Drug Promiscuity in PDB: Protein Binding Site Similarity Is Key. *Plos One* 8, e65894 (2013).

250. Lapinski, P. E. & King, P. D. Regulation of Ras signal transduction during T cell development and activation. *Am J Clin Exp Immunol* 1, 147–153 (2012).

251. Warnecke, N. *et al.* TCR-mediated Erk activation does not depend on Sos and Grb2 in peripheral human T cells. *Embo Rep* 13, 386–391 (2012).

252. Kortum, R. L. *et al.* Targeted Sos1 deletion reveals its critical role in early T-cell development. *Proc National Acad Sci* 108, 12407–12412 (2011).

253. Kortum, R. L., Rouquette-Jazdanian, A. K. & Samelson, L. E. Ras and extracellular signal-regulated kinase signaling in thymocytes and T cells. *Trends Immunol* 34, 259–268 (2013).

254. Zhang, M., Jang, H. & Nussinov, R. PI3K inhibitors: review and new strategies. *Chem Sci* 11, 5855–5865 (2020).

255. Samuels, Y. & Velculescu, V. E. Oncogenic Mutations of PIK3CA in Human Cancers. *Cell Cycle* 3, 1221–1224 (2004).

256. Mizoguchi, M., Nutt, C. L., Mohapatra, G. & Louis, D. N. Genetic Alterations of Phosphoinositide 3-kinase Subunit Genes in Human Glioblastomas. *Brain Pathol* 14, 372–377 (2004).

257. Gharbi, S. I. *et al.* Exploring the specificity of the PI3K family inhibitor LY294002. *Biochem J* 404, 15–21 (2007).

258. Noritake, J., Watanabe, T., Sato, K., Wang, S. & Kaibuchi, K. IQGAP1: a key regulator of adhesion and migration. *J Cell Sci* 118, 2085–2092 (2005).

259. Schnoor, M., Stradal, T. E. & Rottner, K. Cortactin: Cell Functions of A Multifaceted Actin-Binding Protein. *Trends Cell Biol* 28, 79–98 (2018).

260. Chen, B. *et al.* Rac1 GTPase activates the WAVE regulatory complex through two distinct binding sites. *Elife* 6, e29795 (2017).

261. Prunier, C., Prudent, R., Kapur, R., Sadoul, K. & Lafanechère, L. LIM kinases: cofilin and beyond. *Oncotarget* 5, 41749–41763 (2015).

262. Baird, D., Feng, Q. & Cerione, R. A. The Cool-2/α-Pix Protein Mediates a Cdc42-Rac Signaling Cascade. *Curr Biol* 15, 1–10 (2005).

263. Omelchenko, T., Hall, A. & Anderson, K. V. β-Pix-dependent cellular protrusions propel collective mesoderm migration in the mouse embryo. *Nat Commun* 11, 6066 (2020).

264. Yue, J., Huhn, S. & Shen, Z. Complex roles of filamin-A mediated cytoskeleton network in cancer progression. *Cell Biosci* 3, 7 (2013).

265. Shutes, A. *et al.* Specificity and Mechanism of Action of EHT 1864, a Novel Small Molecule Inhibitor of Rac Family Small GTPases*. *J Biol Chem* 282, 35666–35678 (2007).

266. Deacon, S. W. *et al.* An Isoform-Selective, Small-Molecule Inhibitor Targets the Autoregulatory Mechanism of p21-Activated Kinase. *Chem Biol* 15, 322–331 (2008).

267. Sebti, S. M. Protein farnesylation: Implications for normal physiology, malignant transformation, and cancer therapy. *Cancer Cell* 7, 297–300 (2005).

268. Alarcón, B. & Martínez-Martín, N. RRas2, RhoG and T-cell phagocytosis. *Small Gtpases* 3, 97–101 (2012).

269. Garçon, F. *et al.* CD28 provides T-cell costimulation and enhances PI3K activity at the immune synapse independently of its capacity to interact with the p85/p110 heterodimer. *Blood* 111, 1464–1471 (2008).

270. Parry, R. V. *et al.* Ligation of the T cell co-stimulatory receptor CD28 activates the serine-threonine protein kinase protein kinase B. *Eur J Immunol* 27, 2495–2501 (1997).

271. Dütting, S. *et al.* Critical off-target effects of the widely used Rac1 inhibitors NSC23766 and EHT1864 in mouse platelets. *J Thromb Haemost* 13, 827–838 (2015).

272. Semenova, G. & Chernoff, J. Targeting PAK1. *Biochem Soc T* 45, 79–88 (2017).

273. Vazquez, A., Liu, J., Zhou, Y. & Oltvai, Z. N. Catabolic efficiency of aerobic glycolysis: The Warburg effect revisited. *Bmc Syst Biol* 4, 58 (2010).

274. Mookerjee, S. A., Gerencser, A. A., Nicholls, D. G. & Brand, M. D. Quantifying intracellular rates of glycolytic and oxidative ATP production and consumption using extracellular flux measurements. *J Biol Chem* 292, 7189–7207 (2017).

275. Epstein, T., Gatenby, R. A. & Brown, J. S. The Warburg effect as an adaptation of cancer cells to rapid fluctuations in energy demand. *Plos One* 12, e0185085 (2017).

276. Jones, W. & Bianchi, K. Aerobic Glycolysis: Beyond Proliferation. *Front Immunol* 6, 227 (2015).

277. Puchulu-Campanella, E. *et al.* Identification of the Components of a Glycolytic Enzyme Metabolon on the Human Red Blood Cell Membrane*. *J Biol Chem* 288, 848–858 (2013).

278. Windt, G. J. W. & Pearce, E. L. Metabolic switching and fuel choice during T-cell differentiation and memory development. *Immunol Rev* 249, 27–42 (2012).

279. Frauwirth, K. A. & Thompson, C. B. Regulation of T Lymphocyte Metabolism. *J Immunol* 172, 4661–4665 (2004).

280. Thurnher, M. & Gruenbacher, G. T lymphocyte regulation by mevalonate metabolism. *Sci Signal* 8, re4–re4 (2015).

281. Chapman, N. M. & Chi, H. Hallmarks of T-cell Exit from Quiescence. *Cancer Immunol Res* 6, 502–508 (2018).

282. Chang, W.-K., Yang, K. D., Chuang, H., Jan, J.-T. & Shaio, M.-F. Glutamine Protects Activated Human T Cells from Apoptosis by Up-Regulating Glutathione and Bcl-2 Levels. *Clin Immunol* 104, 151–160 (2002).

283. Bachmann, M. F. & Oxenius, A. Interleukin 2: from immunostimulation to immunoregulation and back again. *Embo Rep* 8, 1142–1148 (2007).

284. Ross, S. H. & Cantrell, D. A. Signaling and Function of Interleukin-2 in T Lymphocytes. *Annu Rev Immunol* 36, 411–433 (2018).

285. Mishima, T., Toda, S., Ando, Y., Matsunaga, T. & Inobe, M. Rapid proliferation of activated lymph node CD4+ T cells is achieved by greatly curtailing the duration of gap phases in cell cycle progression. *Cell Mol Biology Lett* 19, 638–648 (2014).

286. Hua, H. *et al.* Targeting mTOR for cancer therapy. *J Hematol Oncol* 12, 71 (2019).

287. Zoncu, R., Efeyan, A. & Sabatini, D. M. mTOR: from growth signal integration to cancer, diabetes and ageing. *Nat Rev Mol Cell Bio* 12, 21–35 (2011).

288. Foster, K. G. *et al.* Regulation of mTOR Complex 1 (mTORC1) by Raptor Ser863 and Multisite Phosphorylation*. *J Biol Chem* 285, 80–94 (2010).

289. Kakumoto, K., Ikeda, J., Okada, M., Morii, E. & Oneyama, C. mLST8 Promotes mTOR-Mediated Tumor Progression. *Plos One* 10, e0119015 (2015).

290. Peterson, T. R. *et al.* DEPTOR Is an mTOR Inhibitor Frequently Overexpressed in Multiple Myeloma Cells and Required for Their Survival. *Cell* 137, 873–886 (2009).

291. Dibble, C. C. *et al.* TBC1D7 Is a Third Subunit of the TSC1-TSC2 Complex Upstream of mTORC1. *Mol Cell* 47, 535–546 (2012).

292. Huang, J. & Manning, B. D. The TSC1–TSC2 complex: a molecular switchboard controlling cell growth. *Biochem J* 412, 179–190 (2008).

293. Yang, H. *et al.* Mechanisms of mTORC1 activation by RHEB and inhibition by PRAS40. *Nature* 552, 368–373 (2017).

294. Long, X., Lin, Y., Ortiz-Vega, S., Yonezawa, K. & Avruch, J. Rheb Binds and Regulates the mTOR Kinase. *Curr Biol* 15, 702–713 (2005).

295. Finlay, D. K. *et al.* PDK1 regulation of mTOR and hypoxia-inducible factor 1 integrate metabolism and migration of CD8+ T cellsmTOR/HIF1 controls CTL metabolism and migration. *J Exp Medicine* 209, 2441–2453 (2012).

296. Laplante, M. & Sabatini, D. M. mTOR Signaling in Growth Control and Disease. *Cell* 149, 274–293 (2012).

297. Shen, K. & Sabatini, D. M. Ragulator and SLC38A9 activate the Rag GTPases through noncanonical GEF mechanisms. *Proc National Acad Sci* 115, 201811727 (2018).

298. Fromm, S. A., Lawrence, R. E. & Hurley, J. H. Structural mechanism for amino acid-dependent Rag GTPase nucleotide state switching by SLC38A9. *Nat Struct Mol Biol* 27, 1017–1023 (2020).

299. Xu, D. *et al.* Evidence for a role for Sestrin1 in mediating leucine-induced activation of mTORC1 in skeletal muscle. *Am J Physiol-endoc M* 316, E817–E828 (2019).

300. Wolfson, R. L. *et al.* Sestrin2 is a leucine sensor for the mTORC1 pathway. *Science* 351, 43–48 (2016).

301. Peng, M., Yin, N. & Li, M. O. Sestrins Function as Guanine Nucleotide Dissociation Inhibitors for Rag GTPases to Control mTORC1 Signaling. *Cell* 159, 122–133 (2014).

302. Chantranupong, L. *et al.* The CASTOR Proteins Are Arginine Sensors for the mTORC1 Pathway. *Cell* 165, 153–164 (2016).

303. Yu, Y. C., Han, J. M. & Kim, S. Aminoacyl-tRNA Synthetases and amino acid signaling. *Biochimica Et Biophysica Acta Bba - Mol Cell Res* 1868, 118889 (2020).

304. Goberdhan, D. C. I., Wilson, C. & Harris, A. L. Amino Acid Sensing by mTORC1: Intracellular Transporters Mark the Spot. *Cell Metab* 23, 580–589 (2016).

305. Rebsamen, M. *et al.* SLC38A9 is a component of the lysosomal amino acid sensing machinery that controls mTORC1. *Nature* 519, 477–481 (2015).

306. Castellano, B. M. *et al.* Lysosomal cholesterol activates mTORC1 via an SLC38A9–Niemann-Pick C1 signaling complex. *Science* 355, 1306–1311 (2017).

307. Soliman, G. A. The integral role of mTOR in lipid metabolism. *Cell Cycle* 10, 861–862 (2011).

308. Sabatini, D. M. Twenty-five years of mTOR: Uncovering the link from nutrients to growth. *Proc National Acad Sci* 114, 11818–11825 (2017).

309. Fenton, T. R. & Gout, I. T. Functions and regulation of the 70kDa ribosomal S6 kinases. *Int J Biochem Cell Biology* 43, 47–59 (2011).

310. Morita, M. *et al.* mTORC1 Controls Mitochondrial Activity and Biogenesis through 4E-BP-Dependent Translational Regulation. *Cell Metab* 18, 698–711 (2013).

311. Morita, M. *et al.* mTOR coordinates protein synthesis, mitochondrial activity and proliferation. *Cell Cycle* 14, 473–480 (2015).

312. Qin, X., Jiang, B. & Zhang, Y. 4E-BP1, a multifactor regulated multifunctional protein. *Cell Cycle* 15, 781–786 (2016).

313. Meyuhas, O. Ribosomal Protein S6 Phosphorylation: Four Decades of Research. *Int Rev Cel Mol Bio* 320, 41–73 (2015).

314. Chauvin, C. *et al.* Ribosomal protein S6 kinase activity controls the ribosome biogenesis transcriptional program. *Oncogene* 33, 474–483 (2014).

315. Philippe, L., Elzen, A. M. G. van den, Watson, M. J. & Thoreen, C. C. Global analysis of LARP1 translation targets reveals tunable and dynamic features of 5′ TOP motifs. *Proc National Acad Sci* 117, 5319–5328 (2020).

316. Ruvinsky, I. & Meyuhas, O. Ribosomal protein S6 phosphorylation: from protein synthesis to cell size. *Trends Biochem Sci* 31, 342–348 (2006).

317. Fingar, D. C. *et al.* mTOR Controls Cell Cycle Progression through Its Cell Growth Effectors S6K1 and 4E-BP1/Eukaryotic Translation Initiation Factor 4E. *Mol Cell Biol* 24, 200–216 (2004).

318. Averous, J., Fonseca, B. D. & Proud, C. G. Regulation of cyclin D1 expression by mTORC1 signaling requires eukaryotic initiation factor 4E-binding protein 1. *Oncogene* 27, 1106–1113 (2008).

319. Holczer, M. *et al.* A Double Negative Feedback Loop between mTORC1 and AMPK Kinases Guarantees Precise Autophagy Induction upon Cellular Stress. *Int J Mol Sci* 20, 5543 (2019).

320. Shackelford, D. B. & Shaw, R. J. The LKB1–AMPK pathway: metabolism and growth control in tumour suppression. *Nat Rev Cancer* 9, 563–575 (2009).

321. Kim, J., Kundu, M., Viollet, B. & Guan, K.-L. AMPK and mTOR regulate autophagy through direct phosphorylation of Ulk1. *Nat Cell Biol* 13, 132–141 (2011).

322. Gwinn, D. M. *et al.* AMPK Phosphorylation of Raptor Mediates a Metabolic Checkpoint. *Mol Cell* 30, 214–226 (2008).

323. Zeng, H. & Chi, H. mTOR signaling in the differentiation and function of regulatory and effector T cells. *Curr Opin Immunol* 46, 103–111 (2017).

324. Chi, H. Regulation and function of mTOR signalling in T cell fate decisions. *Nat Rev Immunol* 12, 325–338 (2012).

325. Dibble, C. C. & Cantley, L. C. Regulation of mTORC1 by PI3K signaling. *Trends Cell Biol* 25, 545–555 (2015).

326. Gorentla, B. K., Wan, C.-K. & Zhong, X.-P. Negative regulation of mTOR activation by diacylglycerol kinases. *Blood* 117, 4022–4031 (2011).

327. Turner, M. S., Kane, L. P. & Morel, P. A. Dominant Role of Antigen Dose in CD4+Foxp3+ Regulatory T Cell Induction and Expansion. *J Immunol* 183, 4895–4903 (2009).

328. Katzman, S. D. *et al.* Duration of antigen receptor signaling determines T-cell tolerance or activation. *Proc National Acad Sci* 107, 18085–18090 (2010).

329. Delgoffe, G. M. *et al.* The mTOR Kinase Differentially Regulates Effector and Regulatory T Cell Lineage Commitment. *Immunity* 30, 832–844 (2009).

330. So, L. *et al.* The 4E-BP–eIF4E axis promotes rapamycin-sensitive growth and proliferation in lymphocytes. *Sci Signal* 9, ra57–ra57 (2016).

331. Myers, D. R., Wheeler, B. & Roose, J. P. mTOR and other effector kinase signals that impact T cell function and activity. *Immunol Rev* 291, 134–153 (2019).

332. Bjur, E. *et al.* Distinct Translational Control in CD4+ T Cell Subsets. *Plos Genet* 9, e1003494 (2013).

333. Delgoffe, G. M. *et al.* The kinase mTOR regulates the differentiation of helper T cells through the selective activation of signaling by mTORC1 and mTORC2. *Nat Immunol* 12, 295–303 (2011).

334. Kurebayashi, Y. *et al.* PI3K-Akt-mTORC1-S6K1/2 Axis Controls Th17 Differentiation by Regulating Gfi1 Expression and Nuclear Translocation of RORγ. *Cell Reports* 1, 360–373 (2012).

335. Yang, K. *et al.* T Cell Exit from Quiescence and Differentiation into Th2 Cells Depend on Raptor-mTORC1-Mediated Metabolic Reprogramming. *Immunity* 39, 1043–1056 (2013).

336. Li, Q. *et al.* Regulating Mammalian Target of Rapamycin To Tune Vaccination-Induced CD8+ T Cell Responses for Tumor Immunity. *J Immunol* 188, 3080–3087 (2012).

337. Shi, J. & Sun, S.-C. TCR signaling to NF-κB and mTORC1: Expanding roles of the CARMA1 complex. *Mol Immunol* 68, 546–557 (2015).

338. Saci, A., Cantley, L. C. & Carpenter, C. L. Rac1 Regulates the Activity of mTORC1 and mTORC2 and Controls Cellular Size. *Mol Cell* 42, 50–61 (2011).

339. Németh, Z. H. *et al.* Disruption of the actin cytoskeleton results in nuclear factor-κB activation and inflammatory mediator production in cultured human intestinal epithelial cells. *J Cell Physiol* 200, 71–81 (2004).

340. KUSTERMANS, G., BENNA, J. E., PIETTE, J. & LEGRAND-POELS, S. Perturbation of actin dynamics induces NF-κB activation in myelomonocytic cells through an NADPH oxidase-dependent pathway. *Biochem J* 387, 531–540 (2005).

341. Rincón, M., Flavell, R. A. & Davis, R. J. Signal transduction by MAP kinases in T lymphocytes. *Oncogene* 20, 2490–2497 (2001).

342. McKee, T. J. & Komarova, S. V. Is it time to reinvent basic cell culture medium? *Am J Physiol-cell Ph* 312, C624–C626 (2017).

343. Garlick, P. J. The Role of Leucine in the Regulation of Protein Metabolism. *J Nutrition* 135, 1553S-1556S (2005).

344. Norton, L. E. & Layman, D. K. Leucine Regulates Translation Initiation of Protein Synthesis in Skeletal Muscle after Exercise. *J Nutrition* 136, 533S-537S (2006).

345. Ananieva, E. A., Powell, J. D. & Hutson, S. M. Leucine Metabolism in T Cell Activation: mTOR Signaling and Beyond. *Adv Nutrition Int Rev J* 7, 798S-805S (2016).

346. Ren, W. *et al.* Amino-acid transporters in T-cell activation and differentiation. *Cell Death Dis* 8, e2655–e2655 (2017).

347. Morris, S. M. Arginine: beyond protein. *Am J Clin Nutrition* 83, 508S-512S (2006).

348. Rodriguez, P. C., Quiceno, D. G. & Ochoa, A. C. l-arginine availability regulates T-lymphocyte cell-cycle progression. *Blood* 109, 1568–1573 (2006).

349. Wang, S. *et al.* Lysosomal amino acid transporter SLC38A9 signals arginine sufficiency to mTORC1. *Science* 347, 188–194 (2015).

350. Carroll, B. *et al.* Control of TSC2-Rheb signaling axis by arginine regulates mTORC1 activity. *Elife* 5, e11058 (2016).

351. Kalhan, S. C. & Hanson, R. W. Resurgence of Serine: An Often Neglected but Indispensable Amino Acid*. *J Biol Chem* 287, 19786–19791 (2012).

352. Fan, S.-J. *et al.* PAT4 levels control amino-acid sensitivity of rapamycin-resistant mTORC1 from the Golgi and affect clinical outcome in colorectal cancer. *Oncogene* 35, 3004–3015 (2016).

353. Dyachok, J., Earnest, S., Iturraran, E. N., Cobb, M. H. & Ross, E. M. Amino Acids Regulate mTORC1 by an Obligate Two-step Mechanism*. *J Biol Chem* 291, 22414–22426 (2016).

354. Bernfeld, E. *et al.* Phospholipase D–dependent mTOR complex 1 (mTORC1) activation by glutamine. *J Biol Chem* 293, 16390–16401 (2018).

355. Song, W., Li, D., Tao, L., Luo, Q. & Chen, L. Solute carrier transporters: the metabolic gatekeepers of immune cells. *Acta Pharm Sinica B* 10, 61–78 (2020).

356. Wang, R. *et al.* The Transcription Factor Myc Controls Metabolic Reprogramming upon T Lymphocyte Activation. *Immunity* 35, 871–882 (2011).

357. Sinclair, L. V. *et al.* Control of amino-acid transport by antigen receptors coordinates the metabolic reprogramming essential for T cell differentiation. *Nat Immunol* 14, 500–508 (2013).

358. Marchingo, J. M., Sinclair, L. V., Howden, A. J. & Cantrell, D. A. Quantitative analysis of how Myc controls T cell proteomes and metabolic pathways during T cell activation. *Elife* 9, e53725 (2020).

359. Hayashi, K., Jutabha, P., Endou, H., Sagara, H. & Anzai, N. LAT1 Is a Critical Transporter of Essential Amino Acids for Immune Reactions in Activated Human T Cells. *J Immunol* 191, 4080–4085 (2013).

360. Milkereit, R. *et al.* LAPTM4b recruits the LAT1-4F2hc Leu transporter to lysosomes and promotes mTORC1 activation. *Nat Commun* 6, 7250 (2015).

361. Palm, W. *et al.* The Utilization of Extracellular Proteins as Nutrients Is Suppressed by mTORC1. *Cell* 162, 259–270 (2015).

362. Lin, H. *et al.* Identification of novel macropinocytosis inhibitors using a rational screen of Food and Drug Administration-approved drugs. *Brit J Pharmacol* 175, 3640–3655 (2018).